
Singularity Structure of Feynman Integrals with Applications to Six-Particle Scattering Processes

Antonela Matijašić



München 2024

Singularity Structure of Feynman Integrals with Applications to Six-Particle Scattering Processes

Antonela Matijašić

Dissertation
der Fakultät für Physik
der Ludwig-Maximilians-Universität
München

vorgelegt von
Antonela Matijašić
aus Poreč (Kroatien)

München, den 31.7.2024

This work is licensed under CC BY 4.0.

<https://creativecommons.org/licenses/by/4.0/>

Erstgutachter: Prof. Dr. Johannes M. Henn

Zweitgutachter: Prof. Dr. Gerhard Buchalla

Tag der mündlichen Prüfung: 16.9.2024

Summary

Scattering amplitudes serve as a bridge between theoretical predictions and experimental data in Quantum Field Theories (QFTs). They are computed in perturbation theory as a series in the coupling constants. Beyond the leading order, computing the contributing Feynman integrals is one of the most critical and often complex steps required to draw predictions from the theory. A well-known method for addressing this involves deriving a system of ordinary differential equations in the canonical form that the Feynman integrals satisfy, where solutions in terms of known functions can be readily obtained. An important aspect of this method lies in understanding the singularity structure of Feynman integrals.

We first introduce several representations of Feynman integrals used in different parts of this thesis. In particular, we introduce two parametric representations suitable for analyzing the singularities of Feynman integrals. Next, we address the question of determining the location of possible kinematic singularities of Feynman integrals. To this end, we first review the Landau equations and a modern approach for finding their solutions based on methods from nonlinear algebra. Next, we use the connection between the singularities of Feynman integrals and symbol alphabets to find the alphabets without ever solving the integrals. Furthermore, we review a method for the analytic computation of Feynman integrals based on differential equations. We argue that knowing the singularity structure and a good basis of Feynman integrals makes the computation more efficient and simplifies finding a solution.

The main contribution of the thesis is an efficient algorithm for finding algebraic letters from the knowledge of the kinematic singularities of Feynman integrals. The algorithm is based on an observed factorization property of algebraic letters. In order to make the algorithm more efficient and ready to use in cutting-edge applications, we introduce a criterion that significantly reduces the size of the problem at hand, allowing us to handle large alphabets appearing in the high-multiplicity problems. Finally, we use the methods discussed in this thesis in a state-of-the-art computation of Feynman integrals that could not be computed without having insight into their singularity structure.

Zusammenfassung

Streuamplituden dienen als Brücke zwischen theoretischen Vorhersagen und experimentellen Daten in Quantenfeldtheorien (QFTs). Sie werden in der Störungstheorie als eine Reihe in den Kopplungskonstanten berechnet. Über die führende Ordnung hinaus ist die Berechnung der beitragenden Feynman-Integrale einer der kritischsten und oft komplexesten Schritte, die erforderlich sind, um Vorhersagen aus der Theorie abzuleiten. Eine bekannte Methode, um dieses Problem anzugehen, besteht darin, ein System gewöhnlicher Differentialgleichungen in der kanonischen Form herzuleiten, die die Feynman-Integrale erfüllen, wobei Lösungen in Form bekannter Funktionen leicht zu ermitteln sind. Ein wichtiger Aspekt dieser Methode besteht darin, die Singularitätsstruktur der Feynman-Integrale zu verstehen.

Zunächst stellen wir verschiedene Darstellungen von Feynman-Integralen vor, die in verschiedenen Teilen dieser Arbeit verwendet werden. Insbesondere stellen wir zwei parametrische Darstellungen vor, die sich für die Analyse der Singularitäten von Feynman-Integralen eignen. Als Nächstes befassen wir uns mit der Frage, wie sich mögliche kinematische Singularitäten von Feynman-Integralen lokalisieren lassen. Zu diesem Zweck werden zunächst die Landau-Gleichungen und ein moderner Ansatz zur Lösung dieser Gleichungen auf der Grundlage von Methoden der nichtlinearen Algebra vorgestellt. Als Nächstes nutzen wir die Verbindung zwischen den Singularitäten von Feynman-Integralen und Symbolalphabeten, um die Alphabete zu finden, ohne die Integrale jemals zu lösen. Darüber hinaus beschreiben wir eine Methode zur analytischen Berechnung von Feynman-Integralen auf der Grundlage von Differentialgleichungen. Wir argumentieren, dass die Kenntnis der Singularitätsstruktur und einer guten Basis von Feynman-Integralen die Berechnung effizienter macht und das Finden einer Lösung vereinfacht.

Der Hauptbeitrag der Dissertation ist ein effizienter Algorithmus zur Ermittlung algebraischer Buchstaben aus der Kenntnis der kinematischen Singularitäten von Feynman-Integralen. Der Algorithmus basiert auf einer beobachteten Faktorisierungseigenschaft algebraischer Buchstaben. Um die Effizienz des Algorithmus zu steigern und ihn für den Einsatz in innovativen Anwendungen zu optimieren, führen wir ein Kriterium ein, das die Größe des vorliegenden Problems erheblich reduziert und es uns ermöglicht, große Alphabete zu verarbeiten, die in Problemen mit hoher Multiplizität auftreten. Schließlich wenden wir die in dieser Arbeit diskutierten Methoden für die Berechnung von Feynman-Integralen an, die ohne die gewonnenen Einsichten in ihre Singularitätsstruktur nicht berechnet werden könnten.

List of Publications

This thesis is based on the author's work conducted at the Max Planck Institute for Physics in Munich from January 2021 to July 2024. Parts of this work have already been presented in the following publications:

Refereed Research Papers:

- J. M. Henn, **A. Matijašić** and J. Miczajka, *One-loop hexagon integral to higher orders in the dimensional regulator*, J. High Energ. Phys. **2023**, 96 (2023) [2210.13505];
- J. M. Henn, **A. Matijašić**, J. Miczajka, T. Peraro, Y. Xu and Y. Zhang, *A computation of two-loop six-point Feynman integrals in dimensional regularization*, J. High Energ. Phys. **2024**, 27 (2024) [2403.19742]

Contents

Contents	viii
1 Introduction	1
2 Feynman Integrals	5
2.1 Loop Momentum Representation	6
2.2 Feynman Parameter Representation	11
2.3 Lee–Pomeransky Representation	15
2.4 Baikov Representation	15
3 Singularity Structure of Feynman Integrals	21
3.1 Landau Equations	22
3.2 Solving Landau Equations	24
3.3 Symbolology of Feynman Integrals	28
3.4 Efficiently Constructing Algebraic (Odd) Letters	29
3.4.1 Mathematical Formulation	31
3.4.2 Finding Allowed Even Letters	33
3.4.3 Constructing Algebraic Letters	34
4 Integration via Differentiation	39
4.1 Integration–by–Parts Identities	40
4.2 Dimension–Shift Identities	42
4.3 Canonical Differential Equations	44
4.4 Solutions to the Canonical Differential Equation	55
4.5 Fixing the Boundary Constants	60
4.6 One–loop Hexagon Function Space	63
4.6.1 Symbol of the Hexagon Integral	67
4.6.2 Limit to Four–Dimensional External Momenta	68
5 Two–Loop Six–Point Feynman Integrals	73
5.1 Kinematics and Conventions	74
5.2 Integral Families	77
5.3 Canonical Bases of Master Integrals	79

5.3.1	Hexagon–Box Family	80
5.3.2	Pentagon–Box Family	81
5.3.3	Double–Box Family	81
5.3.4	Penta–Triangle Family	84
5.3.5	Hexagon–Bubble Family	84
5.4	Efficiently Calculating Feynman Integrals	85
5.5	The Hexagon Alphabet at Two Loops	87
5.5.1	Predicting Alphabet Letters	87
5.5.2	Parity–Even Letters	89
5.5.3	Parity–Odd Letters	91
5.5.4	Letters with Mixed Parity Transformations	94
5.5.5	Summary of Two–Loop Hexagon Alphabet	95
5.6	Solving the Differential Equations	95
5.6.1	Boundary Constants	96
5.6.2	Analytic Properties of the Hexagon Function Space	97
5.6.3	One–Fold Integral Representation for Numerical Evaluations	99
6	Conclusions and Outlook	103
A	Identities among Letters in Four–Dimensional Kinematics	107
	List of Figures	109
	List of Tables	111
	Bibliography	111

Chapter 1

Introduction

The pursuit of a fundamental understanding of the universe has been a cornerstone of human inquiry for centuries. From ancient Greece to the present day, physics has played a central role in this quest, seeking to unravel the mysteries of the cosmos and the laws that govern it. Throughout its history, physics has demonstrated an uncanny ability to uncover hidden patterns and symmetries, revealing the intricate web of relationships that underlies the natural world.

From the majestic sweep of cosmological evolution to the intricate dance of subatomic particles, physics has consistently pushed the boundaries of human knowledge, driven by a deep-seated desire to understand and explain the workings of the universe. Theoretical physics, in particular, has proven to be a powerful tool in this endeavor, providing a framework for distilling complex phenomena into elegant and insightful mathematical descriptions.

In the realm of modern physics, our understanding of the behavior of fundamental particles and forces is rooted in the Standard Model (SM) of particle physics which is built on a framework of Quantum Field Theory (QFT) [1–3]. QFT provides a foundation for describing the interactions between particles in terms of fields that permeate space and time. It has been incredibly successful in describing a wide range of phenomena, from the electron magnetic moment [4, 5] to the Higgs boson [6–10]. The importance of QFT lies in its ability to make precise predictions about the outcomes of high-energy particle collisions, which are crucial for advancing our understanding of the universe at its most fundamental level.

At the heart of QFT lies the concept of scattering amplitudes, which play a central role in computations of the cross sections. The scattering cross section is the primary observable in a particle scattering experiment, like the Large Hadron Collider (LHC) at CERN. It represents the probability of a specific process happening as a function of the particles' energy and momentum.

Triggered by astonishing simplicity emerging from extensive computations [11], a series of breakthroughs founded new techniques for scattering amplitudes as a key field in theoretical high-energy physics; see Ref. [12] and references therein for a recent review. The need for precise theoretical predictions for ongoing and future experiments, coupled

with the desire of theorists for more rigorous tests of their theoretical models, propelled the invention of highly efficient methods that not only calculate amplitudes, but also extract physical quantities from them. The computations enabled by these new techniques uncovered remarkable links between theories relevant to particle scattering and General Relativity. These links extend beyond scattering, offering a fresh outlook on black holes and the physics of gravitational waves detected by the LIGO and Virgo collaborations [13]. Furthermore, the fluctuations that give rise to patterns in the cosmic microwave background (CMB) and to the large-scale structure of the universe can be understood in terms of correlation functions in the early universe, which can be computed using scattering amplitudes methods; see Ref. [14] for a review. Thus, the study of scattering amplitudes is important not only for our understanding of the behavior of fundamental particles but also for our understanding of the universe as a whole.

Just as experimental measurements have limited precision, it is not possible to calculate the desired quantities with arbitrary precision. Therefore, we perform our computations in certain approximations, as an expansion around a small parameter, which is called *perturbation theory*. One of the most powerful tools for computing scattering amplitudes is the Feynman diagram approach, which represents the amplitude as a sum over a set of Feynman diagrams. Each diagram corresponds to a specific contribution to the amplitude arising from the exchange of virtual particles between the colliding particles. The evaluation of Feynman diagrams beyond the leading order gives rise to a set of integrals, known as Feynman integrals, which are a particular type of multidimensional integral. These integrals are a cornerstone of QFT, as they provide a link between the abstract Feynman diagrams and the physical world of concrete particles and interactions.

Despite the importance of Feynman integrals, their evaluation remains a significant challenge in many areas of physics. Feynman integrals are typically represented as multidimensional integrals over the momentum of the virtual particles, and can be evaluated using a variety of analytical and numerical techniques. Numerical methods such as sector decomposition [15, 16], auxiliary mass flow [17, 18], and Monte Carlo integration [19–21] can be used to numerically evaluate the integrals. The choice of method depends on the complexity of the integral, the desired level of precision, and the availability of computational resources. Alternatively, Feynman integrals can be analytically evaluated using direct integration [22, 23]; see also Ref. [24]. A widely adopted modern approach for the analytic computation of Feynman integrals is the method of differential equations [25, 26].

One of the most fascinating aspects of Feynman integrals is their analytic structure, which is the focus of this thesis. In particular, we want to focus on the following question: When can a Feynman integral develop singularities? The answer to this question was first formulated in the 1960s by Landau, Bjorken, and Nakanishi [27–29]. They developed a set of polynomial equations, known as the Landau equations, to determine the locations of the singularities.

Even though Landau equations have been extensively studied since their inception [22, 30–36], finding a systematic and efficient solution for most Feynman integrals relevant to contemporary high-precision calculations remains an unresolved issue. There are two main motivations driving the investigation of this problem. On the one hand, from a

mathematical point of view, we would like to have the definition of the singular locus of Feynman integrals which encapsulates all possible singularities that may occur. On the other hand, from a phenomenological point of view, understanding the full singularity structure enables us to simplify the computation of Feynman integrals via differential equations or even avoid the evaluation of Feynman integrals all together and directly bootstrap the amplitude.

The singularities of Feynman integrals are intricately linked to the concept of symbol letters and alphabets. Symbol letters characterize the types of functions that may appear in the solutions. Hence, recognizing them beforehand is beneficial, even prior to performing any integral computations. There are several methods to directly predict the alphabet, for example, using the Baikov representation [37, 38] or using the so-called Schubert problems [39–42].

The main goal of this thesis is to present an alternative approach to finding a complete alphabet for a given Feynman integral family. Whenever the alphabet includes square root letters, we can separate the alphabet into the polynomial part and the algebraic part. The polynomial part of the alphabet corresponds directly to the solutions of the Landau equations. Although, the algebraic part of the alphabet cannot be accessed directly through the Landau equations, we can algorithmically identify missing algebraic letters from knowledge of the polynomial part of the alphabet and the appearing square roots. Therefore, using a conjectured factorization property [43], we propose an algorithm for finding algebraic letters. In order to make the algorithm more efficient and ready for use in state-of-the-art applications, we introduce a criterion that significantly reduces the size of the problem at hand, allowing us to handle large alphabets.

The thesis is divided into several chapters. In Chapter 2, we introduce several representations of Feynman integrals suitable for studying their analytic properties. In Chapter 3, we address the question of determining the location of possible kinematic singularities of Feynman integrals. For this purpose, we begin by examining the Landau equations and review a method for determining their solutions using techniques from nonlinear algebra and algebraic geometry. Following this, we leverage the relationship between the singularities of Feynman integrals and symbol alphabets to identify the alphabets without directly solving the integrals. Furthermore, in Chapter 4, we review a method for the analytic computation of Feynman integrals based on differential equations. We argue that knowing the singularity structure and a good basis of Feynman integrals makes the computation more efficient and simplifies finding a solution. This is demonstrated on the one-loop hexagon example. Next, in Chapter 5, we apply the algorithm for finding algebraic letters to a cutting-edge computation of planar two-loop six-point Feynman integrals. Finally, we conclude and provide an outlook in Chapter 6.

Chapter 2

Feynman Integrals

Scattering amplitudes have been described as the “most perfect microscopic structures in the Universe” [44]. They are fundamental components in quantum field theory, enabling the prediction of probabilities for the outcome of particle collisions. Consequently, they serve as an essential bridge between theoretical frameworks and experimental data. For instance, they permit the validation of predictions made by the Standard Model of particle physics against the data gathered from the LHC at CERN.

Starting from a Lagrangian for a given quantum field theory, we can derive a set of rules, i.e. Feynman rules, that translate a Feynman diagram to a mathematical expression; see standard QFT textbooks like [2, 3]. Summing over all Feynman diagrams at a given order in perturbation theory gives us an expression for the scattering amplitude of a certain process. Using Feynman rules on any Feynman diagram beyond the tree level will result in an expression involving integrals over undetermined loop momenta. Therefore, we arrive at the expression for a Feynman integral.

In order to make precise theoretical predictions for various scattering processes at the LHC, scattering amplitudes are required at the next-to-leading order (NLO) and next-to-next-to-leading order (NNLO) in perturbation theory [45]. These computations require evaluations of Feynman integrals at the one-loop and two-loop level, respectively. Thus, this chapter is dedicated to the Feynman integrals themselves.

Most quantum field theories have a non-trivial spinor structure in loop Feynman diagrams, therefore resulting in tensor integrals. Although the denominator is consistently represented by a product of scalar propagators in the form $q_i^2 - m_i^2$, where q_i is the momentum and m_i^2 is the mass, due to locality, the numerator might contain multiple Lorentz or Weyl indices in the loop momenta l_i^μ . Through certain manipulations known as tensor reduction [46–48], any tensor quantity can be expressed as a combination of tensor monomials in the external momenta p_i^μ multiplying scalar Feynman integrals. Hence, our focus will be solely on the scalar Feynman integrals.

In this chapter, we introduce several different representations of Feynman integrals. We start with the loop momentum representation in Section 2.1. This representation is the most natural from the perspective of Feynman rules and will be used throughout the Chapters 4 and 5. Furthermore, we also introduce two parametric representations,

namely the Feynman parameter representation in Section 2.2 and the Lee–Pomeransky representation in Section 2.3. Both of these parametrizations are particularly suitable for studying the analytic properties of Feynman integrals in Chapter 3. Lastly, in Section 2.4, we present the Baikov representation.

2.1 Loop Momentum Representation

Feynman integrals correspond to Feynman graphs with loops. Starting with a Feynman graph G , we translate it to a mathematical expression using the Feynman rules.

Consider a connected Feynman graph G with n_{int} internal edges, n_{ext} external edges, and L loops. We associate external momenta $p_i \in \mathbb{R}^{D_{\text{ext}}}$, $i = 1, \dots, n_{\text{ext}}$ to each external edge. Each internal edge is associated with a *propagator* of the form

$$\frac{1}{(q_j^2 - m_j^2)^{\nu_j}}, \quad (2.1)$$

where q_j is the momentum flowing through that edge, m_j is the mass of the corresponding particle and ν_j is the power of the propagator. At each vertex, we impose momentum conservation which allows us to express any internal momentum q_j as a linear combination of independent external momenta p_i and independent loop momenta l_i . Hence, the momentum q_j associated to an edge is

$$q_j = \sum_{r=1}^L \lambda_{jr} l_r + \sum_{r=1}^{n_{\text{ext}}-1} \sigma_{jr} p_r, \quad \lambda_{jr}, \sigma_{jr} \in \{-1, 0, 1\}. \quad (2.2)$$

It follows that the Feynman integral I_G corresponding to the Feynman graph G is obtained by associating external edges with momenta p_i , internal edges with propagators of the form (2.1) and integrating over each independent loop momentum with a measure

$$\int \frac{d^D l_r}{i\pi^{\frac{D}{2}}}. \quad (2.3)$$

Moreover, we multiply the integral with a conventional prefactor

$$e^{L\epsilon\gamma_E}, \quad (2.4)$$

where ϵ is the dimensional regulator and γ_E is the Euler–Mascheroni constant. Without this prefactor, the Euler–Mascheroni constant γ_E would appear in the final result for any Feynman integral.

Thus, we arrive at the definition of a *Feynman integral* I_G

$$I_G = e^{L\epsilon\gamma_E} \int \prod_{r=1}^L \frac{d^D l_r}{i\pi^{\frac{D}{2}}} \prod_{j=1}^{n_{\text{int}}} \frac{1}{(q_j^2 - m_j^2)^{\nu_j}}. \quad (2.5)$$

Here, D is the number of space–time dimensions. We are interested in working in $D = 4$ for standard model computations, but it might be interesting to study integrals in other dimensions.

The same Feynman diagram can generate various Feynman integrals with the same propagator structure but differing in the propagator powers. For example, some propagators might be negative, indicating that they appear in the numerator instead of the denominator. This leads to a generalization of Feynman integrals to *integral families* by allowing arbitrary integer propagator powers $\nu_j \in \mathbb{Z}$.

As noted previously, Feynman integrals depend on the dimensionality of space-time D . In addition, they depend on the exponents of the propagators ν_j . Occasionally, we explicitly write the dependence on the powers of propagators in the following way

$$I_G = I^{(D)}(\nu_1, \dots, \nu_j), \quad \nu_j \in \mathbb{Z}. \quad (2.6)$$

For $\nu_j < 0$, the corresponding factor $(q_j^2 - m_j^2)$ will appear in the numerator. A family of Feynman integrals is defined as a set of propagators with arbitrary propagator powers. Integrals within a family are related to each other through the so-called *integration-by-parts identities* (IBPs) which will be discussed in more detail in Section 4.1.

Dimensional Regularization

Feynman integrals and thus also scattering amplitudes may be divergent in $D = 4$. One way of treating these divergences is by analytically continuing the number of space-time dimensions from four to a generic number of dimensions. Hence, we will be working in

$$D = D_0 - 2\epsilon, \quad (2.7)$$

where ϵ is the dimensional regulator. In general, it can be a noninteger or a complex number. This goes by the name of *dimensional regularization* [49–51].

Feynman integrals and scattering amplitudes are functions of D and are computed as Laurent series expansions around $\epsilon = 0$. In this formalism, loop integration divergences appear as poles in ϵ .

We distinguish between two different types of divergences, ultraviolet (UV) and infrared (IR) divergences. UV divergences arise from the regions where the loop momenta become large and are regulated by assuming that $\epsilon > 0$.

For renormalizable theories, such as the standard model, UV divergences can be absorbed in a redefinition of coupling constants, masses and fields. In those cases, we distinguish between bare (unphysical) parameters and renormalized (physical) parameters. Renormalized parameters are parameters connected to some observable quantity in nature and, therefore, are finite. For example, we can compute the physical coupling constant of some renormalizable theory perturbatively in terms of the bare coupling constant. In this way, we relate the physical coupling to the bare coupling. This relation may contain UV divergences and we can use it to absorb them into the unobservable bare coupling. Doing

this for all parameters of the renormalizable theory ensures that we remove all UV divergences. For a more detailed discussion of regularization and renormalization, see standard QFT textbooks like [1, 2].

On the other hand, IR arise in the scattering processes of massless particles when sufficiently many propagators go on shell simultaneously, i.e. when $q_j^2 - m_j^2 = 0$ for sufficiently many propagators. This may happen when the loop momentum becomes soft

$$l^\mu \rightarrow 0, \quad \mu = 0, \dots, D-1 \quad (2.8)$$

or when it becomes collinear with the momentum of a massless external particle

$$l^\mu \parallel p_i^\mu, \quad p_i^2 = 0. \quad (2.9)$$

We refer to those IR divergences as soft or collinear divergences, respectively. In general, it may be that both soft and collinear divergences arise simultaneously. In dimensional regularization, we regulate those divergences with $\epsilon < 0$.

When considering a scattering process of particles, we assume that we have well-defined asymptotic states with a finite number of particles. This is not the case for massless particles. We cannot distinguish between states with a single massless particle with soft momentum p ($p^2 \rightarrow 0$) or a state with the same massless particle surrounded by a cloud of other soft particles or a state assembled of collinear particles whose momentum sums up to p . This vagueness in the definition of the asymptotic states is the origin of IR divergences in the loop integration.

Unlike UV divergences, IR divergences are not as well understood. One way of treating IR divergences is by using the so-called cross-section method [52, 53]. The argument is that the S -matrix elements themselves are not observable, and therefore there is no problem with them being ill-defined in the presence of IR divergences. The observable quantities are cross sections determined by the square of S -matrix elements integrated over phase-space regions. In this way, IR divergences cancel between real emission contributions, coming from the phase space integration of squared amplitudes with fewer loops but extra radiation in the final state, and virtual contributions coming from the loop integrations. The cancellation of IR divergences in QED was demonstrated in [54] and this approach relies on the theory being Abelian. For non-Abelian gauge theories like QCD, the Kinoshita, Lee, and Nauenberg (KLN) theorem [55, 56] guarantees that all IR divergences cancel order by order in perturbation theory, when summed over all possible degenerate initial and final states. The stronger version of the KLN theorem was recently proven [57]. For recent developments, see Ref. [58] and for a pedagogical review of the subject, see Ref. [59] and references therein.

For the remainder of this thesis, the details on how to properly treat UV and IR divergences will not be important. It is enough to consider Feynman integrals within the dimensional regularization framework where we keep the value of the dimensional regulator ϵ generic so that we regularize both UV and IR divergences simultaneously.

Kinematic Dependence

Lastly, Feynman integrals depend on the kinematic variables. The Feynman integrals defined in equation (2.5) are scalar integrals, and hence they can only depend on the independent external momenta through the Lorentz invariants $p_i \cdot p_j$. The maximal number of independent variables is

$$\frac{n_{\text{ext}}(n_{\text{ext}} - 1)}{2} + n_{\text{int}} - 1. \quad (2.10)$$

The first $n_{\text{ext}}(n_{\text{ext}} - 1)/2$ variables correspond to the scalar products of the external momenta $p_i \cdot p_j$, while the variables n_{int} correspond to the masses of the propagators. Furthermore, we can remove one of the variables by setting it to one because of the scaling invariance. Of course, some of the external or internal masses may be equal or zero, which reduces the number of kinematic variables in the problem.

As we will see in Chapter 4, Feynman integrals evaluate to multi-valued functions. Hence, it is pivotal to specify the domain of kinematic variables. In the remainder of this thesis, we will consider Feynman integrals with massless propagators. The kinematic dependence of these integrals will be encoded in the *Mandelstam variables*

$$s_{ij} = (p_i + p_j)^2, \quad s_{ijk} = (p_i + p_j + p_k)^2. \quad (2.11)$$

These variables take definite signs for the physical momentum configuration that describe the scattering processes depending on which particles are considered incoming and outgoing. Additionally, the signs of the variables are constrained by certain Gram-determinant constraints.

We use the following definition of the *Gram determinant*

$$G \begin{pmatrix} q_1 & \cdots & q_n \\ u_1 & \cdots & u_n \end{pmatrix} = \det(2q_i \cdot u_j), \quad 1 \leq i, j \leq n, \quad (2.12)$$

with a shorthand notation

$$G(q_1, \dots, q_n) = G \begin{pmatrix} q_1 & \cdots & q_n \\ q_1 & \cdots & q_n \end{pmatrix}. \quad (2.13)$$

Additionally, we introduce the notation

$$\bar{G}_n = (-1)^{n-1} G(p_1, \dots, p_n), \quad 1 \leq n \leq n_{\text{ext}}. \quad (2.14)$$

Within the physical scattering region, the Gram determinant constraints take the following form [60]

$$\bar{G}_1 \geq 0, \quad \bar{G}_2 > 0, \quad \bar{G}_3 > 0, \dots, \quad \bar{G}_{D_0} > 0, \quad (2.15)$$

and $\bar{G}_n = 0$ for all $n > D_0$, since there are only D_0 independent momenta in D_0 dimensions. The first inequality differs for massive and massless particles, since \bar{G}_1 is equal to the mass of a particle. In the case of massive particles, we have a strict inequality $\bar{G}_1 > 0$, while for massless particles we have a strict equality $\bar{G}_1 = 0$.

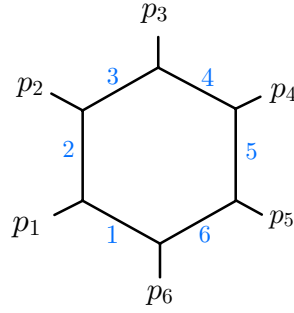


Figure 2.1: One-loop hexagon integral. In our examples, both the external momenta p_i and the propagators are considered to be massless.

Moreover, for all planar Feynman integrals, there is one particularly simple kinematic region where all dimensionally regularized scalar Feynman integrals are real-valued and only diverge on the boundaries where Mandelstam variables vanish. It is defined by a kinematic domain where the \mathcal{F} polynomial, defined in equation (2.28), is non-negative. This region is called the *Euclidean region*. A sufficient condition for the existence of a Euclidean region was given in [61]. Moreover, Feynman integrals in the Euclidean region are completely monotonic functions [62].

In view of the fact that Feynman integrals are multivalued functions, we can compute them in our favorite kinematical region. Then we can obtain the results valid in other kinematical regions by analytic continuation (see, for example, Ref. [63]).

Example: One-Loop Hexagon

To better understand all the notation introduced so far, it is useful to look at a particular example. The main example for this chapter is the one-loop hexagon integral shown in Figure 2.1.

The massless one-loop hexagon family is defined by integrals of the form

$$I^{(D_0)}(\nu_1, \dots, \nu_6) = e^{\epsilon\gamma_E} \int \frac{d^{D_0-2\epsilon}l}{i\pi^{\frac{D_0}{2}}} \frac{1}{\prod_{j=1}^6 \left(l + \sum_{k=1}^{j-1} p_k \right)^{2\nu_j}}, \quad (2.16)$$

with integer propagator powers ν_i . Moreover, the one-loop hexagon integral is the one with all propagator powers equal to one

$$I^{(D_0)}(1, 1, 1, 1, 1, 1) = e^{\epsilon\gamma_E} \int \frac{d^{D_0-2\epsilon}l}{i\pi^{\frac{D_0}{2}}} \frac{1}{\prod_{j=1}^6 \left(l + \sum_{k=1}^{j-1} p_k \right)^2}. \quad (2.17)$$

In principle, this massless six-particle Feynman integral depends on six momenta $p_i \in \mathbb{R}^{D_{\text{ext}}}$ which satisfy $p_i^2 = 0$ and momentum conservation implies

$$\sum_{i=1}^6 p_i = 0 \quad (2.18)$$

if all momenta are taken to be incoming. However, due to the Lorentz symmetry, the kinematic dependence is simplified, and an appropriate set of variables in integer dimensions $D_{\text{ext}} > 4$ are the nine independent Mandelstam invariants

$$\vec{v} = \{s_{12}, s_{23}, s_{34}, s_{45}, s_{56}, s_{61}, s_{123}, s_{234}, s_{345}\} \quad (2.19)$$

with

$$s_{ij} = (p_i + p_j)^2, \quad s_{ijk} = (p_i + p_j + p_k)^2. \quad (2.20)$$

In the Euclidean region, we consider all the variables in equation (2.19) to be negative. For physical momentum configurations describing $2 \rightarrow 4$ or $3 \rightarrow 3$ scattering processes, the Mandelstam invariants take definite signs depending on which particles are incoming and outgoing, respectively. For example:

12 \rightarrow 3456. In the $2 \rightarrow 4$ scattering region with particles 1 and 2 incoming, in addition to the Gram determinant constraints (2.15), the constraints on the Mandelstam invariants are

$$\begin{aligned} s_{12}, s_{34}, s_{35}, s_{36}, s_{45}, s_{46}, s_{56} &> 0, \\ s_{13}, s_{14}, s_{15}, s_{16}, s_{23}, s_{24}, s_{25}, s_{26} &< 0. \end{aligned} \quad (2.21)$$

Note that constraints that go beyond the set of variables introduced in (2.19) can be reexpressed in terms of v_i . For example,

$$s_{35} = s_{345} - s_{34} - s_{45}. \quad (2.22)$$

123 \rightarrow 456. In the $3 \rightarrow 3$ scattering region with particles 1, 2 and 3 incoming, in addition to the Gram determinant constraints (2.15), the Mandelstam invariants satisfy

$$\begin{aligned} s_{12}, s_{13}, s_{23}, s_{45}, s_{46}, s_{56} &> 0, \\ s_{14}, s_{15}, s_{16}, s_{24}, s_{25}, s_{26}, s_{34}, s_{35}, s_{36} &< 0. \end{aligned} \quad (2.23)$$

2.2 Feynman Parameter Representation

The Feynman parameter representation is a parametric representation suitable both for numerical evaluation and for studying the analytic properties of Feynman integrals. In this

representation, we trade the (LD) -fold momentum integrations for (n_{int}) -fold parametric integrations.

Starting from the momentum space representation, we obtain the Feynman parameter representation using the Feynman trick

$$\prod_{j=1}^n \frac{1}{P_j^{\nu_j}} = \frac{\Gamma(\nu)}{\prod_{j=1}^n \Gamma(\nu_j)} \int_{\alpha_j \geq 0} d^n \alpha \delta \left(1 - \sum_{j=1}^n \alpha_j \right) \frac{\prod_{j=1}^n \alpha_j^{\nu_j-1}}{\left(\sum_{j=1}^n \alpha_j P_j \right)^\nu}, \quad (2.24)$$

where $\nu = \sum_{j=1}^{n_{\text{int}}} \nu_j$ and $\nu_j > 0$. The denominators P_j are the propagators of Feynman integrals $P_j = (q_j^2 - m_j^2)$.

We use the translation invariance of the D -dimensional loop integrals to shift each loop momentum l_r in order to complete the square. The integrand then depends only on l_r^2 and all D -dimensional loop integrations can be performed. We arrive at the following representation

$$I_{\text{Feyn}} = e^{L\epsilon\gamma_E} \frac{\Gamma(\nu - \frac{LD}{2})}{\prod_{j=1}^{n_{\text{int}}} \Gamma(\nu_j)} \int_{\alpha_j \geq 0} d^{n_{\text{int}}} \alpha \delta \left(1 - \sum_{j=1}^{n_{\text{int}}} \alpha_j \right) \left(\prod_{j=1}^{n_{\text{int}}} \alpha_j^{\nu_j-1} \right) \frac{\mathcal{U}^{\nu - \frac{(L+1)D}{2}}(\alpha_j)}{\mathcal{F}^{\nu - \frac{LD}{2}}(\alpha_j)}. \quad (2.25)$$

The variables α_j are called Feynman parameters and \mathcal{U} and \mathcal{F} are the first and the second *Symanzik polynomial*, respectively.

The graph polynomials \mathcal{U} and \mathcal{F} are polynomials in the Feynman parameters and can be derived in several ways [64]. One way is by writing the momenta q_j as

$$q_j = \sum_{r=1}^L \lambda_{jr} l_r + \sum_{r=1}^{n_{\text{ext}}-1} \sigma_{jr} p_r. \quad (2.26)$$

Then, we can express the denominator of the integrand in equation (2.24) as

$$\sum_{j=1}^{n_{\text{int}}} \alpha_j P_j = \sum_{r=1}^L \sum_{s=1}^L l_r M_{rs} l_s + \sum_{r=1}^L 2l_r \cdot v_r + J. \quad (2.27)$$

Here, M is a $L \times L$ matrix with entries depending just on the Feynman parameters α_j , v is a L -vector of linear combinations of external momenta and J is scalar. Using these definitions, the graph polynomials are defined as

$$\begin{aligned} \mathcal{U}(\alpha) &= \det(M), \\ \mathcal{F}(\alpha) &= \det(M) \left(v^T M^{-1} v - J \right). \end{aligned} \quad (2.28)$$

The first Symanzik polynomial \mathcal{U} is a homogeneous polynomial of degree L linear in each Feynman parameter α_j . Moreover, each monomial of \mathcal{U} has a coefficient $+1$ if we write

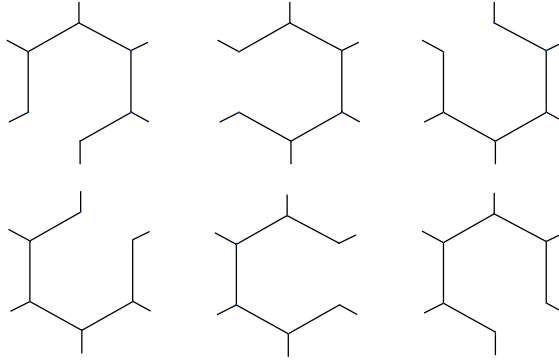


Figure 2.2: The set of spanning trees \mathcal{T}_1 for the one-loop hexagon graph contributing to the \mathcal{U} polynomial.

the polynomial in expanded form. On the other hand, the second Symanzik polynomial \mathcal{F} is a homogeneous polynomial of degree $L + 1$ whose coefficients depend on the kinematic invariants. In case all internal masses are equal to zero, the polynomial \mathcal{F} is also linear in each Feynman parameter α_j .

Starting from the one-loop hexagon integral defined in (2.17), using the Feynman trick (2.24) and expanding the momenta according to (2.27), it follows

$$\begin{aligned}
 M &= \alpha_1 + \alpha_2 + \alpha_3 + \alpha_4 + \alpha_5 + \alpha_6, \\
 v &= \alpha_2 p_1 + \alpha_3(p_1 + p_2) + \alpha_4(p_1 + p_2 + p_3) \\
 &\quad + \alpha_5(p_1 + p_2 + p_3 + p_4) + \alpha_6(p_1 + p_2 + p_3 + p_4 + p_5), \\
 J &= \alpha_3 s_{12} + \alpha_4 s_{123} + \alpha_5 s_{56}.
 \end{aligned} \tag{2.29}$$

From this, we can easily compute the graph polynomials using their definitions in equations (2.28)

$$\begin{aligned}
 \mathcal{U} &= \alpha_1 + \alpha_2 + \alpha_3 + \alpha_4 + \alpha_5 + \alpha_6, \\
 \mathcal{F} &= -s_{12}\alpha_2\alpha_6 - s_{23}\alpha_1\alpha_3 - s_{34}\alpha_2\alpha_4 - s_{45}\alpha_3\alpha_5 - s_{56}\alpha_4\alpha_6 - s_{61}\alpha_1\alpha_5 \\
 &\quad - s_{123}\alpha_3\alpha_6 - s_{234}\alpha_1\alpha_4 - s_{345}\alpha_2\alpha_5,
 \end{aligned} \tag{2.30}$$

and obtain the Feynman parameter representation from equation (2.25).

Another approach to computing the graph polynomials \mathcal{U} and \mathcal{F} is by using concepts from graph theory. Consider a connected graph G with n_{int} internal lines, n_{ext} external lines, and V vertices. The number of loops L of the graph G is given by the *first Betti number*

$$L = n_{\text{int}} - V + 1. \tag{2.31}$$

A *spanning tree* for graph G is a connected subgraph T that contains all the vertices of G and the first Betti number of T is zero. A spanning tree for graph G can be obtained

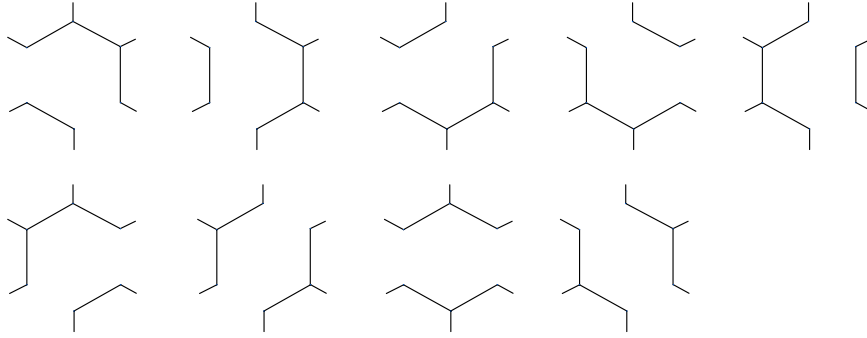


Figure 2.3: The set of spanning 2-forests \mathcal{T}_2 for the one-loop hexagon graph contributing to the \mathcal{F} polynomial.

from G by removing L internal lines. In general, a single graph G has multiple spanning trees. We denote the set of spanning trees as \mathcal{T}_1 .

The first Symanzik polynomial \mathcal{U} is defined as a sum over spanning trees

$$\mathcal{U}(\alpha) = \sum_{T \in \mathcal{T}_1} \prod_{e_i \notin T} \alpha_i, \quad (2.32)$$

where the product runs over the L internal edges that were removed to obtain the spanning tree T .

Similarly, we can define a *spanning 2-forest* as a disjoint union of two disconnected spanning trees T_1 and T_2 which contains all vertices of graph G . Again, a single graph G has multiple spanning 2-forests that can be obtained from G by removing $(L + 1)$ internal lines. We denote the set of spanning 2-forests by \mathcal{T}_2 .

The second Symanzik polynomial is defined as a sum over spanning 2-forests

$$\mathcal{F}(\alpha) = \sum_{(T_1, T_2) \in \mathcal{T}_2} \left(\prod_{e_i \notin (T_1, T_2)} \alpha_i \right) \left(\sum_{p_j \in P_{T_1}} \sum_{p_k \in P_{T_2}} p_j \cdot p_k \right) - \mathcal{U}(\alpha) \sum_{i=1}^{n_{\text{int}}} \alpha_i m_i^2, \quad (2.33)$$

where P_{T_i} denotes the set of external momenta in subgraph T_i .

Let us look at the one-loop hexagon as an example. There are six ways to remove one of the internal edges from the hexagon graph in Figure 2.1, as shown in Figure 2.2. Moreover, there are nine spanning 2-forests which are shown in Figure 2.3. Using the definitions (2.32) and (2.33), it follows that the graph polynomials are the ones found in equation (2.30).

In this section, we described the Feynman parameter representation, which is well suited for studying the analytic properties of Feynman integrals; see chapter 3. Furthermore, we introduced two different methods to compute the graph polynomials \mathcal{U} and \mathcal{F} . For more methods to compute the graph polynomials and original references, see the review [64].

2.3 Lee–Pomeransky Representation

Another closely related representation that uses graph polynomials is the Lee–Pomeransky representation [65]. Here, only one polynomial, which is given as the sum of the graph polynomials $\mathcal{G} = \mathcal{U} + \mathcal{F}$, enters the integrand

$$I_{LP} = e^{L\epsilon\gamma_E} \frac{\Gamma\left(\frac{D}{2}\right)}{\Gamma\left(\frac{(L+1)D}{2} - \nu\right) \prod_{j=1}^{n_{\text{int}}} \nu_j} \int_{\alpha_j \geq 0} d^{n_{\text{int}}} \alpha \left(\prod_{j=1}^{n_{\text{int}}} \alpha_j^{\nu_j-1} \right) \mathcal{G}^{-\frac{D}{2}}. \quad (2.34)$$

In order to derive the Lee–Pomeransky representation it is simpler to work backward and show that it is equivalent to the Feynman representation. In order to pass from (2.34) to (2.25) it is sufficient to insert

$$1 = \int ds \delta\left(s - \sum_{j=1}^{n_{\text{int}}} \alpha_j\right) \quad (2.35)$$

into the equation (2.34), scale the variables $\alpha_j \rightarrow s\alpha_j$ and integrate over s .

If we again choose the massless one-loop hexagon as an example, the \mathcal{G} polynomial takes the following form

$$\begin{aligned} \mathcal{G} = & \alpha_1 + \alpha_2 + \alpha_3 + \alpha_4 + \alpha_5 + \alpha_6 + s_{12}\alpha_2\alpha_6 + s_{23}\alpha_1\alpha_3 + s_{34}\alpha_2\alpha_4 \\ & + s_{45}\alpha_3\alpha_5 + s_{56}\alpha_4\alpha_6 + s_{61}\alpha_1\alpha_5 + s_{123}\alpha_3\alpha_6 + s_{234}\alpha_1\alpha_4 + s_{345}\alpha_2\alpha_5. \end{aligned} \quad (2.36)$$

We obtain the Lee–Pomeransky representation by inserting this polynomial into the equation (2.34) with $L = 1$.

This integral representation is particularly interesting from a mathematical perspective. Up to a prefactor involving Gamma functions and conventional $e^{L\epsilon\gamma_E}$, Feynman integrals in Lee–Pomeransky representation correspond to *generalized Euler integrals* introduced by Gelfand, Kapranov and Zelevinsky [66]

$$\int_{\Gamma} \frac{\alpha_1^{\nu_1} \cdots \alpha_n^{\nu_n}}{f_1^{s_1} \cdots f_1^{s_1}} \frac{d\alpha_1}{\alpha_1} \wedge \cdots \wedge \frac{d\alpha_n}{\alpha_n} = \int_{\Gamma} f^{-s} x^{\nu} \frac{d\alpha}{\alpha}, \quad (2.37)$$

where we used multi-index notation on the right-hand side. For a self-contained introduction to the topic, see Ref. [67].

The Lee–Pomeransky representation is beneficial for counting the number of basis integrals for a given integral family (Section 4.1) and for studying their singularity structure (Section 3.2).

2.4 Baikov Representation

The last representation that we are going to discuss is the Baikov representation [68, 69]. Here, we trade the (LD) -fold integration of loop momentum representation (2.5)

for integration over linearly independent scalar products involving both external and loop momenta.

If we use E to denote the number of independent external momenta, Lorentz invariants involving loop momenta l_i take the following form:

$$\begin{aligned} l_i^2, & \quad 1 \leq i \leq L, \\ l_i \cdot l_j, & \quad 1 \leq i < j \leq L, \\ l_i \cdot p_j, & \quad 1 \leq i \leq L, \quad 1 \leq j \leq E. \end{aligned} \quad (2.38)$$

Hence, we have in total

$$N_V = \frac{L(L+1)}{2} + LE \quad (2.39)$$

linear independent scalar products which we denote by

$$\begin{aligned} \sigma &= \{\sigma_1, \dots, \sigma_{N_V}\} \\ &= \{l_1 \cdot l_1, l_1 \cdot l_2, \dots, l_L \cdot l_L, l_1 \cdot p_1, \dots, l_L \cdot p_E\}. \end{aligned} \quad (2.40)$$

A Feynman graph G has a Baikov representation if $N_V = n_{\text{int}}$ and if we can express any inverse propagator as a linear combination of the linear independent scalar products involving loop momenta and terms independent of loop momenta

$$q_j^2 - m_j^2 = C_{jk} \sigma_k + f_j, \quad \forall 1 \leq k \leq n_{\text{int}}. \quad (2.41)$$

Here, C_n^{ij} are integer constants and f_n are functions of kinematic variables only.

The conditions for a Baikov representation to exist are always satisfied for one-loop Feynman graphs. However, for graphs beyond one loop, this is not always the case. There, we usually see that the number of internal edges n_{int} is smaller than the number of independent scalar products containing loop momenta. The scalar products that cannot be expressed in terms of inverse propagators are called *irreducible scalar products* (ISPs). The solution is to add additional inverse propagators such that all scalar products are expressible as inverse propagators. Therefore, after slight modifications, we can always find the Baikov representation for a Feynman graph G . Later, we will see how this works in practice in a particular example.

Now, we perform a change of the integration variables from loop momenta to the *Baikov variables* z_j

$$z_j = q_j^2 - m_j^2, \quad (2.42)$$

where the Baikov variables are just the inverse propagators. The inverse relation follows from equation (2.41)

$$\sigma_k = (C^{-1})_{kj} (z_j - f_j). \quad (2.43)$$

Next, we decompose the loop momentum into parallel and orthogonal components. This allows us to consistently perform a change of integration variables from l^μ to σ_i . For more

details see Ref. [70, 71]. Finally, we change the variables from σ_i at the Baikov variables z_i and arrive to the Baikov representation

$$I_B = e^{L\epsilon\gamma_E} \frac{[G(p_1, \dots, p_E)]^{\frac{-D+E+1}{2}}}{\pi^{\frac{1}{2}(N_V-L)} \det(C) \prod_{j=1}^L \Gamma\left(\frac{D-E+1-j}{2}\right)} \int_{\mathcal{C}} d^{N_V} z [P(z)]^{\frac{D-L-E-1}{2}} \prod_{k=1}^{N_V} \frac{1}{z_k^{\nu_k}}, \quad (2.44)$$

where $P(z)$ is the Baikov polynomial

$$P(z_1, \dots, z_{N_V}) = G(l_1, \dots, l_L, p_1, \dots, p_E). \quad (2.45)$$

The domain of integration \mathcal{C} is defined by

$$\mathcal{C} = \mathcal{C}_1 \cap \mathcal{C}_2 \cap \dots \cap \mathcal{C}_L, \quad (2.46)$$

with

$$\mathcal{C}_j = \left\{ \frac{G(l_j, l_{j+1}, \dots, l_L, p_1, \dots, p_E)}{G(l_{j+1}, \dots, l_L, p_1, \dots, p_E)} \leq 0 \right\}. \quad (2.47)$$

The Baikov representation is particularly useful for computing residues when one or several propagators go on-shell, i.e. *cuts* of Feynman integrals. Moreover, it can be used to find the canonical bases of Feynman integrals and their symbol alphabets [38, 70].

Example: One-Loop Hexagon

The first example we are going to consider is the one-loop hexagon integral family defined in equation (2.16). Since this is a one-loop example, the conditions for the Baikov representation to exist are immediately satisfied. Therefore, we perform the change of variables to the Baikov variables

$$z_i = \left(l + \sum_{j=1}^{i-1} p_j \right)^2, \quad 1 \leq i \leq 6. \quad (2.48)$$

The Baikov polynomial is defined as

$$P(z_1, z_2, z_3, z_4, z_5, z_6) = G(l, p_1, p_2, p_3, p_4, p_5), \quad (2.49)$$

and we express it in terms of the Baikov variables using the following relations:

$$\begin{aligned} l^2 &= z_1 \\ l \cdot p_1 &= \frac{1}{2}(z_2 - z_1) \\ l \cdot p_2 &= \frac{1}{2}(z_3 - z_2 - s_{12}) \\ l \cdot p_3 &= \frac{1}{2}(z_4 - z_3 + s_{12} - s_{123}) \end{aligned}$$

$$\begin{aligned}
l \cdot p_4 &= \frac{1}{2}(z_5 - z_4 - s_{56} + s_{123}) \\
l \cdot p_5 &= \frac{1}{2}(z_6 - z_5 + s_{56}).
\end{aligned} \tag{2.50}$$

From these relations, we can also read the elements of the C matrix and take its determinant. Therefore, the one-loop hexagon can be written in the Baikov representation as

$$I_{Hex} = e^{\epsilon\gamma_E} \frac{[G(p_1, \dots, p_5)]^{\frac{-D+6}{2}}}{32\pi^{\frac{5}{2}}\Gamma\left(\frac{D-5}{2}\right)} \int_{\mathcal{C}} d^6z [P(z_1, \dots, z_6)]^{\frac{D-7}{2}} \prod_{k=1}^6 \frac{1}{z_k^{\nu_k}}. \tag{2.51}$$

Example: Two-Loop Double-Pentagon

The second example we are considering is the two-loop six-point double-pentagon integral shown in Figure 2.4.

Since this is a two-loop example, the condition for the Baikov representation to exist is not immediately satisfied. The double-pentagon integral has nine inverse propagators:

$$\begin{aligned}
D_1 &= l_1^2, & D_2 &= (l_1 - p_1)^2, & D_3 &= (l_1 - p_1 - p_2)^2, & D_4 &= (l_1 - p_1 - p_2 - p_3)^2, \\
D_7 &= l_2^2, & D_{10} &= (l_2 + p_1 + p_2 + p_3)^2, & D_{11} &= (l_2 + p_1 + p_2 + p_3 + p_4)^2, \\
D_{12} &= (l_2 + p_1 + p_2 + p_3 + p_4 + p_5)^2, & D_{13} &= (l_1 + l_2)^2,
\end{aligned} \tag{2.52}$$

but the number of independent scalar products involving loop momenta for this integral is 13. Therefore, we need to supplement these inverse propagators with four irreducible scalar products.

In general, we need to add any four propagators so that we can express all of the irreducible scalar products in terms of inverse propagators. One way of discerning which propagators to include is to consider the *dual graph* of the original Feynman graph. We use the fact that each momentum can be represented as a difference between two points. In particular, we relate the momenta with points x_i in the dual space

$$\begin{aligned}
p_i &= x_i - x_{i-1}, \quad i = 1, \dots, n_{\text{ext}}, \quad \text{with} \quad p_1 = x_1 - x_{n_{\text{ext}}}, \\
l_j &= x_j - x_1, \quad j = 1, \dots, L.
\end{aligned} \tag{2.53}$$

We call the points x_i *dual coordinates* [72]. It is clear that dual coordinates manifestly satisfy momentum conservation and, therefore, are useful for defining integrals of planar Feynman graphs.

Rewriting the double-pentagon inverse propagators in terms of the dual coordinates

$$\begin{aligned}
D_1 &= x_{1a}^2, & D_2 &= x_{2a}^2, & D_3 &= x_{3a}^2, & D_4 &= x_{4a}^2, \\
D_7 &= x_{1b}^2, & D_{10} &= x_{4b}^2, & D_{11} &= x_{5b}^2, & D_{12} &= x'_{6b} \\
D_{13} &= x_{ab}^2,
\end{aligned} \tag{2.54}$$

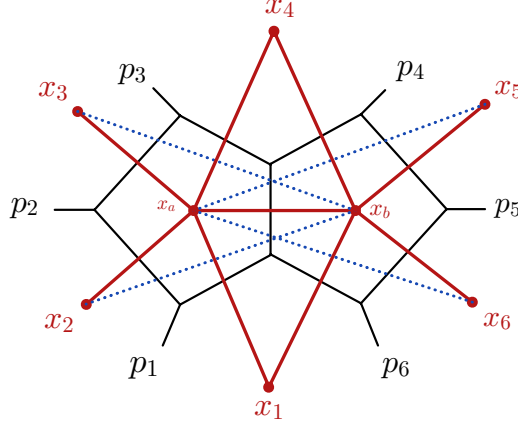


Figure 2.4: Double-pentagon graph and corresponding dual graph. Black lines represent the double-pentagon graph, red lines represent its dual graph and the blue dashed lines represent the irreducible scalar products.

it is easy to see that the missing propagators are $\{x_{5a}^2, x_{6a}^2, x_{2b}^2, x_{3b}^2\}$. Here we identify $l_1 = x_a - x_1$ ($l_2 = x_b - x_1$) and use the short-hand notation $x_{ij} = x_i - x_j$. The missing propagators are easily identified from a dual graph shown in Figure 2.4. The thick red lines represent the inverse propagators that we started with, and the blue dashed lines represent the additional propagators. Now, we can translate them back to loop momentum representation

$$\begin{aligned} D_5 = x_{5a}^2 &= (l_1 - p_1 - p_2 - p_3 - p_4)^2, & D_6 = x_{6a}^2 &= (l_1 - p_1 - p_2 - p_3 - p_4 - p_5)^2 \\ D_8 = x_{2b}^2 &= (l_2 + p_1)^2, & D_9 = x_{3b}^2 &= (l_2 + p_1 + p_2)^2, \end{aligned} \quad (2.55)$$

and use them to express the irreducible scalar products.

With that, we have all of the necessary ingredients to obtain the Baikov representation. As before, we make a change of variables from scalar products involving loop momenta to Baikov variables z_i . The Baikov polynomial in the two-loop case is

$$P(z_1, \dots, z_{13}) = G(l_1, l_2, p_1, p_2, p_3, p_4, p_5), \quad (2.56)$$

while the Gram determinant in the coefficient of the integral remains the same as in the one-loop case. Finally, we arrive at the following representation

$$I_{dp} = e^{2\epsilon\gamma_E} \frac{[G(p_1, \dots, p_5)]^{\frac{-D+6}{2}}}{2048\pi^{\frac{11}{2}} \Gamma\left(\frac{D-5}{2}\right) \Gamma\left(\frac{D-6}{2}\right)} \int_{\mathcal{C}} d^{13}z [P(z_1, \dots, z_{13})]^{\frac{D-8}{2}} \prod_{k=1}^{13} \frac{1}{z_k^{\nu_k}}. \quad (2.57)$$

Starting from two-loop integrals, we can follow another approach where the guiding principle is to keep the number of integration variables as low as possible. In this approach,

we utilize the known results from one loop and perform the change of variables on one of the loops first, while treating the remaining loop momenta as external. This is known as the *loop-by-loop approach* (LbL) [73].

We can start from the right loop in the double-pentagon example. We are considering the one-loop pentagon with p_4, p_5, p_6 and l_1 as independent external momenta, while the loop momentum is l_2 . The Baikov polynomial and the Gram determinant that involve just the external momenta that appear in the Baikov representation (2.44) are

$$P_R = G(l_2, l_1, p_4, p_5, p_6), \quad G(l_1, p_4, p_5, p_6). \quad (2.58)$$

We are left with the left loop which is a pentagon integral with independent external momenta p_1, p_2, p_3, p_6 , and loop momentum l_1 . Hence, the Gram determinants we have to consider are

$$P_L = G(l_1, p_1, p_2, p_3, p_6), \quad G(p_1, p_2, p_3, p_6). \quad (2.59)$$

Since we are considering two pentagons with five Baikov variables each, we end up with a loop-by-loop representation which depends on ten variables

$$I_{dp}^{(LbL)} \sim \int d^{10}z P_R^{\frac{D-6}{2}} [G(l_1, p_4, p_5, p_6)]^{-\frac{D+5}{2}} P_L^{\frac{D-6}{2}} [G(p_1, p_2, p_3, p_6)]^{-\frac{D+5}{2}} \prod_{k=1}^{10} \frac{1}{z_k^{\nu_k}}. \quad (2.60)$$

The advantage of using the loop-by-loop approach is that there are fewer variables in the problem and that the integrand factorizes into several simpler pieces. Both of these help in the analysis of the integral and in the computations of cuts and leading singularities. On the other hand, unlike the standard Baikov representation, the loop-by-loop representation is not unique, since it depends on the loop we start with and the momentum routing we choose.

Chapter 3

Singularity Structure of Feynman Integrals

There are two aspects to the singularity structure of Feynman integrals. First, there may be singularities that occur for any value of the kinematic variables. These are the ultraviolet or infrared divergences of the Feynman integrals briefly described in Chapter 2. Secondly, there may be singularities, which only occur for specific values of the kinematic variables. These are called *Landau singularities* or *kinematic singularities*, and are the central objects of study in this chapter.

Knowing the locations of Landau singularities for a given Feynman integral is crucial for modern high-precision computations. It allows us to make the computations of canonical differential equations satisfied by a family of Feynman integrals more efficient; see Section 4.3 and Chapter 5. In examples discussed in this thesis and more generally in polylogarithmic cases, Landau singularities correspond to zeros and singularities of symbol letters [74, 75]. The symbol encodes many important features of the analytic structure of Feynman integrals. Therefore, knowing the symbol letters in addition to the behaviour in certain physical limits opens the door to potential bootstrap applications.

For example, in planar $\mathcal{N} = 4$ super Yang–Mills (sYM), the function space of planar six-particle scattering is, in fact, conjectured to be known to all loop orders [76]. This conjecture, together with other physical insights, such as behaviour in limits and analytic properties, has been used to bootstrap six-particle amplitudes to staggering loop orders; see Ref. [77, 78].

Determining the positions of kinematic singularities has been a topic of interest for a long time, tracing back to the seminal contributions of Bjorken, Landau, and Nakanishi [27–29]. They formulated a set of polynomial conditions, now referred to as the Landau equations, to identify the singularities. These equations are stated in Section 3.1 where we also give an overview of the literature. In Section 3.2, we review a modern approach to Landau analysis which is best suited for the problems considered in this thesis. In Section 3.3, we discuss a connection between singularities of Feynman integrals and symbol letters. Lastly, in Section 3.4, we describe an efficient algorithm to complete the alphabets with algebraic letters. This algorithm provides key results needed for finding differential

equations satisfied by one-loop and two-loop six-point Feynman integrals in Section 4.3 and Chapter 5, respectively.

The one-loop hexagon alphabet presented throughout this chapter is published in Ref. [79].

3.1 Landau Equations

The main question we want to answer is: When can a Feynman integral develop kinematic singularities? In general, Feynman integrals are too difficult for their analytic properties to be studied after explicit integration. Therefore, we want a way to answer this question that avoids explicit integration.

Identifying the locations of kinematic singularities has been a subject of significant interest for many years, dating back to the foundational work of Bjorken, Landau, and Nakanishi [27–29]. Based on a generalization of a lemma that describes singularities of a function defined by an integral [80–82], these authors derived a system of equations which, in principle, determine locations of singularities of Feynman integrals.

Starting with the loop momentum representation of the Feynman integrals (2.5) and using the Feynman trick (2.24), we arrive to the following Feynman parametrization

$$I = \int \left(\prod_{r=1}^L d^D l_r \right) \left(\prod_{j=1}^{n_{\text{int}}} d\alpha_j \right) \frac{\delta \left(1 - \sum_{j=1}^{n_{\text{int}}} \alpha_j \right)}{\left(\sum_{j=1}^{n_{\text{int}}} \alpha_j (q_j^2 - m_j^2) \right)^{n_{\text{int}}}}, \quad (3.1)$$

where we have omitted all kinematic independent factors since they have no influence on the singularities.

The necessary condition for the integrand of (3.1) to develop singularities is

$$\alpha_j (q_j^2 - m_j^2) = 0 \quad \forall j \in \{1, \dots, n_{\text{int}}\}. \quad (3.2)$$

This condition will be satisfied either when the propagator goes on-shell $q_j^2 = m_j^2$ or when the corresponding Feynman parameter α_j is zero. However, these conditions are not sufficient to guarantee that the Feynman integral will be singular. If these conditions are satisfied at a generic point in the integration region, the integration contour can be deformed so that it avoids the corresponding singularity.

Actual singularities occur if we cannot deform the contour of integration. This happens whenever a singularity lies at an end-point of the integration contour or if two or more singularities approach the contour of integration from opposite sides and coalesce, i.e. they pinch the contour of integration. The pinching occurs for

$$\frac{\partial}{\partial l_i} \sum_{j=1}^{n_{\text{int}}} \alpha_j (q_j^2 - m_j^2) = 0, \quad \forall i \in \{1, \dots, L\}. \quad (3.3)$$

Equations (3.2) and (3.3) together make up the *Landau equations* and serve as a necessary condition for a Feynman integral to develop singularities. However, if a Feynman integral has some nontrivial numerator, some of these singularities might cancel. Moreover, the numerator cannot introduce new singularities.

Following a standard textbook [30], we classify the encountered singularities in the following way. If none of the Feynman parameters is set to zero and all of the propagators are set on-shell, we call those singularities *leading*. In contrast, if some Feynman parameters are zero and the remaining propagators are on-shell, we call those *subleading* singularities. Setting $\alpha_i = 0$ corresponds to pinching the corresponding propagator. Additionally, we can encounter singularities when one or more loop momenta diverge. We call those singularities *second-type* and *mixed* singularities, respectively.

Landau equations and corresponding Landau singularities have received a lot of attention both from physics and mathematics perspectives. Following the original papers [27–29], Pham et al. formally characterized Landau singularities in momentum space [31, 32]; for reviews, see, e.g. [83]. They introduced the notion of a *Landau variety* referring to the projection of the critical set of propagator singularities onto the external kinematic space. Initially, it could only be computed for sufficiently generic integrals, such as those related to one-loop Feynman diagrams with generic masses and no UV/IR divergences. Moreover, Picard–Lefschetz theory was used to examine the local behavior of finite Feynman integrals around real singularities in configurations with generic masses, see [84, 85] for examples. To study singularities of less generic Feynman integrals, i.e. integrals with UV/IR divergences and/or with massless propagators, more careful analysis using blow-ups is needed [86, 87]. Brown [33] and Panzer [22] revisited Landau varieties from the perspective of linear reducibility and algorithmic evaluation of Feynman integrals using multiple polylogarithms. More recently, the Landau variety was studied from the perspective of Whitney stratifications in [36].

Various authors investigated the space–time interpretation of Landau singularities and their relationship to causality and locality in a non-perturbative manner, emphasizing the significance of singularities where all $\alpha_j \geq 0$, for a review see, for example [88]. Singularities where all $\alpha_j \geq 0$, correspond to singularities in the physical scattering region, and there are multiple ways of computing them known in the literature; see [30]. However, for any Feynman integral beyond the one-loop level, these methods become infeasible and difficult to apply systematically.

Using the Lee–Pomeransky representation (2.34), Feynman integrals can be treated as generalized Euler integrals. In that context, methods from the Gelfand–Kapranov–Zelevinsky (GKZ) systems [89] can be used for Feynman integrals; see [90] for a recent overview. In particular, principal A-determinants can be applied to the Landau analysis [91, 92]. In Ref. [93], authors generalized A-discriminants to Landau discriminants.

The majority of results mentioned so far are relevant for Feynman integrals with generic mass configurations. In general, if we take the massless limit on the level of results, we are going to obtain only a subset of singularities [34, 35]. Therefore, methods directly applicable to massless theories were developed. For instance, leading Landau singularities in massless theories can be studied in momentum twistor space [94–96].

As you can see from the extensive, but not complete, literature listed here, Landau equations and singularities are a wide and still active area of research. This is due to the fact that several problems are still not fully resolved. The biggest problem is the fact that we do not know how to systematically account for all singularities in massless cases and when UV/IR singularities are present. Another issue is developing practical tools for systematic Landau analysis that are useful for state-of-the-art applications. A major step in the right direction was made in [34, 35] where both of these issues were addressed.

3.2 Solving Landau Equations

The previous section introduced the Landau equations (3.2) and (3.3), and provided numerous references regarding Landau analysis and its consequences. However, we have yet to discuss how to solve these equations in practice. Consequently, in this section we will review the method presented in [34, 35] which at the time of writing this thesis is the most complete and systematic approach.

In Section 2.3, we introduced the Lee–Pomeransky representation of Feynman integrals (2.34). We repeat that expression for the convenience of the reader

$$I_{LP} \propto \int_{R_+^m} d^m \alpha \mathcal{G}^{-\frac{D}{2}} \prod_{i=1}^m \alpha_i^{\nu_i-1}, \quad (3.4)$$

where we have omitted all kinematic independent prefactors since they do not have influence on the locations of singularities. Moreover,

$$m = \frac{L(L+1)}{2} + L \min(n_{\text{int}} - 1, D_{\text{ext}}) \quad (3.5)$$

is the number of propagators together with the irreducible scalar products. This number corresponds to the number of scalar products involving loop momenta N_V , introduced in Section 2.4, whenever external momenta are defined in a sufficiently high number of space–time dimensions D_{ext} so that all $n_{\text{ext}} - 1$ momenta are independent. The graph polynomial \mathcal{G} is again given by the sum of the two Symanzik polynomials

$$\mathcal{G}(\alpha; \vec{v}) = \mathcal{U}(\alpha) + \mathcal{F}(\alpha; \vec{v}). \quad (3.6)$$

In this setting, the simplest Landau singularity is obtained by solving the critical point equations away from the boundaries

$$\mathcal{G} = \frac{\partial}{\partial \alpha} \mathcal{G} = 0, \quad \alpha \in (\mathbb{C}^*)^m, \quad (3.7)$$

where we used the following notation $\frac{\partial}{\partial \alpha} = \left(\frac{\partial}{\partial \alpha_1}, \dots, \frac{\partial}{\partial \alpha_m} \right)$ and $\mathbb{C}^* = \mathbb{C} \setminus \{0\}$. Solving this system of equations will give us singularities at infinity or the so-called leading second–type singularities.

Note that instead of studying only the leading singularities where all $\alpha_i \neq 0$ and subleading singularities where some $\alpha_i = 0$, more complicated scaling patterns are allowed. In general, a singularity can originate from scalings of the form

$$\alpha_i \rightarrow \varepsilon^{w_i} \alpha_i \quad \text{with} \quad \varepsilon \rightarrow 0. \quad (3.8)$$

The different regions where singularities can occur are given by the set of rational exponents (w_1, \dots, w_m) called *weight*. This allows us to study different configurations obtained by expanding and shrinking edges at specific rates. Moreover, $\alpha_i \in \mathbb{C}$ goes beyond the standard textbook approach, where usually only $\alpha_i \geq 0$ solutions are considered. Therefore, we can detect singularities on any sheet in contrast to the ones just on the physical sheet of the kinematic space.

The majority of remaining Landau singularities are on the boundaries. To classify them, we use the notion of the Newton polytope

$$\mathbf{P} = \text{Newt}(\mathcal{G}), \quad (3.9)$$

which is defined as the convex hull of the columns of an integer matrix A defined by the exponents of Feynman parameters α_i in the graph polynomial \mathcal{G} . For $\mathcal{G} = \sum_{i=1}^s z_i \alpha^{m_s}$, where $\alpha^{m_i} = \alpha_1^{m_{i1}} \dots \alpha_n^{m_{in}}$, the A matrix is

$$A = \begin{pmatrix} m_1 & m_2 & \dots & m_s \\ 1 & 1 & \dots & 1 \end{pmatrix} \in \mathbb{Z}^{(n+1) \times s}. \quad (3.10)$$

Example: If we take the graph polynomial \mathcal{G} of the one-loop hexagon

$$\begin{aligned} \mathcal{G} = & \alpha_1 + \alpha_2 + \alpha_3 + \alpha_4 + \alpha_5 + \alpha_6 + s_{12}\alpha_2\alpha_6 + s_{23}\alpha_1\alpha_3 + s_{34}\alpha_2\alpha_4 \\ & + s_{45}\alpha_3\alpha_5 + s_{56}\alpha_4\alpha_6 + s_{61}\alpha_1\alpha_5 + s_{123}\alpha_3\alpha_6 + s_{234}\alpha_1\alpha_4 + s_{345}\alpha_2\alpha_5, \end{aligned} \quad (3.11)$$

the A matrix is

$$A = \begin{pmatrix} 1 & 0 & 0 & 0 & 0 & 0 & 0 & 1 & 0 & 0 & 0 & 1 & 0 & 1 & 0 \\ 0 & 1 & 0 & 0 & 0 & 0 & 1 & 0 & 1 & 0 & 0 & 0 & 0 & 0 & 1 \\ 0 & 0 & 1 & 0 & 0 & 0 & 0 & 1 & 0 & 1 & 0 & 0 & 1 & 0 & 0 \\ 0 & 0 & 0 & 1 & 0 & 0 & 0 & 0 & 1 & 0 & 1 & 0 & 0 & 1 & 0 \\ 0 & 0 & 0 & 0 & 1 & 0 & 0 & 0 & 0 & 1 & 0 & 1 & 0 & 0 & 1 \\ 0 & 0 & 0 & 0 & 0 & 1 & 1 & 0 & 0 & 0 & 1 & 0 & 1 & 0 & 0 \\ 1 & 1 & 1 & 1 & 1 & 1 & 1 & 1 & 1 & 1 & 1 & 1 & 1 & 1 & 1 \end{pmatrix}. \quad (3.12)$$

The faces of the Newton polytope \mathbf{P} are parametrized by weights $w = (w_1, \dots, w_m)$ that correspond to the scalings (3.8). For each face f of the Newton polytope \mathbf{P} we define the initial form \mathcal{G}_f which contains the leading terms in ε of \mathcal{G} . Then the Landau equations on the boundaries are defined as follows

$$\mathcal{G}_f = \frac{\partial}{\partial \alpha} \mathcal{G}_f = 0, \quad \alpha \in (\mathbb{C}^*)^m. \quad (3.13)$$

Different faces correspond to different types of singularities. In the special case where f is the entire polytope, i.e., for $w = (0, \dots, 0)$, we recover the system of equations in (3.7). The leading Landau singularity corresponds to the facet with $w = (-1, \dots, -1)$, while the subleading singularities are obtained by replacing -1 with 1 or 0 .

The incidence variety Y_f is defined by solutions to the system of equations (3.13)

$$Y_f = \left\{ (\alpha, v) \in (\mathbb{C}^*)^m \times \mathcal{E} : \mathcal{G}_f = \frac{\partial}{\partial \alpha} \mathcal{G}_f = 0 \right\}, \quad (3.14)$$

where \mathcal{E} denotes the kinematic space and v_i are kinematic variables. In general, the incidence variety Y_f can have many irreducible components

$$Y_f = \bigcup_i Y_f^{(i)}. \quad (3.15)$$

In the end, the location of the singularities depends only on the kinematic variables v . Therefore, we need to remove the dependence on the Feynman parameters α . This is done by projecting all components of the incidence variety onto the kinematic space \mathcal{E} . After projection, the components that give rise to singularities for any value $v \in \mathcal{E}$ are ignored since they correspond to UV/IR divergences. The result of all projections is called the *principal Landau determinant* (PLD)

$$\text{PLD}(\mathcal{E}) = \bigcup_{\text{faces } f} \bigcup_{\text{projections } i} \pi \left(Y_f^{(i)} \right) \subset \mathcal{E}, \quad (3.16)$$

where π is the projection operator.

The PLD detects kinematic configurations for which the surface $\{\mathcal{G}(v) = 0\}$ becomes more singular than for generic $v \in \mathcal{E}$. This is quantified by computing the signed *Euler characteristic*

$$\chi_v = |\chi((\mathbb{C}^*)^m \setminus \{\mathcal{G}(v) = 0\})|, \quad (3.17)$$

and checking whether it drops below a generic value χ^* . The Euler characteristic also computes the number of master integrals for a family of Feynman integrals [67, 97, 98]. Master integrals satisfy a system of first-order differential equations; see Section 4.3. Hence, the PLD equivalently detects kinematic configurations for which the rank of the system of differential equations drops. This is demonstrated in Section 4.6.2 for the one-loop hexagon evaluated on the singularity corresponding to the system (3.7).

The methods described in this section are implemented in an open-source `Julia` package `PLD.jl` [34, 35].

Note that there are known examples where the PLD fails to detect all singular components. The authors of Ref. [99] recently proposed an approach based on unitarity and Baikov representation that claims to find those missing components and, therefore, might be used as a complementary approach. The details of this approach go beyond the scope of this thesis.

Example: One–Loop Hexagon

By using PLD.jl for the one–loop hexagon integral (2.17) we find 49 distinct kinematic singularities. The first 40 components of the PLD are:

$$W_1 = s_{12}, \quad W_{i+1} = T^i W_1, \quad i = 1, \dots, 5, \quad (3.18)$$

$$W_7 = s_{123}, \quad W_{i+7} = T^i W_7, \quad i = 1, \dots, 2, \quad (3.19)$$

$$W_{10} = s_{12} - s_{123}, \quad W_{i+10} = T^i W_{10}, \quad i = 1, \dots, 5, \quad (3.20)$$

$$W_{16} = s_{12} - s_{345}, \quad W_{i+16} = T^i W_{16}, \quad i = 1, \dots, 5, \quad (3.21)$$

$$W_{22} = -s_{12} - s_{23} + s_{123}, \quad W_{i+22} = T^i W_{22}, \quad i = 1, \dots, 5, \quad (3.22)$$

$$W_{28} = s_{12} + s_{45} - s_{123} - s_{345}, \quad W_{i+28} = T^i W_{28}, \quad i = 1, \dots, 2, \quad (3.23)$$

$$W_{31} = -s_{12}s_{45} + s_{123}s_{345}, \quad W_{i+31} = T^i W_{31}, \quad i = 1, \dots, 2, \quad (3.24)$$

$$W_{34} = s_{12}(-s_{34} + s_{345}) + s_{345}(s_{34} - s_{56} - s_{345}), \quad W_{i+34} = T^i W_{34}, \quad i = 1, \dots, 5, \quad (3.25)$$

$$W_{40} = G(p_1, p_2, p_3, p_4, p_5). \quad (3.26)$$

Here we employ the cyclic permutation operator T that shifts the external legs by one site,

$$T(p_i) = p_{i+1}, \quad i = 1, \dots, 6 \quad (3.27)$$

and it acts on the variables according to

$$T\vec{v} = \{s_{23}, s_{34}, s_{45}, s_{56}, s_{61}, s_{12}, s_{234}, s_{345}, s_{123}\}. \quad (3.28)$$

These components correspond to the polynomial part of the one–loop hexagon alphabet presented in Ref. [79]. Note that in Ref. [79], W_{40} was defined as

$$\frac{-\Delta_6}{G(p_1, p_2, p_3, p_4, p_5)}, \quad (3.29)$$

since these two factors always appear together in the differential equation. Here, we choose to treat them as separate components, as we treat them differently in Section 3.4.

Next, we have nine components that appear as square root leading singularities of the basis integrals. In Section 4.3, we compute them through the leading singularity analysis in the Baikov representation. From the leading singularity analysis, we know that these singularities are square root singularities. In contrast, from the Landau analysis, we obtain just the arguments of square roots. Therefore, we define the following nine components as follows:

$$W_{41} = \sqrt{\Delta_3(s_{12}, s_{34}, s_{56})}, \quad W_{42} = TW_{41}, \quad (3.30)$$

$$W_{43} = \sqrt{\Delta_5(s_{56}, s_{61}, s_{12}, s_{234}, s_{345}, s_{34})}, \quad W_{i+43} = T^i W_{43}, \quad i = 1, \dots, 5, \quad (3.31)$$

$$W_{49} = \sqrt{\Delta_6}, \quad (3.32)$$

where Δ_i are defined as

$$\begin{aligned}\Delta_3(s_{12}, s_{34}, s_{56}) &= \lambda(s_{12}, s_{34}, s_{56}), \\ \Delta_5(s_{23}, s_{34}, s_{45}, s_{234}, s_{345}, s_{61}) &= (\omega_5(s_{23}, s_{34}, s_{45}, s_{234}, s_{345}) - s_{34}s_{61})^2 \\ &\quad - 4s_{23}s_{34}s_{45}(s_{34} + s_{61} - s_{234} - s_{345}), \\ \Delta_6 &= ((1 + T + T^2)(s_{12}s_{234}s_{45}) - s_{123}s_{234}s_{345})^2 - 4s_{12}s_{23}s_{34}s_{45}s_{56}s_{61},\end{aligned}\tag{3.33}$$

and

$$\begin{aligned}\lambda(s_{12}, s_{34}, s_{56}) &= s_{12}^2 + s_{34}^2 + s_{56}^2 - 2s_{12}s_{34} - 2s_{12}s_{56} - 2s_{34}s_{56}, \\ \omega_5(s_{23}, s_{34}, s_{45}, s_{234}, s_{345}) &= s_{234}s_{345} + s_{23}(s_{34} - s_{234}) + s_{45}(s_{34} - s_{234}).\end{aligned}\tag{3.34}$$

Interestingly, Δ_5 takes a strikingly simple form in terms of the Källén function λ , e.g.

$$\Delta_5(s_{12}, s_{23}, s_{34}, s_{123}, s_{234}, s_{56}) = \lambda(s_{12}s_{34}, s_{13}s_{24}, s_{23}s_{14}).\tag{3.35}$$

In the context of the canonical differential equation (4.38), these components of the Landau variety appear as arguments of $d \log$ forms which we call letters. In particular, the letters listed here are so-called even letters, and they form a part of the full alphabet. We call them even because they are invariant under the action of the Galois group $\sqrt{Q} \rightarrow -\sqrt{Q}$. To complete the alphabet, we also need to include algebraic letters of the form

$$\frac{P - \sqrt{Q}}{P + \sqrt{Q}},\tag{3.36}$$

where P and Q are polynomials in terms of kinematic variables. We call these letters odd, since the $d \log$ changes sign under the action of the Galois group. We postpone the discussion of the algebraic letters to Section 3.4.

3.3 Symbolology of Feynman Integrals

In the simplest cases, the Feynman integrals and the integrated amplitudes are polylogarithmic functions of kinematical variables. The branch cut structure of the polylogarithmic functions is encoded in the symbol [74, 100, 101]. In Ref. [75], it was pointed out that there should be a close connection between the symbol letters and solutions to the Landau equations. In particular, the symbol entries appearing in any amplitude and, in fact, even in individual Feynman integrals should be such that their zeros specify values of external momenta where solutions of the Landau equations exist.

Understanding the symbol letters enables us to compute Feynman integrals in an efficient manner and opens up the possibility to bootstrap amplitudes without computing the Feynman integrals first. There are various approaches to predict the symbol alphabets. In this section, we review the main methods and results, and in the next section, we give our proposition on how to complete the alphabet from the known Landau singularities.

Maximally supersymmetric Yang–Mills theory is often considered to be a perfect toy model due to its simplicity and numerous symmetries [44]. From that perspective, it is no surprise that the connection between the symbol alphabets and Landau singularities is best understood in this setting. Using projective geometry, the authors of Ref. [94] made a connection between the Landau singularities of Feynman integrals appearing in the one- and two-loop maximally-helicity-violating (MHV) amplitudes and the symbols of the amplitudes themselves. Moreover, a series of papers [95, 102, 103] proposed a geometric algorithm for determining a complete set of branch points from the perspective of the amplituhedron [104, 105]. Later, using an analogy between electrical circuits and Feynman integrals, an all-loop result was obtained for a leading Landau singularity of n -particle amplitudes in $\mathcal{N} = 4$ sYM [96]. Using a connection between the letters and the cluster variables [76] of the Grassmannian $\text{Gr}(4, n)$, the symbol alphabets can also be calculated from plabic graphs [106] and tensor diagrams [107].

Based on various results from $\mathcal{N} = 4$ sYM and from diagrammatic coaction [108–112], a systematic study of the singularity structure of one-loop integrals was initiated in [113]. This resulted in a full understanding of the one-loop alphabets and several different practical approaches to compute them. For example, alphabet letters can be computed from the Baikov representation [37, 114] or alternatively from the principal A -determinants of GKZ systems [92].

Going beyond one-loop, we are lacking a full systematic understanding of the relevant alphabets. However, certain results are available in the literature. The so-called Schubert problems were first introduced in $\mathcal{N} = 4$ sYM to find symbol letters from intersections of lines in momentum twistor space [39]. Later, these results were extended to Feynman integrals without dual conformal symmetry by taking certain limits of dual conformal integrals [41], by considering Schubert problems with points at infinity [40] and in the embedding space formalism [42]. Additionally, in Ref. [115] a method using intersection theory is proposed to compute the letters and corresponding rational coefficients of the entries of the differential equations. Finally, a recent result [38] using the recursive structure of the Baikov representation made a significant step towards automatizing the process of finding alphabet letters.

In the next section, we propose an alternative approach to finding a complete alphabet by using the results of the Landau analysis together with a certain observed factorization property of known alphabets.

3.4 Efficiently Constructing Algebraic (Odd) Letters

In Section 3.2, we found the even part of the alphabet as solutions to the Landau equations. Whenever the even part of the alphabet includes square roots, we need to complete the alphabet with algebraic letters. There are several ways to define these letters, but it is convenient to define them in the following form

$$\frac{P - \sqrt{Q}}{P + \sqrt{Q}}, \quad (3.37)$$

where P and Q are polynomials in the kinematic variables. We could consider the numerator or the denominator as a letter, but this particular form makes the action of the Galois group manifest. The letters of the form (3.37) are odd under the sign flip of the square root, i.e.

$$\mathrm{d} \log \left(\frac{P - \sqrt{Q}}{P + \sqrt{Q}} \right) \xrightarrow{\sqrt{Q} \rightarrow -\sqrt{Q}} -\mathrm{d} \log \left(\frac{P - \sqrt{Q}}{P + \sqrt{Q}} \right). \quad (3.38)$$

This property gives a valuable criterion of classification of the functions appearing in the solution.

Although square roots are easy to recognize from the leading singularity analysis, finding the form of the polynomial P in (3.37) is not trivial. Luckily, we can do this algorithmically [43]. If the letter (3.37) is part of the alphabet, it must be possible to factorize the numerator and the denominator separately in the alphabet. This implies that the product of the denominator and numerator is factorized in terms of even letters,

$$\left(P - \sqrt{Q} \right) \left(P + \sqrt{Q} \right) = c \prod_{W_i} W_i^{e_i}, \quad W_i \in \mathbb{A}_{\text{even}}, \quad (3.39)$$

where $c, e_i \in \mathbb{N}$ and \mathbb{A}_{even} is a subset of the full alphabet \mathbb{A} . This indicates that the letter (3.37) is also a solution to the Landau equations. We can use this factorization to find suitable candidates for the polynomial P in two different ways. In both cases, we assume the knowledge of the even alphabet letters and square roots in our problem. In the first approach, we can construct all the possible products of even letters and find the polynomials P . In the second approach, we can make an ansatz for the polynomial P and check if the factorization (3.39) holds.

Example: Three–Mass Triangle Square Root

Let us look at a simple example where we can easily demonstrate the idea behind the algorithm. In Section 3.2, we list the following components of the Landau variety

$$\{s_{12}, s_{34}, s_{56}, \sqrt{\Delta_3(s_{12}, s_{34}, s_{56})}\}. \quad (3.40)$$

These components correspond to the even letters of the three–mass triangle integral at one loop written in terms of the six–point kinematics.

The goal is to find all different polynomials P such that equation (3.39) is satisfied for $Q = \Delta_3(s_{12}, s_{34}, s_{56})$. Since $\Delta_3(s_{12}, s_{34}, s_{56})$ is a degree two polynomial in Mandelstams, we can make an ansatz for a degree two polynomial P and check whether equation (3.39) holds for some coefficient c and exponents e_i . Alternatively, we can construct different products of even letters with some coefficient c and check if

$$P(\vec{v})^2 = Q(\vec{v}) + c \prod_{W_i} W_i^{e_i} \quad (3.41)$$

is a perfect square. We are going to follow the second approach, which will be discussed in the next section.

Considering all different products of degree two consisting from the first three elements of the list (3.40), we find the following polynomials P_i

$$\begin{aligned} P_1^2 &= \Delta_3(s_{12}, s_{34}, s_{56}) + 4s_{12}s_{34} = (s_{12} + s_{34} - s_{56})^2, \\ P_2^2 &= \Delta_3(s_{12}, s_{34}, s_{56}) + 4s_{34}s_{56} = (-s_{12} + s_{34} + s_{56})^2, \\ P_3^2 &= \Delta_3(s_{12}, s_{34}, s_{56}) + 4s_{12}s_{56} = (s_{12} - s_{34} + s_{56})^2. \end{aligned} \quad (3.42)$$

Thus, we can construct three different odd letters for this square root. Before we add them to the alphabet, we have to make sure that the letters are multiplicatively independent. In this case, we can immediately check that

$$1 = \frac{s_{12} + s_{34} - s_{56} - \sqrt{\Delta_3}}{s_{12} + s_{34} - s_{56} + \sqrt{\Delta_3}} \cdot \frac{-s_{12} + s_{34} + s_{56} - \sqrt{\Delta_3}}{-s_{12} + s_{34} + s_{56} + \sqrt{\Delta_3}} \cdot \frac{s_{12} - s_{34} + s_{56} - \sqrt{\Delta_3}}{s_{12} - s_{34} + s_{56} + \sqrt{\Delta_3}}. \quad (3.43)$$

Hence, there are only two multiplicatively independent solutions. The full three-mass triangle alphabet reads

$$\left\{ s_{12}, s_{34}, s_{56}, \sqrt{\Delta_3}, \frac{s_{12} + s_{34} - s_{56} - \sqrt{\Delta_3}}{s_{12} + s_{34} - s_{56} + \sqrt{\Delta_3}}, \frac{-s_{12} + s_{34} + s_{56} - \sqrt{\Delta_3}}{-s_{12} + s_{34} + s_{56} + \sqrt{\Delta_3}} \right\}, \quad (3.44)$$

where $\sqrt{\Delta_3} = \sqrt{\Delta_3(s_{12}, s_{34}, s_{56})}$.

Although this appears to be an easy problem to solve, complications occur when the same square root is embedded in a larger alphabet. If we now take the full polynomial part of the one-loop hexagon alphabet (3.18) – (3.26), we have 444 different products of letters which result in a degree-two polynomial. After considering all of them, we find three additional solutions

$$\begin{aligned} P_4 &= \Delta_3 + 4 \left(s_{123}^2 - s_{12}s_{123} + s_{34}s_{123} - s_{56}s_{123} + s_{12}s_{56} \right) = (s_{12} - s_{34} + s_{56} - 2s_{123})^2, \\ P_5 &= \Delta_3 + 4 \left(s_{234}^2 + s_{12}s_{234} - s_{34}s_{234} - s_{56}s_{234} + s_{34}s_{56} \right) = (-s_{12} + s_{34} + s_{56} - 2s_{234})^2, \\ P_6 &= \Delta_3 + 4 \left(s_{345}^2 - s_{12}s_{345} - s_{34}s_{345} + s_{56}s_{345} + s_{12}s_{34} \right) = (s_{12} + s_{34} - s_{56} - 2s_{345})^2. \end{aligned} \quad (3.45)$$

All three solutions are multiplicatively independent; therefore, in a larger alphabet, we need to consider all of them.

The question that naturally arises is how to find all possible solutions (or at least sufficiently many) for a given set of square roots and a given set of polynomial letters.

3.4.1 Mathematical Formulation

Let $W_i(\vec{v}) \in \mathbb{Z}[\vec{v}]$ for $i = 1, \dots, m$ be a set of homogeneous polynomials in kinematic variables \vec{v} with integer coefficients. Let $Q(\vec{v}) \in \mathbb{Z}[\vec{v}]$ be another homogeneous polynomial with integer coefficients of degree q . We want to find all sets $\{e_1, \dots, e_m, c, P(\vec{v})\}$ with the property

$$P(\vec{v})^2 = Q(\vec{v}) + c \prod_{W_i} W_i^{e_i}, \quad (3.46)$$

where $e_i \in \mathbb{N}$, $c \in \mathbb{Q}$ and $P(v) \in \mathbb{Z}[\vec{v}]$ is a homogeneous polynomial of degree $q/2$.

In other words, we are looking for all quadratic completions of $Q(\vec{v})$ that factorize over even alphabet letters $\mathbb{A}_{\text{even}} = \{W_1, \dots, W_m\}$.

Several remarks are in order. First of all, it is crucial to work with homogeneous polynomials Q because this allows us to find a complete set of solutions. It is not clear at the moment how to check whether we constructed all allowed solutions in the non-homogeneous case.

For Feynman integrals, this will be the case when we work with unconstrained Mandelstam invariants. For example, for six-point kinematics with D -dimensional external momenta $\{p_1, \dots, p_6\} \in \mathbb{R}^{D_{\text{ext}}}$ we can build nine unconstrained Mandelstam invariants $\vec{v} = \{s_{12}, \dots, s_{345}\}$. In this case, polynomials Q_i are homogeneous polynomials of degrees two, four, six, and ten, where we consider arguments of square roots in equations (3.30) – (3.30) and products of two different arguments. If we restrict ourselves to four-dimensional external states, we will introduce an additional non-trivial constraint on the Mandelstam variables, effectively reducing the number of independent variables from nine to eight. The constraint is a degree-five polynomial in the variables \vec{v} that is quadratic in any of the Mandelstams. It is also invariant under arbitrary permutations of external momenta. This constraint will break the homogeneity of the polynomials Q_i .

The second remark is about the assumed form of the odd letters (3.37). There are cases in the literature, for example [41, 116, 117], where odd letters have an additional polynomial in front of the square root

$$\frac{P_i - P_j \sqrt{Q}}{P_i + P_j \sqrt{Q}}. \quad (3.47)$$

In cases where there are no masses on the propagators, it is possible to rewrite these letters in the form (3.37). However, when the propagators are massive, we could not re-express all the letters such that there is no polynomial in front of a square root. This is not an obstacle, as the same analysis applies to these letters if we assume $P_j = \sqrt{P_j^2}$. Moreover, in the examples considered in this thesis, it is sufficient to consider cases with square-free square roots. Thus, we focus our discussion on the letters of the form (3.37).

The last remark is about the size of the problem at hand. Looking at the square roots listed in the one-loop hexagon example in Section 3.2, the highest degree polynomial we have to consider is of degree ten corresponding to the product $\Delta_{5,i} \Delta_6$. In this example, $m = 40$ where the first 30 letters are of degree one, nine letters are of degree two, and one letter is of degree five. Using this alphabet as an example, we can perform a back-of-the-envelope calculation for the naive approach to the problem. For a polynomial of degree ten, we would need to construct, store, and check roughly 10^8 different products of even letters for a single choice of coefficient c . The other approach where we make an ansatz for the polynomial P and check whether it factorizes is, in fact, even worse. For the same Q of degree ten and if we only allowed coefficients between -2 and 2 in the polynomial P , we would have $\sim 10^{989}$ possible polynomials, which we would need to check. For comparison, the age of the universe is $\sim 10^{17}$ seconds and the lower bound on the mean life of a proton is 10^{36} seconds [118].

The problem becomes even worse when we embed the same square roots into a larger alphabet at two loops. In this example $m = 400$ where the first 90 letters are of degree one, 291 letters are of degree two, 18 letters are of degree three, and one letter is of degree five. Note that this even alphabet is conjectured and it is possibly over-complete, i.e. it is not necessary that all letters appear in the differential equation. A priori, we do not have a criterion which would reduce the size of the alphabet and therefore also the size of the ansatz. Looking at the same polynomial $Q = \Delta_{5,i}\Delta_6$ of degree ten as at one-loop, we would have roughly 10^{15} different possible products. Here we did not take into account different possibilities for the coefficients c .

There is still some hope left! Performing factorization (3.39) for the known alphabet letters, for example, from Ref. [116, 119], we see that only a small subset of even letters appears for a given polynomial Q . Hence, we need to find a criterion to restrict the construction just to this allowed subset of even letters for each polynomial Q_i .

3.4.2 Finding Allowed Even Letters

As described in the previous section, we cannot construct all possible products for a given polynomial Q because the number of these products is too large. Therefore, we need a way to reduce the number of allowed even letters W_i for each polynomial Q .

Assume that we know the factorization of an odd letter, and that a particular letter $W_i(\vec{v})$ appears in the product on the right-hand side of equation (3.39),

$$P(\vec{v})^2 = Q(\vec{v}) + cW_i(\vec{v}) \prod_{j \neq i} W_j^{e_j}. \quad (3.48)$$

Here, we assume $e_i = 1$ without the loss of generality. Then, for every $\vec{v}_0 \in \mathbb{Q}^n$, where n is the number of kinematic variables, such that $W_i(\vec{v}_0) = 0$, it follows

$$\sqrt{Q(\vec{v}_0)} \in \mathbb{Q}. \quad (3.49)$$

This holds for any letter that appears in the factorization. Thus, we can use it to constrain the set of allowed letters for each polynomial Q_i .

Now, we reverse the logic for unknown factorizations and unknown polynomials P . We use property (3.49) to systematically find the list of allowed letters for each polynomial Q_i by going to the variety defined by $W_i = 0$. Even letters W_i are in general polynomials in terms of Mandelstam invariants, and therefore we can find the solutions for $W_i = 0$ for all letters in our even alphabet. Next, we plug in one of the solutions into the square root \sqrt{Q} and check

$$\sqrt{Q(v)}|_{W_j=0} \stackrel{?}{\in} \mathbb{Q}. \quad (3.50)$$

We can simply check whether this is true by inserting integer values for variables \vec{v} . If Q becomes a perfect square on the support of the solution $W_j = 0$, then we add the letter W_j to the list of allowed letters.

Going through solutions for all even letters one by one and checking whether (3.49) holds, results in a drastically reduced list of allowed even letters for a given square root.

Algorithm 1 The algorithm for construction of algebraic letters

Input: Square root $\sqrt{Q_i}$, list of even letters \mathbb{A}_{even} , value of coefficient c

Output: List of algebraic letters involving a square root $\sqrt{Q_i}$

```

1: for all  $W_j \in \mathbb{A}_{even}$  do
2:   if  $\sqrt{Q_i}|_{W_j=0} \in \mathbb{Q}$  then
3:     add  $W_j$  to the allowed letters list  $\mathbb{A}_{allowed}$ 
4:   end if
5: end for
6: construct all products  $R_k = \prod_{W_j \in \mathbb{A}_{allowed}} W_j^{e_j}$  of degree  $q$ 
7: for all  $R_k$  do
8:   if  $\sqrt{Q + cR_k}$  is perfect square then
9:      $P_k = \sqrt{Q + cR_k}$ 
10:  end if
11: end for
12: return list of  $\frac{P_k - \sqrt{Q_i}}{P_k + \sqrt{Q_i}}$ 

```

For instance, in the two-loop hexagon alphabet example, for all Q_i we get less than ten allowed letters, drastically reducing the number of possible products we can construct.

3.4.3 Constructing Algebraic Letters

Once we find allowed even letters for each polynomial Q , we can begin with the construction of odd letters. We do this by constructing all possible products of even letters of a certain degree.

Whenever we are working with dimensionful variables such as Mandelstam variables, the even letters $W_i \in \mathbb{A}_{even}$ are homogeneous polynomials, and therefore their products are also homogeneous polynomials. Moreover, polynomials Q_i are also homogeneous polynomials of a certain degree q . If the degree of the polynomial Q is q , then we construct all possible products of even letters W_i of the same degree q . Of course, W_i are taken from the reduced list of allowed letters. In this way, we take into account all possible powers e_i in equation (3.46). Using equation (3.46), we check whether the constructed product completes the square by evaluating it for integer values of \vec{v} and a specific value of the coefficient c . If the product completes the square, we take the square root of (3.46) and construct the odd letter of the form (3.37). The main steps of the algorithm are presented in the Algorithm 1 and a public implementation of this algorithm is currently in preparation.

The algorithm was tested on several known examples where we reproduced or found equivalent algebraic letters. The examples include the one-mass pentagon alphabet [116], the four-mass double-box alphabet [41] and the one-loop hexagon alphabet which is presented in this section. Moreover, we used it to predict the two-loop hexagon alphabet described in Section 5.5.

Note that we tested the algorithm for integer values of $c \in [-10, 10]$ for the even

alphabet given in Section 3.2. The algorithm produces results only for $c = \pm 4$, which is consistent with various known alphabets.

In addition, the constructed letters might not be independent. Therefore, before proceeding with further usage, we remove dependent letters from the list. Once we know the full allowed alphabet, we can use it for bootstrap approaches and reconstruction of differential equations. The latter application is demonstrated throughout Chapter 4 and Chapter 5.

It should be noted that the produced alphabet could be overcomplete in the sense that not all letters are relevant for the integrals we are considering. For the purpose of fitting the entries of the canonical differential equations, this is not an issue since the coefficients of the additional letters will end up being zero. However, in the bootstrap approaches, it may happen that we do not have enough physical insights to fully determine the solution.

Example: One–Loop Hexagon

Finally, we are in a position to complete the one–loop hexagon alphabet with the odd letters. We use the even letters defined in equations (3.18) – (3.26) and the square roots given in equations (3.30) – (3.32) as well as their products as input for our algorithm.

First, we consider all letters with a single square root. There are 43 independent letters:

$$W_{50} = \frac{-s_{12} + s_{34} - s_{56} - \sqrt{\Delta_3(s_{12}, s_{34}, s_{56})}}{-s_{12} + s_{34} - s_{56} + \sqrt{\Delta_3(s_{12}, s_{34}, s_{56})}}, \quad W_{51} = TW_{50}, \quad (3.51)$$

$$W_{52} = \frac{s_{12} - s_{34} - s_{56} - \sqrt{\Delta_3(s_{12}, s_{34}, s_{56})}}{s_{12} - s_{34} - s_{56} + \sqrt{\Delta_3(s_{12}, s_{34}, s_{56})}}, \quad W_{53} = TW_{52}, \quad (3.52)$$

$$W_{54} = \frac{s_{12} - s_{34} + s_{56} - 2s_{123} - \sqrt{\Delta_3(s_{12}, s_{34}, s_{56})}}{s_{12} - s_{34} + s_{56} - 2s_{123} + \sqrt{\Delta_3(s_{12}, s_{34}, s_{56})}}, \quad (3.53)$$

$$W_{i+54} = T^i W_{54}, \quad i = 1, \dots, 5, \quad (3.54)$$

$$W_{60} = \frac{s_{23}s_{34} - s_{23}s_{56} - s_{34}s_{123} + s_{123}s_{234} + s_{12}(-s_{23} + s_{234}) - \sqrt{\Delta_{5,1}}}{s_{23}s_{34} - s_{23}s_{56} - s_{34}s_{123} + s_{123}s_{234} + s_{12}(-s_{23} + s_{234}) + \sqrt{\Delta_{5,1}}}, \quad (3.55)$$

$$W_{i+60} = T^i W_{60}, \quad i = 1, \dots, 5, \quad (3.56)$$

$$W_{66} = \frac{-s_{23}s_{34} - s_{23}s_{56} + s_{34}s_{123} + s_{123}s_{234} + s_{12}(s_{23} - s_{234}) - \sqrt{\Delta_{5,1}}}{-s_{23}s_{34} - s_{23}s_{56} + s_{34}s_{123} + s_{123}s_{234} + s_{12}(s_{23} - s_{234}) + \sqrt{\Delta_{5,1}}}, \quad (3.57)$$

$$W_{i+66} = T^i W_{66}, \quad i = 1, \dots, 5, \quad (3.58)$$

$$W_{72} = \frac{s_{23}s_{34} + s_{23}s_{56} - s_{34}s_{123} - 2s_{23}s_{234} + s_{123}s_{234} - s_{12}(s_{23} + s_{234}) - \sqrt{\Delta_{5,1}}}{s_{23}s_{34} + s_{23}s_{56} - s_{34}s_{123} - 2s_{23}s_{234} + s_{123}s_{234} - s_{12}(s_{23} + s_{234}) + \sqrt{\Delta_{5,1}}}, \quad (3.59)$$

$$W_{i+72} = T^i W_{72}, \quad i = 1, \dots, 5, \quad (3.60)$$

$$W_{78} = \frac{R_1 - \sqrt{\Delta_{5,1}}}{R_1 + \sqrt{\Delta_{5,1}}}, \quad W_{i+78} = T^i W_{78}, \quad i = 1, \dots, 5, \quad (3.61)$$

$$W_{84} = \frac{R_2 - \sqrt{\Delta_{5,1}}}{R_2 + \sqrt{\Delta_{5,1}}}, \quad W_{i+84} = T^i W_{84}, \quad i = 1, \dots, 5, \quad (3.62)$$

$$W_{90} = \frac{s_{34}s_{61}s_{123} - s_{12}s_{45}s_{234} - s_{23}s_{56}s_{345} + s_{123}s_{234}s_{345} - \sqrt{\Delta_6}}{s_{34}s_{61}s_{123} - s_{12}s_{45}s_{234} - s_{23}s_{56}s_{345} + s_{123}s_{234}s_{345} + \sqrt{\Delta_6}}, \quad (3.63)$$

$$W_{i+90} = T^i W_{90}, \quad i = 1, \dots, 2, \quad (3.64)$$

where R_i are the polynomials

$$\begin{aligned} R_1 &= s_{23}(-s_{34} + s_{56} - 2s_{123}) + s_{12}(s_{23} + 2s_{56} - 2s_{123} - s_{234}) \\ &\quad + s_{123}(s_{34} - 2s_{56} + 2s_{123} + s_{234}), \\ R_2 &= s_{23}(s_{34} + s_{56} - 2s_{234}) + (2s_{56} - s_{123} - 2s_{234})(s_{34} - s_{234}) + s_{12}(-s_{23} + s_{234}). \end{aligned} \quad (3.65)$$

and $\Delta_{5,1}$ is a shorthand notation for the pentagon square root

$$\Delta_{5,1} = \Delta_5(s_{12}, s_{23}, s_{34}, s_{123}, s_{234}, s_{56}). \quad (3.66)$$

Next, we consider all different products of two square roots. There are 27 independent letters with two square roots that can be constructed:

$$W_{93} = \frac{R_3 - \sqrt{\Delta_3(s_{12}, s_{34}, s_{56})\Delta_{5,1}}}{R_3 + \sqrt{\Delta_3(s_{12}, s_{34}, s_{56})\Delta_{5,1}}}, \quad W_{i+93} = T^i W_{93}, \quad i = 1, \dots, 5, \quad (3.67)$$

$$W_{99} = \frac{R_4 - \sqrt{\Delta_{5,1}\Delta_6}}{R_4 + \sqrt{\Delta_{5,1}\Delta_6}}, \quad W_{i+99} = T^i W_{99}, \quad i = 1, \dots, 5, \quad (3.68)$$

$$W_{105} = \frac{R_5 - \sqrt{\Delta_{5,1}\Delta_{5,6}}}{R_5 + \sqrt{\Delta_{5,1}\Delta_{5,6}}}, \quad W_{i+105} = T^i W_{105}, \quad i = 1, \dots, 5, \quad (3.69)$$

$$W_{111} = \frac{R_6 - \sqrt{\Delta_{5,1}\Delta_{5,5}}}{R_6 + \sqrt{\Delta_{5,1}\Delta_{5,5}}}, \quad W_{i+110} = T^i W_{111}, \quad i = 1, \dots, 5, \quad (3.70)$$

$$W_{117} = \frac{R_7 - \sqrt{\Delta_{5,1}\Delta_{5,4}}}{R_7 + \sqrt{\Delta_{5,1}\Delta_{5,4}}}, \quad W_{i+117} = T^i W_{117}, \quad i = 1, 2, \quad (3.71)$$

where

$$\begin{aligned} R_3 &= s_{12}^2(s_{23} - s_{234}) + s_{12}(-2s_{23}(s_{34} + s_{56}) + s_{34}(-2s_{56} + s_{123}) + (s_{34} + s_{56} + s_{123})s_{234}) \\ &\quad + (s_{34} - s_{56})(s_{23}(s_{34} - s_{56}) + s_{123}(-s_{34} + s_{234})), \\ R_4 &= s_{12}^2 s_{45} s_{234} (s_{234} - s_{23}) - [s_{23} (s_{34} - s_{56}) + s_{123} (s_{234} - s_{34})] \times \end{aligned}$$

$$\begin{aligned}
& [s_{34}s_{61}s_{123} + (s_{23}s_{56} - s_{123}s_{234})s_{345}] + s_{12} \left\{ s_{23}^2 s_{56} (2s_{34} - s_{345}) \right. \\
& + s_{123}s_{234} [s_{34}(s_{45} + s_{61}) - s_{234}(s_{45} + s_{345})] + s_{23} [s_{234}(s_{45}s_{56} + (s_{56} + s_{123})s_{345}) \\
& \left. + s_{34}(-2s_{56}s_{61} + s_{45}(s_{234} - 2s_{56}) + s_{123}(s_{61} - 2s_{234})) \right\}. \tag{3.72}
\end{aligned}$$

We do not explicitly write the expressions for degree five polynomials R_5 , R_6 and R_7 since they are lengthy and not needed for expressing the results of this thesis.

Combining all the components of the Landau variety (3.18) – (3.32) and all the odd letters that we constructed (3.51) – (3.71), allows us to conjecture the one-loop hexagon alphabet \mathbb{A}_{1-loop} . Note that this conjectured alphabet might be overcomplete, that is, it is not necessary that all the letters listed throughout this chapter are needed to express the canonical differential equation, as we will see in the following chapter.

Before we move to an application of the constructed alphabet in the next chapter, a remark about the efficiency of the algorithm is in order. In Section 3.4.1, we commented on the size of the problem in a naive approach where we would need to construct and check roughly 10^8 different products of even letters which result in the degree-ten polynomial. If we assumed that it takes roughly 0.1 seconds to check each possibility, it would take us about 116 days to check all possible polynomials and construct the letter W_{99} . However, using a simple `Mathematica` implementation of the Algorithm 1 on a laptop¹, we find the same letter in 0.6 seconds. The improvement in the computation time becomes even more evident for larger alphabets. If we embed the same square root in a much bigger two-loop alphabet, the number of different products would be 10^{15} in the naive approach, and we would need more than a million years to check all of them assuming that we have resources to store them first. However, using the Algorithm 1, we get the result in about 3 seconds.

¹The timings are obtained on a MacBook Air with Apple M2 chip with 16 GB of memory.

Chapter 4

Integration via Differentiation

Feynman rules offer a fully systematic approach to formulating the expression of any scattering amplitude in perturbation theory. As we add more external particles and more loops, the number of Feynman diagrams increases significantly. Although the exploration of alternative techniques is a thrilling field of study [104, 105, 120, 121], in order to make precise theoretical predictions, Feynman integrals are still a crucial ingredient. Therefore, in this chapter, we are going to introduce a method for the analytic computation of Feynman integrals.

At the end of the day, if we only care about getting numerical values for our integrals, Feynman integrals can be numerically evaluated using methods such as sector decomposition [15, 16] or the auxiliary mass flow method [17] (as implemented in AMFlow [18]). However, for integrals with many propagators, these methods become exceedingly computationally expensive and insufficient for phenomenological applications. In phenomenological applications, we want to compute cross sections where the necessary ingredients in the computations are scattering amplitudes. In turn, scattering amplitudes can be written as linear combinations of Feynman integrals. In order to compute a cross section, scattering amplitudes have to be integrated over the phase space. This means evaluating them hundreds of thousands of times. Hence, speed and numerical stability are essential, which is easier to achieve with analytic results.

Additionally, when calculating an integral numerically, one loses the opportunity to learn about the analytic properties of the resulting function, in particular its singularities and branch structure. Therefore, there is strong motivation from both a phenomenological and a theoretical point of view to calculate Feynman integrals as analytically as possible.

We could attempt to obtain analytic results using direct integration, for example, by leveraging the Feynman parametrization, but this method rapidly becomes infeasible. Moreover, we could use algorithms for symbolic integration of Feynman integrals, such as the one implemented in `HyperInt` [22]. However, these methods apply only to a small subset of linearly reducible graphs, which are a subset of Feynman integrals that can be evaluated in terms of polylogarithmic functions.

The method of differential equations [122, 123] has proved to be a very powerful tool towards this goal. Of course, being a multivariate function of Mandelstam variables, the

value of a Feynman integral is completely determined once we know all of its first derivatives and their values at some arbitrary point in phase space. Since the derivatives of Feynman integrals (2.5) with respect to external variables can be expanded in terms of the same family of integrals, there is a completely algorithmic way to express them in terms of basis integrals of the respective family using *integration-by-parts* (IBP) identities, see Section 4.1.

In Section 4.2, we introduce relations between integrals in different numbers of space-time dimensions. These relations prove to be useful for finding basis integrals that satisfy the differential equation in canonical form. In Section 4.3, we demonstrate how to obtain a differential equation satisfied by basis integrals. Furthermore, we argue that, with an appropriate basis, the differential equation simplifies significantly. We call such a basis canonical basis and the corresponding differential equation is said to be in the canonical form. Using the one-loop hexagon family as an example, we demonstrate how to find the canonical basis. In Section 4.4, we establish a formal solution of the canonical differential equation in terms of iterated integrals. Moreover, we introduce a class of special functions needed to express the solution. To fully specify the solution, we fix the boundary values in Section 4.5. Finally, in Section 4.6, we describe the one-loop hexagon function space, the symbol of the hexagon integral, and the $D_{\text{ext}} \rightarrow 4$ limit, where we recover well-known results.

Parts of this chapter, related to finding the canonical basis of the one-loop hexagon integral family and the corresponding function space, were already presented in [79]. Hence, we closely follow that discussion when presenting these results.

4.1 Integration-by-Parts Identities

In Section 2.1, we introduced the concept of integral families. We began with a Feynman integral corresponding to a Feynman diagram and allowed for arbitrary propagator powers. In a sense, by doing this, we made the problem even more challenging since we went from one integral to infinitely many. However, integrals within an integral family are not independent. There are relations between integrals with different propagator powers. *Integration-by-parts identities* (IBPs) provide these relations [124, 125].

A family of Feynman integrals in the loop momentum representation is defined as

$$I_G(\nu_1, \dots, \nu_n) = e^{L\epsilon\gamma_E} \int \prod_{r=1}^L \frac{d^D l_r}{i\pi^{\frac{D}{2}}} \prod_{j=1}^n \frac{1}{(q_j^2 + m_j^2)^{\nu_j}}, \quad (4.1)$$

where $n = n_{\text{int}} + n_{\text{ISP}}$ is the number of propagators together with possible irreducible scalar products that were introduced in section 2.4. We have to include the ISPs to ensure that we can express any scalar product involving loop momentum as inverse propagators and terms independent of loop momentum. Integrals, where all indices corresponding to the internal edges satisfy $\nu_i > 0$, are called *top topology* integrals. In contrast, integrals where some of the propagator powers satisfy $\nu_i \leq 0$ are called *sub-topology* integrals. Moreover, integrals where the same ν_i are greater than zero belong to the same *sector*.

Feynman integrals in the dimensional regularization are translation invariant

$$\int d^D l f(l) = \int d^D l f(l + q). \quad (4.2)$$

We expand the right-hand side for small q and obtain the following expression

$$\begin{aligned} \int d^D l f(l) &= \int d^D l f(l) + q^\mu \int d^D l \frac{\partial}{\partial q^\mu} f(l + q) \Big|_{q=0} + \mathcal{O}(q^2) \\ &= \int d^D l f(l) + q^\mu \int d^D l \frac{\partial}{\partial q^\mu} f(l) + \mathcal{O}(q^2). \end{aligned} \quad (4.3)$$

This implies that total derivatives vanish in dimensional regularization

$$\int \frac{d^D l}{i\pi^{\frac{D}{2}}} \frac{\partial}{\partial l^\mu} [q^\mu f(l)] = 0, \quad (4.4)$$

where vector q can be any linear combination of the loop momentum l and external momenta p and $f(l)$ is the integrand of a Feynman integral.

Working out the derivatives in equation (4.4) and using a bit of algebra, we can show that the action of the differential operator on the rest of the integrand can be written in terms of the integrals within the same integral family but with different propagator powers.

Let us look at our favorite one-loop hexagon example again. The integral family is defined in equation (2.16). For instance, for $q = l$ the equation (4.4) results in

$$\begin{aligned} &\left[(D - 2\nu_1 - \nu_2 - \nu_3 - \nu_4 - \nu_5 - \nu_6) - j_1^- \left(\sum_{i=2}^6 \nu_i j_i^+ \right) + \right. \\ &\left. + s_{12} \nu_4 j_4^+ + s_{123} \nu_3 j_4^+ + s_{56} \nu_5 j_5^+ \right] I^{(D)}(\nu_1, \nu_2, \nu_3, \nu_4, \nu_5, \nu_6) = 0, \end{aligned} \quad (4.5)$$

where we j_i^+ and j_i^- are raising and lowering operators, respectively, defined as

$$j_i^\pm I^{(D)}(\nu_1, \dots, \nu_i, \dots, \nu_n) = I^{(D)}(\nu_1, \dots, \nu_i \pm 1, \dots, \nu_n). \quad (4.6)$$

As we can see, IBPs relate integrals with different propagator powers, and as already anticipated, only a finite number of integrals is independent [126]. Hence, the integrals in an integral family form a finite-dimensional vector space, and the independent integrals form a basis of this space. The basis integrals are commonly referred to as *master integrals*.

Based on equation (4.4), we can construct a sufficient number of IBP relations, forming a system of linear equations. This system of equations allows us to express more complicated integrals in terms of basis integrals, which are usually simpler given an ordering criterion. This procedure is called IBP reduction and its output are master integrals. The basis is of course not unique and it depends on the choice of the ordering criteria. The choice of the basis makes all the difference when we want to analytically evaluate the integrals, as will be demonstrated in Section 4.3.

Solving systems of linear equations is, in principle, straightforward, but can become rather computationally heavy, especially when the dimension of vector space becomes large. Hence, several implementations based on the Laporta algorithm [127] are publicly available on the market for automatic and efficient IBP reductions [128–136].

Although this is a widely used method in state-of-the-art computations, there are several bottlenecks. The first bottleneck arises from the simplification of large rational coefficients in the IBP identities. This is addressed by employing finite field methods, as outlined in Refs. [137, 138]. In essence, the necessary computations are carried out for kinematics with integer values modulo a large prime number. Subsequently, after sufficient data about the resulting rational functions is obtained, they can be analytically reconstructed. This is implemented, for example, in [139]. A further limitation is the number of linear equations that are included in the system which is often bigger than necessary. To reduce the size of the problem, more direct procedures have been developed based on algebraic geometry [140–142], intersection theory [143–146], syzygies [147, 148], and Gröbner basis [149].

4.2 Dimension–Shift Identities

As we will see in the remainder of this chapter and in Chapter 5, considering Feynman integrals in different numbers of space-time dimensions D is often useful. For example, depending on the dimension D , an integral can be finite or divergent. Moreover, integrals in different numbers of dimensions D evaluate to pure functions. This property is important for finding a canonical basis of master integrals, which will be introduced in the following section.

In fact, if D differs from D' by integer multiples of two, these integrals are related to the D' integrals by *dimension shift identities* [47, 150].

Using the Baikov representation (2.44), we can derive the dimension lowering relations that relate the integrals in the dimensions $(D + 2)$ and the dimensions D . We start with an integral in $(D + 2)$ dimensions

$$I_B^{(D+2)} = C \frac{[G(p_1, \dots, p_E)]^{\frac{-(D+2)+E+1}{2}}}{\prod_{j=1}^L \Gamma\left(\frac{(D+2) - E + 1 - j}{2}\right)} \int_{\mathcal{C}} d^{N_V} z [P(z)]^{\frac{(D+2)-L-E-1}{2}} \prod_{k=1}^{N_V} \frac{1}{z_k^{\nu_k}}, \quad (4.7)$$

where C denotes all factors that do not depend on the number of dimensions. Next, we separate all appropriate factors to recognize the D -dimensional integral

$$I_B^{(D+2)} = \frac{[G(p_1, \dots, p_E)]^{-1}}{\prod_{j=1}^L \frac{D - E + 1 - j}{2}} \int_{\mathcal{C}} d^{N_V} z [P(z)]$$

$$\times C \frac{[G(p_1, \dots, p_E)]^{\frac{-D+E+1}{2}}}{\prod_{j=1}^L \Gamma\left(\frac{D-E+1-j}{2}\right)} [P(z)]^{\frac{D-L-E-1}{2}} \prod_{k=1}^{N_V} \frac{1}{z_k^{\nu_k}}. \quad (4.8)$$

The first row shows the additional factors compared to the D -dimensional integral we recognize in the second row. The product in the denominator of the first row comes from using the following property of the Gamma function

$$\Gamma(z+1) = z\Gamma(z). \quad (4.9)$$

Using the lowering operator j_i^- we can pull out the Baikov polynomial out of the integral and write

$$I^{(D+2)} = \frac{[G(p_1, \dots, p_E)]^{-1}}{\prod_{j=1}^L \frac{D-E+1-j}{2}} P(j_1^-, \dots, j_{N_V}^-) I^{(D)}. \quad (4.10)$$

Similarly, we can derive the dimension raising relations, relating the integrals in the D and $(D+2)$ dimensions. Using the graph polynomials \mathcal{U} and \mathcal{F} defined in equation (2.28), we can write another parametric representation of Feynman integrals

$$I_{Sch}^{(D)} = e^{L\epsilon\gamma_E} \frac{1}{\prod_{k=1}^{n_{\text{int}}} \Gamma(\nu_k)} \int_{\alpha_k \geq 0} d^{n_{\text{int}}} \alpha \left(\prod_{k=1}^{n_{\text{int}}} \alpha_k^{\nu_k-1} \right) \frac{1}{\mathcal{U}^{\frac{D}{2}}} e^{-\frac{\mathcal{F}}{\mathcal{U}}}. \quad (4.11)$$

This is the so-called *Schwinger parametrization* and it is closely related to the Feynman parametrization introduced in Section 2.2.

We expand the fraction in equation (4.11) with \mathcal{U}

$$I_{Sch}^{(D)} = e^{L\epsilon\gamma_E} \frac{1}{\prod_{k=1}^{n_{\text{int}}} \Gamma(\nu_k)} \int_{\alpha_k \geq 0} d^{n_{\text{int}}} \alpha \left(\prod_{k=1}^{n_{\text{int}}} \alpha_k^{\nu_k-1} \right) \frac{\mathcal{U}}{\mathcal{U}^{\frac{D+2}{2}}} e^{-\frac{\mathcal{F}}{\mathcal{U}}}. \quad (4.12)$$

We recognize that the additional factor of \mathcal{U} in the denominator increases the number of dimensions by two. The additional factor of \mathcal{U} in the numerator is interpreted as follows. Recall that the graph polynomial \mathcal{U} is a homogeneous polynomial of degree L linear in each parameter α_i . Each instance of parameter α_i in the numerator acts like a raising operator j_i^+ . Hence, we have the following relation

$$I^{(D)} = \mathcal{U}(j_1^+, \dots, j_{n_{\text{int}}}^+) I^{(D+2)}. \quad (4.13)$$

Let us look at the one-loop hexagon example again. The hexagon integral in $(D+2)$ dimensions is related to the same integral in D dimensions through the following relation

$$I^{(D+2)}(\nu_1, \nu_2, \nu_3, \nu_4, \nu_5, \nu_6) = \frac{G(l, p_1, p_2, p_3, p_4, p_5)}{\left(\frac{D-5}{2}\right) G(p_1, p_2, p_3, p_4, p_5)} I^{(D)}(\nu_1, \nu_2, \nu_3, \nu_4, \nu_5, \nu_6) \quad (4.14)$$

Here, similar to the IBPs case, we can expand the Gram determinant in the numerator in terms of the lowering operator j_i^- . Likewise, we find the following relation between the integrals in D dimensions and $(D + 2)$ dimensions

$$I^{(D)}(\nu_1, \nu_2, \nu_3, \nu_4, \nu_5, \nu_6) = \sum_{i=1}^6 j_i^+ I^{(D+2)}(\nu_1, \nu_2, \nu_3, \nu_4, \nu_5, \nu_6). \quad (4.15)$$

These relations will turn out to be quite important for finding a "good" basis of master integrals, as we shall see in the next section and in Chapter 5.

4.3 Canonical Differential Equations

The main finding of Section 4.1 is the existence of a finite-dimensional basis for a given family of Feynman integrals. Typically, this basis is determined by establishing a sufficient number of IBP relations. With this basis, any integral within the family can be expressed as a linear combination of these basis integrals, involving rational coefficients in the kinematic variables and space-time dimensions D . Hence, it is sufficient to compute the basis integrals. We will employ differential equations in the kinematic variables for this purpose [122, 123, 151].

Rather than computing the Feynman integral directly, we first derive a differential equation of the Feynman integral with respect to the kinematic variables. In the next step, we solve this differential equation, thereby finding the required Feynman integral. Specifically, we examine a system of differential equations for a basis of master integrals. This method has the benefit of dealing with only first-order differential equations.

We start with a loop momentum representation of a Feynman integral family, e.g. the one-loop hexagon family (2.16). The integrand is given in terms of momenta, but we want to take derivatives in terms of the kinematical variables. Therefore, we need to construct differential operators that can act on the integrand directly.

It is straightforward to rewrite the Mandelstams in terms of scalar products,

$$s_{i,i+1,\dots,i+k} = 2 \sum_{l=i}^{i+k} \sum_{m=l+1}^{i+k} p_l \cdot p_m. \quad (4.16)$$

In fact, to determine the derivatives, it is best to reintroduce $s_{12\dots n-1} = m_n^2$ as a nonzero variable and only restrict it to the constraint surface in the end.

At six points, we have 10 variables

$$\begin{aligned} s_{12} &= 2p_1 \cdot p_2, & s_{23} &= 2p_2 \cdot p_3, & s_{34} &= 2p_3 \cdot p_4, & s_{45} &= 2p_4 \cdot p_5 \\ s_{123} &= 2(p_1 \cdot p_2 + p_2 \cdot p_3 + p_1 \cdot p_3), & s_{234} &= 2(p_2 \cdot p_3 + p_3 \cdot p_4 + p_2 \cdot p_4), \\ s_{345} &= 2(p_3 \cdot p_4 + p_4 \cdot p_5 + p_3 \cdot p_5), \\ s_{56} &= s_{1234} = 2(p_1 \cdot p_2 + p_2 \cdot p_3 + p_3 \cdot p_4 + p_1 \cdot p_3 + p_2 \cdot p_4 + p_1 \cdot p_4), \\ s_{61} &= s_{2345} = 2(p_2 \cdot p_3 + p_3 \cdot p_4 + p_4 \cdot p_5 + p_2 \cdot p_4 + p_3 \cdot p_5 + p_2 \cdot p_5), \end{aligned}$$

allowing us to rewrite the derivatives according to

$$\begin{aligned}
\frac{\partial}{\partial s_{12}} &= \left(\frac{\partial}{\partial p_1 \cdot p_2} - \frac{\partial}{\partial p_1 \cdot p_3} \right), \\
\frac{\partial}{\partial s_{23}} &= \left(\frac{\partial}{\partial p_1 \cdot p_4} - \frac{\partial}{\partial p_1 \cdot p_3} + \frac{\partial}{\partial p_2 \cdot p_3} - \frac{\partial}{\partial p_2 \cdot p_4} \right), \\
\frac{\partial}{\partial s_{34}} &= \left(\frac{\partial}{\partial p_2 \cdot p_5} - \frac{\partial}{\partial p_2 \cdot p_4} + \frac{\partial}{\partial p_3 \cdot p_4} - \frac{\partial}{\partial p_3 \cdot p_5} \right), \\
\frac{\partial}{\partial s_{45}} &= \left(\frac{\partial}{\partial p_4 \cdot p_5} - \frac{\partial}{\partial p_3 \cdot p_5} \right), \\
\frac{\partial}{\partial s_{123}} &= \left(\frac{\partial}{\partial p_1 \cdot p_3} - \frac{\partial}{\partial p_1 \cdot p_4} \right), \\
\frac{\partial}{\partial s_{234}} &= \left(\frac{\partial}{\partial p_1 \cdot p_5} - \frac{\partial}{\partial p_1 \cdot p_4} + \frac{\partial}{\partial p_2 \cdot p_4} - \frac{\partial}{\partial p_2 \cdot p_5} \right), \\
\frac{\partial}{\partial s_{345}} &= \left(\frac{\partial}{\partial p_3 \cdot p_5} - \frac{\partial}{\partial p_2 \cdot p_5} \right), \\
\frac{\partial}{\partial s_{1234}} &= \left(\frac{\partial}{\partial p_1 \cdot p_4} - \frac{\partial}{\partial p_1 \cdot p_5} \right), \\
\frac{\partial}{\partial s_{2345}} &= \left(\frac{\partial}{\partial p_2 \cdot p_5} - \frac{\partial}{\partial p_1 \cdot p_5} \right), \\
\frac{\partial}{\partial s_{12345}} &= \frac{\partial}{\partial p_1 \cdot p_5}.
\end{aligned} \tag{4.24}$$

Now we would like to rewrite the derivatives in terms of scalar products of momenta in terms of derivatives with respect to momenta, since these can be easily applied to Feynman integrals. In general, we make the ansatz

$$\frac{\partial}{\partial p_i \cdot p_j} = \sum_{k=1}^{n-1} a_k p_k \cdot \frac{\partial}{\partial p_i} \tag{4.25}$$

and impose

$$\frac{\partial}{\partial p_i \cdot p_j} p_l \cdot p_m = \delta_{il} \delta_{jm} + \delta_{im} \delta_{jl}. \tag{4.26}$$

Clearly,

$$\frac{\partial}{\partial p_i \cdot p_j} p_l \cdot p_m = \sum_{k=1}^{n-1} a_k p_k \cdot p_l \delta_{im} + \sum_{k=1}^{n-1} a_k p_k \cdot p_m \delta_{il}, \tag{4.27}$$

Hence, we can satisfy the constraint by choosing [132]

$$a_k = \mathbb{G}_{jk}^{-1}, \tag{4.28}$$

where $\mathbb{G}_{ij} = p_i \cdot p_j$, $i, j = 1, \dots, n-1$ is the Gram matrix. By symmetry, we have the two alternative representations

$$\begin{aligned} \frac{\partial}{\partial p_i \cdot p_j} &= \sum_{k=1}^{n-1} (\mathbb{G}^{-1})_{jk} p_k \cdot \frac{\partial}{\partial p_i} \\ &= \sum_{k=1}^{n-1} (\mathbb{G}^{-1})_{ik} p_k \cdot \frac{\partial}{\partial p_j}. \end{aligned} \quad (4.29)$$

Expanding one these expressions and substituting it back into (4.24) allows us to write down the differential operators with respect to kinematic variables in terms of operators with respect to momenta thus allowing us to act directly on the Feynman integrals.

When acting with such differential operators on the Feynman integrals, we have to perform algebraic manipulations similar to those when deriving the IBP relations. Again, we obtain integrals within the same integral family but with different propagator powers, which we re-express in terms of the basis integrals \vec{I} . Particularly, we arrive at a system of first-order partial differential equations,

$$\frac{\partial \vec{I}}{\partial s_i} = A_{s_i}(\epsilon, \vec{v}) \vec{I}, \quad \forall s_i \in \vec{v}. \quad (4.30)$$

Here, $A_{s_i}(\epsilon, \vec{v})$ is a $N \times N$ matrix with rational coefficients depending both on the kinematic variables and on the space-time dimension through the dimensional regulator ϵ , and N is the number of master integrals.

Using the standard notation for the total differential

$$d = \sum_k ds_k \frac{\partial}{\partial s_k}, \quad s_k \in \vec{v}, \quad (4.31)$$

we can rewrite the system of partial differential equations (4.30) in a compact form

$$d\vec{I} = A(\epsilon, \vec{v}) \vec{I}, \quad (4.32)$$

where A is a matrix-valued one-form

$$A(\epsilon, \vec{v}) = \sum_k A_{s_k}(\epsilon, \vec{v}) ds_k. \quad (4.33)$$

The matrices A_{s_k} have to satisfy *integrability conditions*

$$\frac{\partial A_{s_i}}{\partial s_j} - \frac{\partial A_{s_j}}{\partial s_i} + [A_{s_i}, A_{s_j}] = 0, \quad (4.34)$$

since the partial derivatives of the basis integrals commute

$$\left[\frac{\partial}{\partial s_i}, \frac{\partial}{\partial s_j} \right] \vec{I} = 0. \quad (4.35)$$

These integrability conditions serve as a check for an implementation of the differential equations.

In summary, we showed that every integral family has an integral basis. This basis satisfies a linear system of first-order differential equations (4.32), which can be determined using a fully algorithmic approach. However, their solutions are typically not systematic. In addition, the selection of the basis is arbitrary. We have the freedom to choose any basis that we like as long as it spans the whole vector space. A new basis \vec{I}' satisfies a system of differential equations equivalent to (4.32)

$$d\vec{I}' = B(\epsilon, \vec{v})\vec{I}', \quad (4.36)$$

where

$$B_{s_k} = T \cdot A_{s_k} T^{-1} + \frac{\partial T}{\partial s_k} \cdot T^{-1}, \quad (4.37)$$

and T is a transformation matrix from the basis \vec{I} to the basis \vec{I}' .

It was conjectured that a particular choice of basis can simplify differential equations, making the solution more accessible [152]. The differential equation takes the following *canonical form*

$$d\vec{I} = \epsilon \left(d\tilde{A}(\vec{v}) \right) \vec{I}, \quad (4.38)$$

where, in general,

$$\tilde{A} = \sum_k c_k \omega_k(\vec{v}). \quad (4.39)$$

Here, c_k are constant rational matrices, and ω_k are differential one-forms that have only simple poles. The sole dependence on the dimensional regulator ϵ is through the overall factor on the right-hand side. Consequently, it is straightforward to find a general solution to the canonical differential equation as a Laurent series in ϵ where each term in the expansion is given in terms of iterated integrals; see Section 4.4.

For the differential equation in the canonical form (4.38), the integrability condition (4.34) becomes

$$\begin{aligned} \partial_{s_j} \tilde{A}_i - \partial_{s_i} \tilde{A}_j &= 0, \\ [\tilde{A}_i, \tilde{A}_j] &= 0, \end{aligned} \quad (4.40)$$

where

$$\tilde{A}_{s_k} = \frac{\partial \tilde{A}}{\partial s_k}. \quad (4.41)$$

In the cases we are considering in this thesis, the one-forms that appear in the canonical differential equation (4.38) can be written in terms of logarithmic one-forms, i.e. $d\log$ -forms. Hence, the $d\tilde{A}(\vec{v})$ matrix takes the following form

$$d\tilde{A} = \sum_k c_k d\log(W_k), \quad (4.42)$$

where W_i are algebraic functions of the kinematic variables. We refer to the one-forms as *letters* and the collection of all independent letters as the *alphabet*. Note that in this thesis, we will refer to the arguments of the one-forms W_k as letters, instead of the complete one-forms $d \log(W_k)$.

Once we have the differential equation in canonical form (4.38), we can read off the letters as independent entries of the \tilde{A} matrix. However, knowing the alphabet in advance is beneficial for reducing the overall computation time since we can perform numerical fits to find the coefficients in front of the letters. The letters W_i encode the singularity structure of the basis integrals and therefore can be predicted through Landau analysis, which is covered in Chapter 3. Furthermore, they also specify which class of special functions is needed to write a solution, see Section 4.4.

The basis that satisfies the differential equation in canonical form is called the *canonical basis*. Such a basis should have simple properties under the differentiation. To define what we exactly mean by “simple”, let us introduce the notion of *transcendental weight*. A function f has transcendental weight k if we need to perform k iterated integrals to define it. For example, the ordinary logarithm has transcendental weight one, since

$$\log(x) = \int_0^x \frac{dt}{t}. \quad (4.43)$$

Clearly, $\mathcal{T}(f_1 f_2) = \mathcal{T}(f_1) + \mathcal{T}(f_2)$, where \mathcal{T} denotes the transcendental weight.

In addition, if the transcendental weight of a function f is reduced by differentiation

$$\mathcal{T}(df) = \mathcal{T}(f) - 1, \quad (4.44)$$

we call these functions *pure functions*. Consequently, if functions f_1 and f_2 are pure functions of weight k , so is any \mathbb{Q} -linear combination of them. Moreover, if f_1 and f_2 are pure functions of weight k_1 and k_2 , respectively, then their product is a pure function of weight $\mathcal{T}(f_1 f_2) = k_1 + k_2$. Finally, a function f that is given as a sum of terms with the same transcendental weight is said to have a *uniform transcendental weight (UT)*.

Let us look at the transcendental weight of the canonical differential equation (4.38)

$$\mathcal{T}(d\vec{I}) = \mathcal{T}(\epsilon) + \mathcal{T}(d\tilde{A}) + \mathcal{T}(\vec{I}). \quad (4.45)$$

It is conventional to assign transcendental weight -1 to the dimensional regulator ϵ . Moreover, since the matrix $d\tilde{A}$ is written in terms of $d \log$ -forms, it has zero transcendental weight. It follows

$$\mathcal{T}(d\vec{I}) = \mathcal{T}(\vec{I}) - 1. \quad (4.46)$$

Therefore, integrals in the canonical basis are pure functions. The reverse holds as well; any pure function satisfies a differential equation in canonical form. Through this thesis, we will interchangeably refer to the basis satisfying the canonical differential equation as the canonical basis or UT basis.

Although it is feasible to begin with a generic basis produced by the IBP reduction procedure and subsequently determine the transformation to the canonical basis [26, 153–156],

this approach is generally quite challenging. This procedure is simplified and automated if we already know at least one pure integral in the top sector [157–159].

Ideally, we would like to have an UT basis from the beginning, since this simplifies finding a solution and makes the whole computation more efficient. There are several guiding principles that can help in finding such integrals. Although a general proof is not currently known, it has been observed that integrals with constant *leading singularities* [160, 161] exhibit characteristics of pure functions. The loop integrand contains all the information about the rational factors that arise after integration, which could spoil the properties of pure functions. If the integrand possesses only simple poles in the integration variables, one can systematically extract the rational factors by computing (multi-variate) residues. The “maximal” that fix all integrations are referred to as leading singularities [30, 162]. Therefore, one way of obtaining pure functions is by normalizing basis integrals by the inverse leading singularities. One particularly important result is that D -gons in D dimensions normalized by its leading singularities are pure functions [163]. This will be demonstrated in the one-loop hexagon example below.

An alternative method to reveal the properties of pure functions is by using an appropriate $d \log$ representation [164], where the integrand is expressed in a logarithmic differential form

$$\mathcal{I} = \sum c_I d \log(r_{i_1}) \wedge \dots \wedge d \log(r_{i_n}). \quad (4.47)$$

Here, c_I are algebraic functions of kinematic variables and r_i are algebraic functions of kinematic variables and integration variables. The coefficients c_I are the leading singularities and can be computed by taking residues to localize all integrations. The hypothesis behind this approach suggests that integrands possessing a $d \log$ representation with constant leading singularities evaluate to pure functions [161, 165]. There is a lot of evidence to support this statement, and important steps have been taken to better understand it [166].

Algorithmically, all $d \log$ forms with constant leading singularities can be derived for a specific integral family. The initial proposal for this algorithm can be found in Ref. [167]. The algorithm with subsequent refinements was implemented into a Mathematica package `DlogBasis` [168]. The systematic approach of the method, coupled with the remarkable simplicity of the derived pure integrals compared to other techniques, has contributed to its great success.

Example: One-loop Hexagon Differential Equation

Let us finally look at a specific example where we are going to demonstrate how to find the canonical differential equation starting from the IBP reduction procedure. Our main example will again be the one-loop hexagon integral family defined in equation (2.16).

Using IBP identities (4.4), all integrals in the hexagon family can be reduced to a basis of 33 master integrals when the external momenta are considered to be ($D_{\text{ext}} > 4$)-dimensional. We use a combination of `FIRE` [128] and `LiteRed` [132] to perform the reductions automatically. A convenient basis choice I_j is spanned by six cyclic permutations

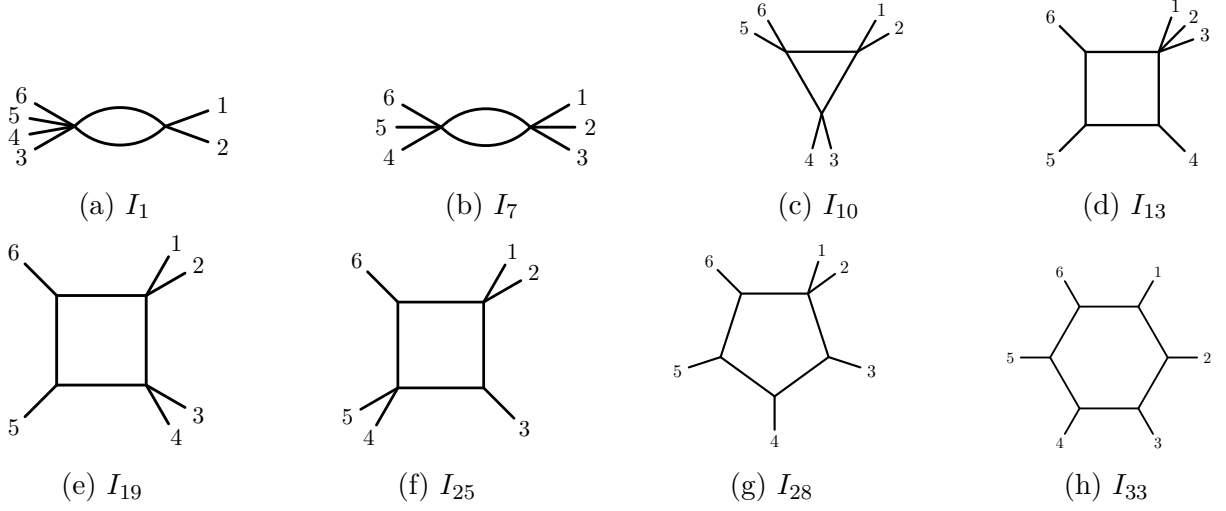


Figure 4.1: Graphical representations of the integrals in the IBP basis of the one-loop hexagon integral family. The figure is adapted from Ref. [79].

of the massive bubble integral

$$I_i = T^{i-1} I^{(4)}(1, 0, 1, 0, 0, 0), \quad i = 1, \dots, 6, \quad (4.48)$$

three cyclic permutations of the massive bubble integral

$$I_{6+i} = T^{i-1} I^{(4)}(1, 0, 0, 1, 0, 0), \quad i = 1, \dots, 3, \quad (4.49)$$

two cyclic permutations of the three-mass triangle integral

$$I_{9+i} = T^{i-1} I^{(4)}(1, 0, 1, 0, 1, 0), \quad i = 1, 2, \quad (4.50)$$

six cyclic permutations of the one-mass box integral

$$I_{11+i} = T^{i-1} I^{(4)}(0, 0, 1, 1, 1, 1), \quad i = 1, \dots, 6, \quad (4.51)$$

six cyclic permutations of the two-mass-hard box integral

$$I_{17+i} = T^{i-1} I^{(4)}(0, 1, 0, 1, 1, 1), \quad i = 1, \dots, 6, \quad (4.52)$$

three cyclic permutations of the two-mass-easy box integral

$$I_{23+i} = T^{i-1} I^{(4)}(0, 1, 1, 0, 1, 1), \quad i = 1, 2, 3, \quad (4.53)$$

six cyclic permutations of the one-mass pentagon integral

$$I_{26+i} = T^{i-1} I^{(4)}(0, 1, 1, 1, 1, 1), \quad i = 1, \dots, 6, \quad (4.54)$$

and the hexagon integral

$$I_{33} = I^{(4)}(1, 1, 1, 1, 1, 1). \quad (4.55)$$

The basis integrals are shown in Figure 4.1.

The integrals in this basis do not have uniform transcendentality and therefore satisfy the differential equation (4.32) but do not satisfy a differential equation in the canonical form (4.38).

Constructing a UT Basis. To determine a UT basis, we use the observation that n -point and $(n-1)$ -point integrals in $D = n - 2\epsilon$ dimensions have uniform transcendental weight if they are normalized by their leading singularities in $D = n$ dimensions [163]. Therefore, for the construction of an UT basis, we prefer to include integrals in $D = 2 - 2\epsilon$ and $D = 6 - 2\epsilon$ dimensions. In fact, if D_0 differs from four by integer multiples of two, these integrals are related to the $D_0 = 4$ integrals by dimension shift identities introduced in Section 4.2. Explicitly, this allows us to express bubble integrals in two dimensions through bubble integrals in four dimensions as

$$I^{(2)}(1, 0, 1, 0, 0, 0) = \frac{2(1 - 2\epsilon)}{s_{12}} I^{(4)}(1, 0, 1, 0, 0, 0), \quad (4.56)$$

as well as pentagon integrals in six dimensions through box and pentagon integrals in four dimensions

$$I^{(6)}(0, 1, 1, 1, 1, 1) = \frac{1}{2\epsilon G(p_2, p_3, p_4, p_5)} \vec{c}_P \cdot \vec{I}_P, \quad (4.57)$$

where

$$\vec{I}_P = (I_{12} \quad I_{17} \quad I_{18} \quad I_{22} \quad I_{24} \quad I_{27}) \quad (4.58)$$

and

$$\begin{aligned} c_{P1} &= s_{34}s_{45}(s_{234}s_{345} - s_{34}s_{61} + s_{23}(s_{345} - s_{34}) + s_{45}(s_{34} - s_{234})), \\ c_{P2} &= s_{23}s_{34}(s_{23}(s_{34} - s_{345}) - s_{34}(s_{61} + s_{45}) + s_{234}(s_{345} + s_{45})), \\ c_{P3} &= s_{45}(-2s_{23}s_{61}s_{34} + s_{23}s_{234}(s_{34} + s_{345}) + s_{234}(s_{61}s_{34} - s_{34}s_{45} + s_{234}(-s_{345} + s_{45}))), \\ c_{P4} &= s_{23}(-2s_{61}s_{34}s_{45} + s_{34}s_{345}(-s_{23} + s_{61} + s_{45}) + s_{345}(s_{23}s_{345} + s_{234}(-s_{345} + s_{45}))), \\ c_{P5} &= (s_{61}s_{34} - s_{234}s_{345})(s_{61}s_{34} - s_{234}s_{345} + s_{23}(-s_{34} + s_{345}) + s_{234}s_{45} - s_{34}s_{45}), \\ c_{P6} &= 2s_{23}s_{34}s_{45}(s_{61}s_{34} - s_{234}s_{345}). \end{aligned} \quad (4.59)$$

Finally, the six-dimensional hexagon integral can be decomposed into four-dimensional pentagon and hexagon integrals according to

$$I^{(6)}(1, 1, 1, 1, 1, 1) = \frac{1}{2(1 + 2\epsilon)G(p_1, p_2, p_3, p_4, p_5)} \vec{c}_H \cdot \vec{I}_H, \quad (4.60)$$

where

$$\vec{I}_H = (I_{27} \quad I_{28} \quad I_{29} \quad I_{30} \quad I_{31} \quad I_{32} \quad I_{33}) \quad (4.61)$$

and

$$\begin{aligned} c_{Hi} &= -T^i G(l, p_1, \dots, p_4; p_5, p_1, \dots, p_4) \Big|_{l \cdot p_j = -\sum_{k < j} p_k \cdot p_j - \frac{1}{2} p_j^2}, \quad i = 1, \dots, 6 \\ c_{H7} &= -G(l, p_1, \dots, p_5) \Big|_{l \cdot p_j = -\sum_{k < j} p_k \cdot p_j - \frac{1}{2} p_j^2}. \end{aligned} \quad (4.62)$$

Using these dimension-shift identities, we can establish an intermediate basis, where the bubbles are two-dimensional, the triangles and boxes four-dimensional and the pentagons and hexagon six-dimensional integrals, i.e.

$$\bar{I}_i = \hat{d}^{-2} I_i, \quad i = 1, \dots, 9,$$

$$\begin{aligned}\bar{I}_i &= I_i, & i &= 11, \dots, 26, \\ \bar{I}_i &= \hat{d}^2 I_i, & i &= 27, \dots, 33\end{aligned}\quad (4.63)$$

with the dimension–shift operator \hat{d} . This basis is still not of uniform transcendental weight, as we are still missing leading singularities in the normalization.

Leading Singularities from the Baikov Representation. To transform the above basis of the master integrals into a basis where every single element is a pure function of uniform transcendental weight we normalize the integrals by their leading singularities. Calculating the leading singularities of one–loop integrals is most straightforward in the Baikov representation introduced in Section 2.4.

The leading singularity can be easily extracted by taking the residue at $z_i = 0$ starting from the representation given in equation (2.44). We can neglect all coefficients in front of the integral that are kinematic–independent constants since they have no impact on the UT property of an integral. Hence, the leading singularity of an integral takes the form

$$\text{LS}(I(\nu_1, \dots, \nu_n)) = [G(p_1, \dots, p_E)]^{\frac{E-D+1}{2}} \text{Res}_{z_i=0} P(z) \frac{1}{z_1^{\nu_1} \dots z_n^{\nu_n}}. \quad (4.64)$$

The expression becomes even simpler if all propagator powers $\nu_j = 1$:

$$\text{LS}(I^{(D)}(1, \dots, 1)) = [G(p_1, \dots, p_E)]^{\frac{E-D+1}{2}} \text{Res}_{z_i=0} P(z) \frac{1}{z_1^{\nu_1} \dots z_n^{\nu_n}}. \quad (4.65)$$

Defining a Gram determinant on the maximal cut as

$$G^*(q_1, \dots, q_{n-1}; u_1, \dots, u_n) = G(l, q_1, \dots, q_{n-1}; u_1, \dots, u_n)|_{l \cdot p_j = -\sum_{k < j} p_k \cdot p_j - \frac{1}{2} p_j^2}, \quad (4.66)$$

for the one–loop n –point integrals in n or $(n + 1)$ dimensions we can further rewrite the leading singularity as

$$\text{LS}(I^{(D)}(\underbrace{1, \dots, 1}_{n \text{ entries}})) = \begin{cases} \sqrt{G^*(p_1, \dots, p_{n-1})}^{-1}, & \text{if } D = n, \\ \sqrt{G(p_1, \dots, p_{n-1})}^{-1}, & \text{if } D = n + 1. \end{cases} \quad (4.67)$$

Using this expression, we can easily calculate the leading singularities for our basis of integrals, namely¹

$$\begin{aligned}\text{LS}(I^{(2)}(1, 0, 1, 0, 0, 0)) &= s_{12}^{-1}, \\ \text{LS}(I^{(2)}(1, 0, 0, 1, 0, 0)) &= s_{123}^{-1}, \\ \text{LS}(I^{(4)}(1, 0, 1, 0, 1, 0)) &= \sqrt{\Delta_3(s_{12}, s_{34}, s_{56})}^{-1}, \\ \text{LS}(I^{(4)}(0, 0, 1, 1, 1, 1)) &= (s_{34}s_{45})^{-1},\end{aligned}$$

¹Note that due to (2.15), the leading singularities of the three–mass triangle and of the one–mass pentagon integrals are purely imaginary in physical regions.

$$\begin{aligned}
\text{LS}(I^{(4)}(0, 1, 0, 1, 1, 1)) &= (s_{234}s_{45})^{-1}, \\
\text{LS}(I^{(4)}(0, 1, 1, 0, 1, 1)) &= (s_{234}s_{345} - s_{34}s_{61})^{-1} \\
\text{LS}(I^{(6)}(0, 1, 1, 1, 1, 1)) &= \sqrt{\Delta_5(s_{23}, s_{34}, s_{45}, s_{234}, s_{345}, s_{61})}^{-1} \\
\text{LS}(I^{(6)}(1, 1, 1, 1, 1, 1)) &= \sqrt{\Delta_6}^{-1},
\end{aligned} \tag{4.68}$$

and the permutations thereof, where the arguments of square roots are defined in (3.32).

Finally, having started with the four-dimensional basis I , after using dimension-shift identities to construct the basis \bar{I} we can further transform it into a basis of uniform transcendental weight \tilde{I} , by normalizing it according to

$$\tilde{I}_i = \frac{\bar{I}_i}{\text{LS}(\bar{I}_i)} \times \begin{cases} \epsilon, & i = 1, \dots, 9, \\ \epsilon^2, & i = 10, \dots, 26, \\ \epsilon^3, & i = 27, \dots, 33. \end{cases} \tag{4.69}$$

Here, the explicit powers of ϵ make sure that not only is every single integral of uniform transcendental weight but that all the different integrals also have vanishing transcendental weight, c.f. [84].² Since the finite part of the pentagon and hexagon integrals in four dimensions are transcendental functions of weight three, their epsilon expansion in arbitrary dimensions starts at order ϵ^3 and the first correction to the four-dimensional result is of order ϵ^4 .

Acting with the differential operators on the UT basis integrals (4.69), we find the following system of partial differential equations

$$\frac{\partial \tilde{I}}{\partial s_i} = \epsilon \tilde{A}_{s_i} \tilde{I}. \tag{4.70}$$

In principle, we could find the logarithmic DE matrix \tilde{A} by integrating the entries of \tilde{A}_{s_i} into logarithms. This would provide us with a constructive determination of the hexagon alphabet \mathbb{A}_{1-loop} . However, we find that it is more efficient to start with an educated ansatz for the alphabet, constructed in Chapter 3, and fit it to the derivatives with respect to Mandelstam invariants entry by entry.

As a result, the integrals in the UT basis (4.69) satisfy the canonical differential equation

$$d\tilde{I} = \epsilon d\tilde{A}(\vec{v})\tilde{I}, \tag{4.71}$$

where d is the total differential in terms of the nine kinematic variables

$$d = \sum_{i=1}^6 ds_{i,i+1} \frac{\partial}{\partial s_{i,i+1}} + \sum_{i=1}^3 ds_{i,i+1,i+2} \frac{\partial}{\partial s_{i,i+1,i+2}}. \tag{4.72}$$

Moreover, \tilde{A} is a matrix of logarithmic forms

$$\tilde{A}_{jk} = \sum_{i=1}^{104} c_{jk}^i \log(W_i), \tag{4.73}$$

²Recall that ϵ has transcendental weight -1 .

where c_{jk}^i are rational matrices and the arguments of $d \log$ are algebraic functions of kinematic variables. By performing a linear fit, we observe that the conjectured alphabet from Chapter 3 is too big and that the last 15 letters (3.69) – (3.71) are not part of the one-loop hexagon alphabet.

We can understand why those 15 letters do not appear in the differential equation matrix by looking at a toy example. Assume the following UT basis

$$\left(\sqrt{Q_1} f_1, \sqrt{Q_2} f_2, f_3 \right)^T, \quad (4.74)$$

satisfying the canonical differential equation (4.38). Since all functions in the basis have a definite parity behaviour under the action of the Galois group $\sqrt{Q_i} \rightarrow -\sqrt{Q_i}$, this property is also reflected in the \tilde{A} matrix of the canonical differential equation. Therefore, \tilde{A} has the following schematic form

$$\tilde{A} = \begin{pmatrix} \sum_{W_i \in \mathbb{A}_{\text{even}}} c_i W_i & c_j \frac{P_1 - \sqrt{Q_1} \sqrt{Q_2}}{P_1 + \sqrt{Q_1} \sqrt{Q_2}} & c_k \frac{P_1 - \sqrt{Q_1}}{P_1 + \sqrt{Q_1}} \\ & \sum_{W_i \in \mathbb{A}_{\text{even}}} c_i W_i & c_l \frac{P_1 - \sqrt{Q_2}}{P_1 + \sqrt{Q_2}} \\ & & \sum_{W_i \in \mathbb{A}_{\text{even}}} c_i W_i \end{pmatrix}. \quad (4.75)$$

From this toy example, it is easy to see that odd letters with two square roots appear only in the entries that relate the two functions normalized by those square roots.

The 15 letters that do not appear in the hexagon differential equation have two different pentagon square roots in the argument, hence, they can only appear in the entries of the \tilde{A} matrix that relate the two corresponding pentagons. Considering that two pentagons do not “talk” to each other in the hexagon differential equation, those letters do not appear in the one-loop alphabet. However, we cannot rule out the possibility that those letters might be a part of the alphabet at higher loop orders.

A machine-readable expression of the \tilde{A} matrix is provided in the ancillary files of Ref. [79].

4.4 Solutions to the Canonical Differential Equation

In Section 4.3, we demonstrated the procedure of deriving differential equations satisfied by basis integrals of a specific Feynman integral family. Additionally, we anticipated that having an UT basis simplifies the process of finding a solution. This is the primary objective of this section. In this section, we will outline a formal solution to the canonical differential equation and present a class of special functions pertinent to the Feynman integrals discussed in this thesis.

Once we have the differential equation in the canonical form (4.38), the formal solution can be written as a path-ordered integral.

$$\tilde{I}(\vec{v}, \epsilon) = \mathbb{P} \exp\left(\epsilon \int_{\gamma} d\tilde{A}\right) \cdot \vec{b}, \quad (4.76)$$

where γ denotes a path from a boundary point \vec{v}_0 to \vec{v} and $\vec{b} = \tilde{I}(\vec{v}_0)$ is a vector of master integral values at the boundary point \vec{v}_0 . This equation is to be understood as a Laurent expansion around $\epsilon = 0$,

$$\tilde{I}(\vec{v}, \epsilon) = \sum_{k=0}^{\infty} \epsilon^k \tilde{I}^{(k)}(\vec{v}). \quad (4.77)$$

Substituting this expansion in the canonical differential equation (4.38), we see that the equation decouples order by order in ϵ

$$d\tilde{I}^{(k+1)}(\vec{v}) = \sum_{k \geq 0} (d\tilde{A}(\vec{v})) \tilde{I}^{(k)}(\vec{v}) \quad (4.78)$$

The $(k+1)$ -th term in the expansion is then given by a $(k+1)$ -fold iterated integral along the contour γ of the matrix differential form \tilde{A}

$$\tilde{I}^{(k+1)}(\vec{v}) = \int_{\gamma} (d\tilde{A}(\vec{v})) \tilde{I}^{(k)}(\vec{v}) + \vec{b}^{(k)}, \quad (4.79)$$

where $\vec{b}^{(k)}$ are weight k boundary values which we discuss in the following section. We can rewrite this equation in terms of *Chen iterated integrals* [169]

$$\tilde{I}^{(k)}(\vec{v}) = \sum_{k'=0}^k \sum_{i_1, \dots, i_{k'} \in \mathbb{A}} a^{(i_1)} \dots a^{(i_{k'})} \vec{b}^{(k-k')} [W_{i_1}, \dots, W_{i_{k'}}]_{\vec{v}_0}(\vec{v}), \quad (4.80)$$

where

$$[W_{i_1}, \dots, W_{i_k}]_{\vec{v}_0}(\vec{v}) = \int_{\gamma} d \log W_k(\vec{v}') [W_{i_1}, \dots, W_{i_{k-1}}]_{\vec{v}_0}, \quad (4.81)$$

and $[]_{\vec{v}_0} = 1$. In order for the integral to be well-defined, it has to be homotopy invariant i.e. it should be independent of the choice of the contour as long as the singularities are not crossed. Since the differential equation satisfies the integrability conditions (4.40), the solution (4.80) is homotopy invariant, but the separate integrals (4.81) are not.

Special Functions

Iterated integrals naturally arise as solutions to the differential equations satisfied by Feynman integrals. If our primary objective is to obtain numerical values of Feynman integrals, it becomes advantageous to express their solutions in terms of well-established functions, since computer codes may exist for their evaluation and manipulation.

The best understood class of iterated integrals are *multiple polylogarithms* (MPLs). These types of functions are already known from the mathematics literature [170–174].

The *Goncharov polylogarithms* (GPLs) or *multiple polylogarithms* are recursively defined in the integral representation as [100, 175]

$$G(a_1, a_2, \dots, a_n; x) = \int_0^x \frac{dt}{t - a_1} G(a_2, \dots, a_n; t), \quad \forall n \in \mathbb{N}, \quad a_n \neq 0, \quad (4.82)$$

where the recursion starts with

$$G(; x) = 1. \quad (4.83)$$

Here, the number n counts the number of recursions and denotes the weight of the GPL.

If $a_n = 0$, then the GPLs are divergent, and we need to regularize them. This is usually done by defining

$$G(\underbrace{0, \dots, 0}_n; x) = \frac{1}{n!} \log^n(x). \quad (4.84)$$

The GPLs have intricate mathematical properties. For instance, they obey a shuffle product rule, which transforms the vector space of GPLs into an algebra. In addition, GPLs have a rich branch-cut structure. The details of their mathematical properties go beyond the scope of this work. The interested reader may find more on this topic in Chapter 8 of Ref. [71]. Another useful reference for manipulating and evaluating GPLs is the *Mathematica* package `PolyLogTools` [23].

MPLs also have a definition in terms of nested sums [176, 177]

$$\text{Li}_{n_1, \dots, n_m}(x_1, \dots, x_m) = \sum_{0 < k_1 < k_2 < \dots < k_m} \frac{x_1^{k_1} x_2^{k_2} \dots x_m^{k_m}}{k_1^{n_1} k_2^{n_2} \dots k_m^{n_m}}, \quad (4.85)$$

where the number $(n_1 + \dots + n_m)$ indicates the weight and the number m denotes the depth of MPLs. Note that these two numbers are not equal, in general, for the nested sum representation. The relations between the two representations are given by

$$\begin{aligned} \text{Li}_{n_1, \dots, n_m}(x_1, \dots, x_m) &= (-1)^m G_{n_1, \dots, n_m} \left(\frac{1}{x_1}, \frac{1}{x_1 x_2}, \dots, \frac{1}{x_1 \dots x_m}; 1 \right) \\ G_{n_1, \dots, n_m}(z_1, \dots, z_m; y) &= (-1)^m \text{Li}_{n_1, \dots, n_m} \left(\frac{y}{z_1}, \frac{z_1}{z_2}, \dots, \frac{z_{m-1}}{z_m} \right), \end{aligned} \quad (4.86)$$

where we used the following notation

$$G_{n_1, \dots, n_m}(z_1, \dots, z_m; y) = G(\underbrace{0, \dots, 0}_{n_1-1}, z_1, \dots, z_m, \underbrace{0, \dots, 0}_{n_m-1}, z_m; y). \quad (4.87)$$

The multiple polylogarithms contain ordinary logarithm and *classical polylogarithms* as special cases

$$\begin{aligned} G(a; x) &= \log \left(1 - \frac{x}{a} \right) \\ G(\underbrace{0, \dots, 0}_{n-1}, a; x) &= -\text{Li}_n \left(\frac{x}{a} \right). \end{aligned} \quad (4.88)$$

Classical polylogarithms can also be defined recursively in terms of iterated integration or via nested sums

$$\text{Li}_n(x) = \int_0^x \frac{dy}{y} \text{Li}_{n-1}(y)$$

$$= \sum_{k=1}^{\infty} \frac{x^k}{k^n}, \quad \forall n \in \mathbb{N}. \quad (4.89)$$

The recursion starts with the ordinary logarithm $\text{Li}_1(x) = -\log(1-x)$.

Additionally, the values of multiple polylogarithms at $x_1 = \dots = x_m = 1$ are known as *multiple ζ -values*

$$\zeta_{n_1, \dots, n_m} = \text{Li}_{n_1, \dots, n_m}(\underbrace{1, \dots, 1}_m), \quad (4.90)$$

and in special case of depth one they correspond to *Riemann ζ -functions*

$$\zeta_n = \text{Li}_n(1) = \sum_{k=1}^{\infty} \frac{1}{k^n}. \quad (4.91)$$

For even n , the Riemann ζ -functions evaluate to powers of π .

Since the early days of quantum field theory, it has been known that not all Feynman integrals fall into the class of MPLs [178]. Less understood classes of special functions such as elliptic polylogarithms [179, 180], modular forms [181, 182] and Calabi-Yau manifolds also appear [183–188]. We will not go into the details of these functions, as they go beyond the scope of this thesis. The interested reader can find more relevant references in the review [189]. Note that the Feynman integrals considered in this work are in the MPL class of iterated integrals at least up to transcendental weight two, where we have found the explicit function basis, see Sections 4.6 and 5.6.3.

The Symbol

The symbol [190, 191] is a powerful mathematical tool which captures the main analytical and combinatorial properties of polylogarithmic functions. Given that the symbol captures the main properties of polylogarithmic functions, a necessary condition for the two expressions written in terms of MPLs to be equal is that they have the same symbol. It was first introduced in physics to simplify long expressions written in terms of GPLs [74] and later became an ubiquitous tool for bootstrap approaches [78, 192–196]. Moreover, the symbol encodes the cluster adjacency properties of scattering amplitudes in $\mathcal{N} = 4$ super Yang–Mills theory [197, 198] and certain Feynman integrals [199]. For an introduction to cluster algebras, see, for example, [200–204].

The symbol can be defined through its action on the Chen iterated integrals where it maps a k -fold iterated integral to the k -fold tensor product

$$\mathcal{S}([W_1, \dots, W_k]_{\vec{v}_0}(\vec{v})) = d \log(W_1) \otimes \dots \otimes d \log(W_k), \quad (4.92)$$

of $d \log$ forms. Since all of the factors of the symbol have the $d \log$ sign, we will omit it to simplify the notation and write instead

$$\mathcal{S}([W_1, \dots, W_k]_{\vec{v}_0}(\vec{v})) = W_1 \otimes \dots \otimes W_k. \quad (4.93)$$

We can extend the definition of the symbol to the transcendental functions whose total differential is a linear combination of $d \log$ -forms multiplied by transcendental functions of weight minus one

$$df^{(n)} = \sum_i c_i f^{(n-1)} d \log(W_i), \quad (4.94)$$

where c_i are rational coefficients and $f^{(n)}$ denotes a function of transcendental weight n . One additional requirement is that the total differential of lower-weight functions can again be written in the same manner.

Additionally, we will use $\mathcal{S}^{(k)}(f)$ to denote the symbol of the weight- k part of f , i.e. if f has an expansion

$$f = \sum_k \epsilon^k f^{(k)} \quad (4.95)$$

then we define

$$\mathcal{S}^{(k)}(f) = \mathcal{S}(f^{(k)}). \quad (4.96)$$

The symbol map inherits many properties from iterated integrals. First, the symbol map is linear. Second, the symbol of a product of two functions is mapped into the shuffle product of their respective symbols

$$\mathcal{S}(f \cdot g) = \mathcal{S}(f) \sqcup \mathcal{S}(g), \quad (4.97)$$

where \sqcup denotes the shuffle product of tensors. For example,

$$(a \otimes b) \sqcup c = a \otimes b \otimes c + a \otimes c \otimes b + c \otimes a \otimes b. \quad (4.98)$$

Additionally, the additivity of the logarithm $\log(ab) = \log(a) + \log(b)$, translates into the following basic properties

$$\begin{aligned} \dots \otimes (ab) \otimes \dots &= \dots \otimes a \otimes \dots + \dots \otimes b \otimes \dots \\ \dots \otimes a^n \otimes \dots &= n(\dots \otimes a \otimes \dots). \end{aligned} \quad (4.99)$$

Next, since the the total differential of any constant is zero, any symbol with constant entries vanishes

$$\dots \otimes c \otimes \dots = 0, \quad \text{for } c = \text{const}. \quad (4.100)$$

Some of the information is lost due to this last property. Consequently, there is no algorithm that recovers this information in order to go from a symbol to a function that works in general.

Lastly, we can ask whether every possible \mathbb{Q} -linear combination of tensors

$$F = \sum_{i_1, \dots, i_k} c_{i_1, \dots, i_k} W_{i_1} \otimes \dots \otimes W_{i_k}, \quad (4.101)$$

corresponds to some function f , such that $\mathcal{S}(f) = F$. Such a function f exists if and only if F satisfies the integrability conditions [205]

$$\sum_{i_1, \dots, i_k} c_{i_1, \dots, i_k} d \log(W_{i_j}) \wedge d \log(W_{i_{j+1}}) W_{i_1} \otimes \dots \otimes W_{i_{j-1}} \otimes W_{i_{j+2}} \otimes W_{i_k} = 0, \quad (4.102)$$

for all $1 \leq j \leq k - 1$ and where \wedge denotes the wedge product of differential forms. Hence, there is a finite number of integrable symbols of any transcendental weight for a given symbol alphabet.

4.5 Fixing the Boundary Constants

To uniquely fix a solution of the first-order canonical DE, we have to provide boundary information for all of the integrals at a single point in the space of kinematical variables.

There are two different approaches that we can follow to fix the boundary values. The first approach is to use one of the available software on the market like `AMFlow` [17, 18] or `pySecDec` [16, 206–208] to numerically evaluate basis integrals at a particular point with high precision. Afterwards, we can use this information to fully fix the solutions of the canonical differential equations.

Another approach is to use physical arguments such as certain physical limits [209] or the absence of spurious singularities [168, 210] to put constraints on the boundary values. Using these arguments, we can usually fix all of the boundary values up to an overall normalization factor. This normalization factor can be determined by computing a simple integral like the bubble integral at one loop or the sunrise integral at two loops.

Using the one-loop hexagon differential equation as the example, we will see how we can determine the values of our integral basis at the point

$$\vec{v}_0 = \{-1, -1, -1, -1, -1, -1, -1, -1, -1\} \quad (4.103)$$

up to weight four in the ϵ expansion by imposing the absence of certain spurious singularities and by matching to the analytical solution of a bubble integral which is known analytically

$$\tilde{I}_1 = \epsilon e^{\epsilon\gamma_E} \frac{\Gamma(-\epsilon)^2 \Gamma(1 + \epsilon)}{\Gamma(-2\epsilon)(-s_{12})^\epsilon}. \quad (4.104)$$

To be a bit more explicit, even though the Feynman integrals in our basis are manifestly finite throughout the Euclidean region, this is not true for the DE matrix A . In fact, the vanishing (or divergence) of any of the hexagon letters

$$W_i = 0, \quad (4.105)$$

defines a hypersurface that might intersect the Euclidean region. The situation is sketched in Fig. 4.2. Imposing finiteness of the solution to the canonical differential equation (4.38) on any of these hypersurfaces severely constrains the possible boundary values at the point \vec{v}_0 , c.f. [210]. Hence, we will determine the c_{ij} in the expansion

$$\tilde{I}_i(\vec{v}_0) = \sum_{j=0}^4 c_{ij} \epsilon^j. \quad (4.106)$$

We also denote the vector of boundary constants as

$$\vec{b} = \tilde{I}(\vec{v}_0). \quad (4.107)$$

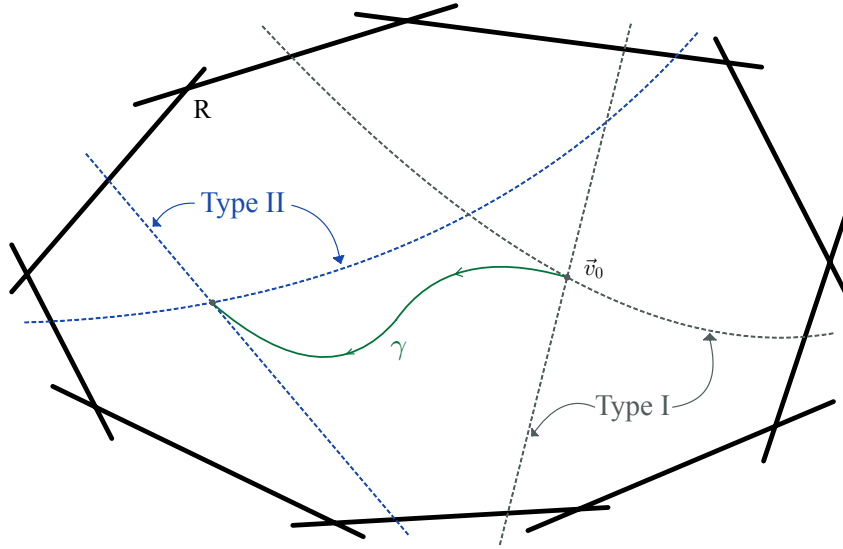


Figure 4.2: Schematic representation of the Euclidean region R which is bounded by the inequalities $s_{ij} < 0$ and $s_{ijk} < 0$ (solid black lines). The dashed lines represent different hypersurfaces where some alphabet letters W_j vanish.

In the following analysis, we will call spurious letter singularities at the bulk point \vec{v}_0 *type-I singularities* and singularities on any other hypersurfaces that do not contain \vec{v}_0 *type-II singularities*; see Figure 4.2.

Absence of Type-I Singularities

We parameterize the paths that start at the boundary point \vec{v}_0 by an infinitesimal parameter δ to remove spurious letter divergences at that point. Then, the divergent letters will have an expansion in δ according to

$$\log W_j = c_j \log \delta + \mathcal{O}(1). \quad (4.108)$$

The set of letters vanishing at \vec{v}_0 is given by

$$\mathbb{A}_0 = \{W_{10}, \dots, W_{21}, W_{28}, \dots, W_{33}\}. \quad (4.109)$$

Since the master integrals are supposed to diverge only on the boundaries of the Euclidean region, the boundary vector must be such that

$$\lim_{\delta \rightarrow 0} A \vec{b} = \text{finite}. \quad (4.110)$$

Using different parametrizations to approach the boundary point on different curves, we find that this requirement constrains \vec{b} (non-perturbatively in ϵ) to be of the form

$$\vec{b} = \{b_1, b_1, b_1, b_1, b_1, b_1, b_1, b_1, b_1, b_1, b_{10}, b_{11}, b_{12}, b_{13}, b_{14}, b_{15}, b_{16}, b_{17}, b_{18}, b_{19}, b_{20}, b_{21},$$

$$\begin{aligned}
& -b_{12} + b_{14} - b_{15} + b_{17} + b_{18} - b_{19} + b_{21}, -b_{13} + b_{14} - b_{16} + b_{17} + b_{18} - b_{20} + b_{21}, \\
& 0, 0, 0, 0, 0, 0, 0, 0, 0, 0\}.
\end{aligned} \tag{4.111}$$

Absence of Type-II Singularities

Beyond the singular letters at the point \vec{v}_0 , there are additional letters that diverge at some other point in the Euclidean region, for example

$$\log W_{22} = \log(-s_{12} - s_{23} + s_{123}). \tag{4.112}$$

In order to prevent these singularities from appearing in our differential equation solution, we perform the integration from the boundary point \vec{v}_0 to the hypersurface where the additional letters diverge. By enforcing the absence of logarithmic divergences, we further restrict the boundary constants b_i . Given that we typically lack a non-perturbative solution to (4.38), these constraints are perturbative in ϵ . A convenient path from \vec{v}_0 to the hypersurface where W_{21} vanishes is given by

$$\vec{v} = \{-1, -(1-x)^2, -1, -(1-x)^2, -1, -(1-x)^2, -1+x, -1+x, -1+x\}, \tag{4.113}$$

which satisfies the Gram constraint. On this line, the hexagon alphabet simplifies to

$$\mathbb{A} \rightarrow \mathbb{A}_{\text{line}} = \{x, 1-x, x-\rho, x-\bar{\rho}\}, \tag{4.114}$$

with $\rho = \frac{1}{2}(1 + i\sqrt{3})$. Hence, there are four potential singular points on the line. The absence of type-I singularities ensures that all $\log x$ singularities are dropped. The $\log(1-x)$ singularities lie on the boundary of the Euclidean region and hence are not necessarily unphysical. Finally, the singularities at the points ρ and $\bar{\rho}$ are nonphysical, and we can further determine the boundary values by imposing them to drop out.

Using POLYLOGTOOLS [23], it is straightforward to integrate the differential equation with the alphabet (4.114) into GPLs with entries $\{0, 1, \rho, \bar{\rho}\}$. To isolate the singularities, we use shuffle identities to bring the GPLs to a convenient Lyndon basis [211], see also Chapter 8 of Ref. [71]. Then, imposing that all $\log(x-\rho)$ drop out for $x \rightarrow \rho$ (and similarly for $x \rightarrow \bar{\rho}$), we can fully determine the boundary values order by order in ϵ . Up to weight four, we find the following non-vanishing boundary constants,

$$\begin{aligned}
b_{1,\dots,9} &= -2 + \zeta_2 \epsilon^2 + \frac{14}{3} \zeta_3 \epsilon^3 + \frac{47}{8} \zeta_4 \epsilon^4 + \mathcal{O}(\epsilon^5), \\
b_{10,11} &= i(6 \operatorname{Im}[\operatorname{Li}_2(1-\rho^2)] + 2\pi \log(3)) \epsilon^2 \\
&\quad + i\left(\frac{10}{9} \pi \zeta_2 + 12 \operatorname{Im}[\operatorname{Li}_3(1-\rho^2)] + \pi \log^2(3)\right) \epsilon^3 \\
&\quad + i\left(-3\zeta_2 \operatorname{Im}[\operatorname{Li}_2(1-\rho^2)] + 24 \operatorname{Im}[\operatorname{Li}_4(1-\rho^2)]\right. \\
&\quad \left. + \frac{16}{3} \operatorname{Im}[\operatorname{Li}_4(1+\rho^2)] + \frac{\pi}{3} \log^3(3) + 12\pi \zeta_2 \log(3)\right) \epsilon^4 + \mathcal{O}(\epsilon^5),
\end{aligned}$$

$$\begin{aligned}
b_{12,\dots,17} &= 2 - 3\epsilon^2\zeta_2 - \frac{20}{3}\epsilon^3\zeta_3 - \frac{43}{8}\epsilon^4\zeta_4 + \mathcal{O}(\epsilon^5), \\
b_{18,\dots,23} &= 1 - \epsilon^2\frac{\zeta_2}{2} + \epsilon^3\frac{\zeta_3}{3} + \epsilon^4\left(\frac{17}{16}\zeta_4 + 6 \operatorname{Im}[\operatorname{Li}_2(1 - \rho^2)]^2\right. \\
&\quad \left. + \frac{2}{3}\pi^2 \log^2(3) + 4\pi \log(3) \operatorname{Im}[\operatorname{Li}_2(1 - \rho^2)]\right) + \mathcal{O}(\epsilon^5).
\end{aligned} \tag{4.115}$$

Both Li_n and ζ_n are functions of transcendental weight n and therefore the boundary values are of uniform transcendental weight. In addition, the constants appearing in equation (4.115) are embedded in the basis of polylogarithms at sixth roots of unity discussed in Ref. [212].

Moreover, the inverse leading singularities of all pentagon integrals and the hexagon integral vanish on the entire line, leading to trivial boundary conditions for these functions. With these constants determined, we have full analytic control over the entire function space at weight four on the line given by (4.113).

The boundary constants in Eq. (4.115) are valid in the Euclidean region. To obtain the boundary constants in the physical scattering regions defined in the example in Section 2.1, we can either perform an analytic continuation or determine the boundary constants directly in the physical region of interest following a similar procedure [210].

4.6 One-loop Hexagon Function Space

Although canonical differential equations can be solved to any desired order in the dimensional regulator ϵ by employing iterated integrals (4.80 – 4.81), for the calculation of physical scattering amplitudes, it is common practice to determine them up to the finite part. It is conjectured that an L -loop Feynman integral in D dimensions can at most involve transcendental functions of weight $\lfloor \frac{LD}{2} \rfloor$. This statement was proven for generic masses in Ref. [84]. As a consequence, we are interested in the solution of the canonical differential equation (4.38) up to weight four in the dimensional regulator ϵ .

At weights one and two, we can explicitly integrate the iterated integrals (4.80) into special functions such that they are well-defined in the whole Euclidean region. Moreover, the only integrals that contribute at these weights are the ones coming from the subsectors, thus their function space is already known [213–215].

At weight one, we need to perform a one-fold integration over the $d \log$ kernel

$$\log(x) = \int_0^x \frac{dt}{t} \tag{4.116}$$

Therefore, the only function that can appear is the logarithm

$$f_i^{(1)} = \log(-s_{ii+1}), \quad i = 1, \dots, 6, \tag{4.117}$$

$$f_{i+6}^{(1)} = \log(-s_{ii+1i+2}), \quad i = 1, \dots, 3. \tag{4.118}$$

The minus sign in the argument of the logarithm is included so that the functions are well-defined within the Euclidean region.

At weight two, we construct the initial basis as

$$\{f^{(2)}, (f^{(1)}f^{(1)}), \zeta_2\}, \quad (4.119)$$

where $f^{(2)}$ are weight–two functions and $(f^{(1)}f^{(1)})$ are products of two weight–one functions given in (4.118). Genuine weight–two functions that can appear are dilogarithms Li_2 . We chose the arguments of these functions so that they are well defined in the Euclidean region. Genuine weight two functions that appear are:

$$\begin{aligned} f_1^{(2)} &= \text{Li}_2\left(1 - \frac{s_{12}}{s_{123}}\right), & f_{i+1}^{(2)} &= T^i f_1^{(2)}, & i &= 1, \dots, 5, \\ f_7^{(2)} &= \text{Li}_2\left(1 - \frac{s_{23}}{s_{123}}\right), & f_{i+7}^{(2)} &= T^i f_7^{(2)}, & i &= 1, \dots, 5, \\ f_{13}^{(2)} &= \text{Li}_2\left(1 - \frac{s_{12}s_{45}}{s_{123}s_{345}}\right), & f_{i+13}^{(2)} &= T^i f_{13}^{(2)}, & i &= 1, \dots, 2, \\ f_{16}^{(2)} &= \text{Tri}(s_{12}, s_{34}, s_{56}), & f_{17}^{(2)} &= \text{Tri}(s_{23}, s_{45}, s_{61}), \end{aligned} \quad (4.120)$$

where the $\text{Tri}(a, b, c)$ function is the Bloch–Wigner dilogarithm

$$\begin{aligned} \text{Tri}(a, b, c) &= -\text{Li}_2\left(-\frac{2b}{a-b-c-\sqrt{\Delta_3(a, b, c)}}\right) - \text{Li}_2\left(-\frac{2c}{a-b-c-\sqrt{\Delta_3(a, b, c)}}\right) \\ &\quad - \frac{\pi^2}{6} - \frac{1}{2} \log\left(\frac{c}{b}\right) \log\left(\frac{a-b+c-\sqrt{\Delta_3(a, b, c)}}{a+b-c-\sqrt{\Delta_3(a, b, c)}}\right) \\ &\quad - \frac{1}{2} \log\left(\frac{2b}{-\sqrt{\Delta_3(a, b, c)}+a-b-c}\right) \log\left(\frac{2c}{-\sqrt{\Delta_3(a, b, c)}+a-b-c}\right). \end{aligned} \quad (4.121)$$

This basis of special functions is sufficient to express the solution up to weight two for any master integral in our one–loop hexagon integral basis.

We still need to get weight three and four parts of the solution. We could try to find a similar basis of functions at higher weight consisting of classical polylogarithms like Li_3 and Li_4 and multiple polylogarithms like $\text{Li}_{2,2}$. Finding such a basis of functions is not easy, since it is not generally understood which arguments to use in order for them to form a basis and for their symbol to belong to the given alphabet. Moreover, we could also demand that such functions be well defined in a desired kinematic region. In general, there is no completely algorithmic way to find such functions even though there are systematic strategies [101]. Computing the symbol of a classical polylogarithm

$$\mathcal{S}(\text{Li}_n(R)) = -(1-R) \otimes \underbrace{R \otimes \dots \otimes R}_{(n-1) \text{ entries}}, \quad (4.122)$$

we see that both R and $(1-R)$ must factorize in terms of the letters of the alphabet W_i

$$R = c \prod_{i \in \mathbb{A}} W_i^{e_i}, \quad 1-R = c' \prod_{i \in \mathbb{A}} W_i^{e'_i}. \quad (4.123)$$

Another requirement is that the arguments of the polylogarithms have to be dimensionless which puts constraints on allowed powers c_i and c'_i . However, there is no algorithmic way to solve these constraints which in turn makes finding allowed arguments quite difficult especially when considering bigger alphabets.

Additionally, at higher weights, there is a proliferation of terms that may lead to a slowdown in numerical evaluations. This is a consequence of functional identities that relate different arguments of polylogarithms. For example, already at weight two, the dilogarithm satisfies two reflection identities [216]

$$\begin{aligned}\mathrm{Li}_2\left(\frac{1}{x}\right) &= -\mathrm{Li}_2(x) - \frac{\pi^2}{6} - \frac{1}{2}\log^2(-x), \\ \mathrm{Li}_2(1-x) &= -\mathrm{Li}_2(x) + \frac{\pi^2}{6} - \log(x)\log(1-x),\end{aligned}\quad (4.124)$$

which tell us that dilogarithms

$$\left\{\mathrm{Li}_2(x), \mathrm{Li}_2\left(\frac{1}{1-x}\right), \mathrm{Li}_2\left(\frac{x-1}{x}\right), -\mathrm{Li}_2\left(\frac{1}{x}\right), -\mathrm{Li}_2(1-x), -\mathrm{Li}_2\left(\frac{x}{x-1}\right)\right\} \quad (4.125)$$

are all equivalent modulo elementary functions. There are even more complicated identities like the five-term identity

$$\mathrm{Li}_2(x) + \mathrm{Li}_2(y) + \mathrm{Li}_2\left(\frac{1-x}{1-xy}\right) + \mathrm{Li}_2(1-xy) + \mathrm{Li}_2\left(\frac{1-y}{1-xy}\right) = \quad (4.126)$$

$$\frac{\pi^2}{6} - \log(x)\log(1-x) - \log(y)\log(1-y) + \log\left(\frac{1-x}{1-xy}\right) + \log\left(\frac{1-y}{1-xy}\right). \quad (4.127)$$

Identities similar to these also exist for higher-weight functions. For example, one of the identities at weight three is

$$\mathrm{Li}_3(x) + \mathrm{Li}_3(1-x) + \mathrm{Li}_3\left(1 - \frac{1}{x}\right) = \zeta_3 + \frac{1}{6}\log^3(x) + \frac{\pi^2}{6}\log(x) - \frac{1}{2}\log^2(x)\log(1-x). \quad (4.128)$$

There are many more identities similar to this that make finding an optimal basis of functions difficult. Equivalent arguments of polylogarithms produce branch cuts in different locations of the kinematic space. Therefore, we might end up writing a very complicated zero if we do not account for all different relations between the arguments, which slows down numerical evaluations.

To avoid an increase in the number of terms at higher weights, we follow a hybrid approach suggested in Ref. [217]. Assuming that we know the boundary value at the point \vec{v}_0 up to weight $(n+2)$ and function basis up at weight n

$$f^{(n)}(\vec{v}) = [W_{i_1}, \dots, W_{i_n}]_{\vec{v}_0}(\vec{v}), \quad (4.129)$$

we can use that information to set up a one-fold integration to obtain weight $-(n+1)$ and weight $-(n+2)$ functions. Setting up a straight path from the boundary point \vec{v}_0 to some end point \vec{v}_i

$$\gamma(t) = (1-t)\vec{v}_0 + t\vec{v}_i, \quad (4.130)$$

we obtain weight $-(n+1)$ functions as a one-fold integral over the weight $-n$ functions

$$\tilde{I}^{(n+1)}(\vec{v}_i) = \vec{b}^{(n+1)} + \int_0^1 dt_1 \frac{d\tilde{A}}{dt_1} \vec{f}^{(n)}(t_1). \quad (4.131)$$

At weight $(n+2)$, we need to perform two integrations over the weight $-n$ functions

$$\tilde{I}^{(n+2)}(\vec{v}_i) = \vec{b}^{(n+2)} + \int_0^1 dt \frac{d\tilde{A}}{dt} \vec{b}^{(n+1)} + \int_0^1 dt_1 \int_0^{t_1} dt_2 \frac{d\tilde{A}}{dt_1} \frac{d\tilde{A}}{dt_2} \vec{f}^{(n)}(t_2). \quad (4.132)$$

Using integration by parts with respect to t_1 , we rewrite the two-fold integration as a one-fold integration

$$\tilde{I}^{(n+2)}(\vec{v}_i) = \vec{b}^{(n+2)} + \int_0^1 dt \left(\frac{d\tilde{A}}{dt} \vec{b}^{(n+1)} + (\tilde{A}(1) - \tilde{A}(0)) \frac{d\tilde{A}}{dt} \vec{f}^{(n)}(t) \right). \quad (4.133)$$

Although the representations given in equations (4.131) and (4.133) hold globally, both the weight $-n$ functions and the differential equation matrix \tilde{A} are multivalued functions. Therefore, we must make sure that they are evaluated on the right Riemann sheet and that an analytic continuation is performed in an appropriate way if the contour γ goes beyond the region of analyticity where the boundary point \vec{v}_0 lies.

Going back to our one-loop hexagon example, the finite part of the pentagon and hexagon integrals are transcendental functions of weight three, and the first correction is of weight four. These functions are obtained using the one-fold integral representation (4.131) and (4.133) from the known weight-two functions and the boundary value at the point \vec{v}_0 .

We choose several points in the bulk of the Euclidean region (see Table 4.1) and construct straight paths to those points. The point $\vec{v}^{(1)}$ corresponds to the point $K^{(3)}$ from Ref. [218] while the points $\vec{v}^{(2)}$ and $\vec{v}^{(3)}$ are generic points within the Euclidean region. Implementing the one-fold integration in `Mathematica` using the `NIntegrate` function, we numerically evaluate all of our basis integrals. Moreover, we compare the numerical values obtained using the one-fold integral representation with the values obtained using `AMFlow` and find that the results are in complete agreement.

Even by using a simple `Mathematica` implementation of one-fold integration, running times are significantly faster compared to state-of-the-art software for numerical evaluation of Feynman integrals such as `pySecDec` and `AMFlow`. For example, it takes around ~ 1 minute to evaluate all of the basis integrals using the one-fold integral representation, while it takes ~ 10 minutes to do the same with `AMFlow` on the same machine.

Moreover, explicit expressions of polylogarithms at high transcendental weight often fall short compared to the performance of one-fold integral representations in terms of

Kinematic point	\tilde{I}_{33}
$\vec{v}^{(1)} = \left\{ -1, -1, -1, -1, -1, -1, -\frac{1}{2}, -\frac{5}{8}, -\frac{17}{14} \right\}$	$1.69878610466574714627i\epsilon^3$ $+ 6.62873216549319714468i\epsilon^4$ $+ \mathcal{O}(\epsilon^5)$
$\vec{v}^{(2)} = \left\{ -\frac{2}{3}, -\frac{7}{10}, -\frac{9}{11}, -\frac{15}{17}, -\frac{24}{29}, -\frac{30}{37}, -\frac{37}{43}, -\frac{47}{53}, -\frac{53}{59} \right\}$	$1.2966474952363382027i\epsilon^3$ $+ 5.241756401399539064i\epsilon^4$ $+ \mathcal{O}(\epsilon^5)$
$\vec{v}^{(3)} = \left\{ -\frac{7}{9}, -\frac{4}{5}, -\frac{29}{33}, -\frac{47}{51}, -\frac{77}{87}, -\frac{97}{111}, -\frac{39}{43}, -\frac{49}{53}, -\frac{55}{59} \right\}$	$0.81389548925976547185i\epsilon^3$ $+ 3.2221858302838235961i\epsilon^4$ $+ \mathcal{O}(\epsilon^5)$

Table 4.1: Numerical evaluation of the hexagon integral at several kinematic points. The values correspond to the UT hexagon integral and are obtained using the one-fold integral representation.

computational efficiency [213–215, 217]. Therefore, since the highest transcendental weight required in two-loop computations in $D = 4 - 2\epsilon$ dimensions is weight four, having an explicit basis of functions up to weight two allows us to numerically evaluate all necessary functions in an efficient way.

For phenomenological applications of our results, a necessary requirement is the evaluation of the hexagon integrals in the $2 \rightarrow 4$ physical scattering region. Although the same differential equations are satisfied as in the Euclidean region, the transition to the physical scattering region requires additional refinements. One approach is to determine the values of the entire basis of integrals at a particular boundary point within the physical domain and solve the differential equations with a new boundary value. Alternatively, we could use a suitable analytic continuation to transfer the information from our known boundary point to the desired physical region. This involves navigating a complex landscape of analytic functions to ensure that the data obtained on the Euclidean plane are seamlessly extended to the relevant physical scattering domain.

4.6.1 Symbol of the Hexagon Integral

Of course, the most interesting integral in our basis is the massless hexagon integral. In this section, we discuss its finite part and its order epsilon part in generic external spacetime dimensions D_{ext} . The finite part of the hexagon integral was first calculated in Ref. [219]. Using the canonical differential equation matrix \tilde{A} and the boundary constants determined in section 4.5, it is straightforward to determine the symbols for the $\mathcal{O}(1)$ and $\mathcal{O}(\epsilon)$ parts of the hexagon integral. In agreement with Ref. [219], we find

$$\mathcal{S}^{(3)}(\tilde{I}_{33}) = (u_1 \otimes u_2 + u_2 \otimes u_1 - \sum_{j=1}^3 u_j \otimes (1 - u_j)) \otimes y_3 + (\text{cyclic}) \quad (4.134)$$

where we used the dual–conformal cross ratios

$$u_1 = \frac{s_{12}s_{45}}{s_{123}s_{345}}, \quad u_2 = \frac{s_{23}s_{56}}{s_{234}s_{123}}, \quad u_3 = \frac{s_{34}s_{61}}{s_{345}s_{234}}, \quad (4.135)$$

as well as the parity–odd dual–conformal letters

$$y_1 = \frac{1 + u_1 - u_2 - u_3 - \sqrt{\Delta}}{1 + u_1 - u_2 - u_3 + \sqrt{\Delta}}, \quad y_2 = \frac{1 + u_2 - u_3 - u_1 - \sqrt{\Delta}}{1 + u_2 - u_3 - u_1 + \sqrt{\Delta}}, \quad y_3 = \frac{1 + u_3 - u_1 - u_2 - \sqrt{\Delta}}{1 + u_3 - u_1 - u_2 + \sqrt{\Delta}}, \quad (4.136)$$

where $\Delta = (1 - u_1 - u_2 - u_3)^2 - 4u_1u_2u_3$ and it is related to the leading singularity of the hexagon integral through the following relation

$$\sqrt{\Delta_6} = s_{123}s_{234}s_{345}\sqrt{\Delta}. \quad (4.137)$$

Both u_i and y_i form threefold orbits under cyclic permutations of the external points.

At weight four, the symbol of the hexagon decomposes according to³

$$\mathcal{S}^{(4)}(\tilde{I}_{33}) = \mathcal{S}^{(3)}(\tilde{I}_{33}) \otimes W_{hex} + \sum_{i=1}^6 T_i \left(\mathcal{S}^{(3)}(\tilde{I}_{27}) \otimes W_{100} \right) + \frac{1}{2} \sum_{i=1}^3 T_i (\Omega \otimes W_{90}), \quad (4.138)$$

where we remind the reader that \tilde{I}_{27} and its permutations are the one–mass pentagons and Ω is given by the following combination of box integrals

$$\begin{aligned} \Omega = & \mathcal{S}^{(3)}(\tilde{I}_{18}) + \mathcal{S}^{(3)}(\tilde{I}_{19}) + \mathcal{S}^{(3)}(\tilde{I}_{21}) + \mathcal{S}^{(3)}(\tilde{I}_{22}) \\ & - \mathcal{S}^{(3)}(\tilde{I}_{13}) - \mathcal{S}^{(3)}(\tilde{I}_{16}) - \mathcal{S}^{(3)}(\tilde{I}_{24}) - \mathcal{S}^{(3)}(\tilde{I}_{25}) - \mathcal{S}^{(3)}(\tilde{I}_{26}). \end{aligned} \quad (4.139)$$

By inspecting the expressions for the symbol at weight three and four, we can determine the reduced alphabets that are necessary to describe the hexagon integral at weight three and weight four respectively. They read

$$\mathbb{A}_{hex}^{(3)} = \{u_1, u_2, u_3, 1 - u_1, 1 - u_2, 1 - u_3, y_1, y_2, y_3\} \quad (4.140)$$

and

$$\mathbb{A}_{hex}^{(4)} = \mathbb{A} \setminus \{W_{41}, \dots, W_{48}\}. \quad (4.141)$$

Starting at weight five, all 104 letters of the one–loop hexagon alphabet appear in the symbol.

4.6.2 Limit to Four–Dimensional External Momenta

It is well known that for four–dimensional external momenta, the hexagon integral can be decomposed into a linear combination of pentagon integrals [220–224], i.e.

$$I_{33} = -\frac{1}{2} \sum_{j,k=1}^6 (S^{-1})_{jk} I_{26+j}, \quad (4.142)$$

³We note that $W_{hex} = -\Delta_6/G(p_1, p_2, p_3, p_4, p_5)$, $W_{90} = 1/y_3$, $W_{91} = 1/y_1$ and $W_{92} = 1/y_2$.

with

$$S = -\frac{1}{2} \begin{pmatrix} 0 & 0 & s_{45} & s_{123} & s_{23} & 0 \\ 0 & 0 & 0 & s_{56} & s_{234} & s_{34} \\ s_{45} & 0 & 0 & 0 & s_{61} & s_{345} \\ s_{123} & s_{56} & 0 & 0 & 0 & s_{12} \\ s_{23} & s_{234} & s_{61} & 0 & 0 & 0 \\ 0 & s_{34} & s_{345} & s_{12} & 0 & 0 \end{pmatrix}. \quad (4.143)$$

In this section, we show that this identity comes out of the differential equation for free as a finiteness condition in four-dimensional kinematics. When the kinematics are generated by four-dimensional vectors, the nine Mandelstam invariants are not independent anymore but they satisfy the Gram determinant constraint,

$$G(p_1, p_2, p_3, p_4, p_5) = 0. \quad (4.144)$$

A parameterization of the external degrees of freedom that hardwires this constraint, as well as momentum conservation and on-shell conditions, can be provided by choosing a momentum twistor configuration [225]. We employ a particular parameterization [226, 227]

$$\begin{aligned} s_{12} &= x_1, \\ s_{23} &= x_1 x_5, \\ s_{34} &= \frac{x_1 [x_5 - x_2 x_3 x_6 + x_3 x_5 (1 + x_2 - x_2 x_7)]}{x_2}, \\ s_{45} &= x_1 \left[x_5 - x_5 x_7 - (1 + x_3) x_4 (x_5 (-1 + x_7) + x_8) + \frac{x_2 x_3 x_4 (x_5 (-1 + x_7) + x_6 x_8)}{x_5} \right], \\ s_{56} &= \frac{x_1 x_3 [(x_2 - x_5) x_5 (-1 + x_7) + (-x_5 + x_2 x_6) x_8]}{x_5}, \\ s_{61} &= \frac{x_1 x_2 x_3 x_4 [x_5 (-x_6 + x_7) + x_6 x_8]}{x_5}, \\ s_{123} &= x_1 x_8, \\ s_{234} &= x_1 x_3 (x_2 x_6 - x_5 x_7), \\ s_{345} &= x_1 \left\{ x_6 + x_4 \left\{ -1 + x_6 + x_3 \left[-1 + x_6 + x_2 \left(-1 + x_7 + \frac{x_6 x_8}{x_5} \right) \right] \right\} \right\} \end{aligned} \quad (4.145)$$

where $x_i \in \mathbb{R}$ are unconstrained variables.

In terms of the momentum twistor variables, the leading singularities of the pentagons and the hexagons become perfect squares. However, substituting the parametrization into the differential equation matrix \tilde{A} , a subset of logarithmic letters diverges, namely

$$\mathbb{A}_{\text{div}} = \{W_{hex}, W_{99}, \dots, W_{104}\}. \quad (4.146)$$

Since $W_{hex} = -\Delta_6/G(p_1, p_2, p_3, p_4, p_5)$, it is obvious why it diverges. However, the divergence of the logs of the letters W_{96}, \dots, W_{101} are less straightforward and require some

explanation. Let us focus on W_{96} since the behaviour of the other letters follows from cyclic permutations. It takes the form

$$W_{99} = \frac{R_4 - \sqrt{\Delta_{5,1}\Delta_6}}{R_4 + \sqrt{\Delta_{5,1}\Delta_6}}, \quad (4.147)$$

where

$$\Delta_{5,1} = \Delta_5(s_{12}, s_{23}, s_{34}, s_{123}, s_{234}, s_{56}) \quad (4.148)$$

and R_4 is a homogeneous polynomial of degree four. The exact form of R_4 is provided in Section 3.4, but it is not important for this discussion. By inspection, one finds

$$\Delta_{5,1}\Delta_6 = R_4^2 - 4s_{12}s_{23}s_{34}(s_{23}s_{56} - s_{123}s_{234})G(p_1, p_2, p_3, p_4, p_5) \quad (4.149)$$

which is valid for arbitrary D -dimensional kinematics. Clearly, in the limit of four-dimensional external kinematics, the product of $\Delta_{5,1}$ and Δ_6 approaches the square of R_4 and we have

$$W_{99} \Big|_{D_{\text{ext}} \rightarrow 4} \rightarrow \frac{R_4 - |R_4|}{R_4 + |R_4|}. \quad (4.150)$$

Depending on the sign of R_4 , the letter W_{95} will either vanish or diverge in the limit $D \rightarrow 4$, hence its logarithm will go to $\mp\infty$.

The divergent letters appear only in the last row of the matrix, i.e. the derivative of the hexagon integral, and correspond to the coefficients of the pentagon and hexagon integrals in this derivative. Hence, for the four-dimensional limit of the hexagon integral to be finite, these divergences must cancel. To approach the surface where the Gram determinant constraint holds more carefully, we deform the two-particle Mandelstam invariants by a small parameter δ , i.e.

$$s_{i,i+1} \rightarrow s_{i,i+1} + \delta, \quad i = 1, \dots, 6, \quad (4.151)$$

explicitly breaking the Gram determinant constraint at order $\mathcal{O}(\delta)$. Then, the divergent letters take the form⁴

$$W_i = -c_i \log(\delta) + \mathcal{O}(1), \quad W_i \in \mathbb{A}_{\text{div}}, \quad (4.152)$$

where the signs of the $\log(\delta)$ divergence depend of the sign of R_4 , i.e.

$$c_{99+i} = \text{sgn}(T^i R_4), \quad i = 0, \dots, 5, \quad (4.153)$$

whereas $c_{40} = -1$. The requirement that the logarithmic divergence cancels leads to a very simple identity for the UT integrals in four-dimensional kinematics, namely

$$\tilde{I}_{33} = \sum_{j=0}^5 c_{99+j} \tilde{I}_{27+j}. \quad (4.154)$$

⁴Note that this analysis is valid for a generic point in four-dimensional kinematics, at which no other letters diverge. At more special points, there can be additional constraints emerging from the differential equation.

Interestingly, comparing with the well-known identity (4.142), we find after dividing (4.154) by Δ_6

$$\frac{\Delta_{5,j}}{\Delta_6} = \left(\frac{1}{2} \sum_{k=1}^6 (S^{-1})_{jk} \right)^2 \quad (4.155)$$

on the momentum twistor parametrization. Hence, after taking into account the signs c_i , the identity we find from the canonical differential equation for the UT integrals is equivalent to (4.142).

At the level of the weight-four symbol of the hexagon integral, the four-dimensional limit implies

$$\lim_{D_{\text{ext}} \rightarrow 4} \mathcal{S}^{(4)}(\tilde{I}_{33}) = \frac{1}{2} \sum_{i=1}^3 T_i(\Omega \otimes W_{90}), \quad (4.156)$$

where Ω is the linear combination of weight-three symbols of box-integrals given in eq. (4.139).

Relations between Letters in Four-Dimensional Kinematics

Beyond the divergent letters, there are additional dependencies among the letters that emerge in four-dimensional kinematics. For ease of discussion, we consider only the case where all $c_i = -1$. Other cases can be obtained through Galois transformations that map the corresponding square roots to their negatives (and thereby invert the respective odd letters). The complete set of identities is

$$\begin{aligned} T^{i-1} \left(\frac{W_{90}}{W_{65}W_{66}} \right) &= 1, \quad i = 1, \dots, 6 \\ T^{i-1} (W_{93}W_{95}W_{97}) &= 1, \quad i = 1, 2 \\ T^{i-1} \left(\frac{W_{72}W_{74}W_{84}}{W_{61}W_{67}W_{78}} \right) &= 1, \quad i = 1, \dots, 6 \\ T^{i-1} \left(\frac{W_{78}W_{81}W_{90}W_{91}W_{92}}{W_{62}W_{65}W_{68}W_{71}W_{74}W_{77}} \right) &= 1, \quad i = 1, 2, 3. \end{aligned} \quad (4.157)$$

The hexagon alphabet reduces to 89 independent letters on the support of these identities.

At last, we can compare the results valid for $D_{\text{ext}} > 4$ and $D_{\text{ext}} = 4$ kinematics. We find it very convenient to work in a $D_{\text{ext}} > 4$ setting and only fix the dimensionality to four at the very end by using momentum twistor variables (4.145) which satisfy the Gram determinant constraint (4.144). Although the integral family is slightly larger in $D_{\text{ext}} > 4$, we profit from a more systematic understanding of the alphabet and manifest realizations of permutation invariance. While at one loop, the single additional independent integral in $D_{\text{ext}} > 4$ kinematics is not a vast complication, at two-loops there is a bigger trade-off between additional integrals and alphabet letters on the one hand and clearer structures and free movement in the nine-dimensional kinematic space on the other hand.

In this chapter, we have outlined a method for the analytical computation of Feynman integrals. We began with an integral family and used the IBP reduction method in Section 4.1 to relate it to a basis of integrals. Dimension shift identities were also introduced, connecting integrals in D dimensions with those in $(D + 2)$ or $(D - 2)$ dimensions, which helped in finding a UT basis. This basis facilitates the simplification of the differential equation in the canonical form; see Section 4.3. Another essential component of the canonical differential equation (4.38), along with the UT basis, are the alphabet letters that act as arguments for the dlog forms. Alphabet letters encode the singularity structure of Feynman integrals, see Chapter 3, and specify the types of possible solutions. To fully specify the solution in Section 4.4, we have determined the boundary values at a specific point in Section 4.5.

Finally, we are in a position to apply these techniques to a state-of-the-art computation of planar two-loop six-point Feynman integral families in the next chapter.

Chapter 5

Two-Loop Six-Point Feynman Integrals

The last few years have seen substantial advancements in the computation of two-loop Feynman integrals, scattering amplitudes, and cross sections. Analytical calculations for two-loop five-point massless integrals have been achieved [210, 213, 228–230], offering a comprehensive set for $2 \rightarrow 3$ massless scattering process.

In particular, a dedicated computer implementation has been established for efficient and reliable evaluation of five-point Feynman integrals in the physical region, detailed in Ref. [214]. Analytical progress has already found applications in various amplitude computations [231–245] and phenomenological processes [246–250].

In addition, all master integrals for two-loop five-point scattering with one off-shell leg [116, 119, 251, 252] were calculated analytically and the results were further optimized for fast evaluation of the functions in the physical scattering region [215].

On the other hand, for the production of four or more jets, i.e., for the $2 \rightarrow 4$ massless scattering process, only NLO cross sections are known in the literature [253, 254]. On the amplitude side, one-loop six-gluon [255, 256] and photon amplitudes [257–260] are known. However, only the special case of all plus helicities for the two-loop six-gluon amplitudes is presented in the literature [261, 262].

On the Feynman integrals side, in Ref. [226], the potential of computing two-loop six-point integrals in dimensional regularization via integrals with uniform transcendentality weights and the canonical differential equation was demonstrated. The maximal cuts of a UT basis for genuine (non-factorizable) two-loop six-point massless planar integrals were found and the diagonal blocks of the canonical differential equations and symbol letters were calculated. Based on these results, we computed the off-diagonal blocks for three out of six integral families in [263].

In this chapter, we review the computation we performed in [263] where the double-box, pentagon-triangle, and hexagon-bubble families were computed. Moreover, we extend these results to two additional families, namely the pentagon-box family and the hexagon-box family. Hence, the only missing family at the time of writing this thesis is the double-pentagon family.

This chapter is organized as follows. In Section 5.1, we review the six-point kinematics and set up conventions that are used throughout the chapter. In Section 5.3, we present the complete UT basis for the two-loop six-point hexagon-box, pentagon-box, double-box, pentagon-triangle and hexagon-bubble families. In Section 5.4, we describe how to efficiently calculate the differential equation by fitting against an ansatz in terms of the hexagon alphabet. To that end, we employ an efficient method to find algebraic symbol letters introduced in Section 3.4. In Section 5.5, we identify all the symbol letters that appear in the canonical differential equations for those five families, defining the symbol alphabet. In Section 5.6, the boundary values at a specific point are obtained analytically based on the singularity structure of the canonical differential equations in the Euclidean region. Furthermore, we set up integration paths in the Euclidean region to solve the canonical differential equations. The weight one and two parts of those integrals are presented in terms of classical polylogarithms, while weight three and four parts are presented as one-fold iterated integrals suitable for fast numerical evaluation.

The majority of this chapter follows the structure of Ref. [263] where the results for three families, the double-box, pentagon-triangle and hexagon-bubble families, are presented. The discussion is altered in several places to provide additional information about the UT basis and the two new families. Additionally, labels of the alphabet letters are modified to accommodate a larger alphabet needed to express the remaining two families.

5.1 Kinematics and Conventions

Kinematics of the massless six-point Feynman integrals were introduced in the example of Section 2.1. There are nine independent kinematic invariants for the momenta defined in $D_{\text{ext}} > 4$

$$\vec{v} = \{s_{12}, s_{23}, s_{34}, s_{45}, s_{56}, s_{61}, s_{123}, s_{234}, s_{345}\} \quad (5.1)$$

with

$$s_{ij} = (p_i + p_j)^2, \quad s_{ijk} = (p_i + p_j + p_k)^2. \quad (5.2)$$

Since only four vectors can be independent in four dimensions, there is a linear relation among any five momenta. After using momentum conservation to eliminate p_6 , the remaining constraint is captured by the vanishing of the following Gram determinant,

$$G(1, 2, 3, 4, 5) = 0. \quad (5.3)$$

This reduces the number of independent Mandelstam variables from nine to eight.

Throughout this chapter, we use a scheme such that external momenta are in four dimensions, while the loop integration is $(4 - 2\epsilon)$ -dimensional. At the level of the amplitudes, this is compatible with both the 't Hooft-Veltman and the four-dimensional helicity scheme. An advantage of computing in this scheme is that we can use a momentum twistor

parametrization [225] to rationalize the majority of square roots in the canonical differential equation. Furthermore, in this convention, the number of irreducible scalar products is smaller than the corresponding number for D -dimensional external momenta; see Section 5.2 for the discussion.

To fully describe the kinematics of a scattering process, in addition to the parity-even invariants mentioned earlier, it is essential to determine the sign of a parity-odd pseudo-scalar invariant [30]. A pseudo-scalar can be formed by contracting the antisymmetric Levi-Civita tensor with any four momenta of the scattering process, i.e.

$$\epsilon_{ijkl} \equiv 4\sqrt{-1} \epsilon_{\mu_1\mu_2\mu_3\mu_4} p_i^{\mu_1} p_j^{\mu_2} p_k^{\mu_3} p_l^{\mu_4}, \quad 1 \leq i, j, k, l \leq 6. \quad (5.4)$$

Only one of these objects is independent, since the product of two ϵ_{ijkl} may be written in terms of a Gram determinant. In particular, the squares of the pseudo scalars equal

$$\epsilon_{ijkl}^2 = G(i, j, k, l). \quad (5.5)$$

Spinor-Helicity Variables

In spinor-helicity variables the sign of the ϵ_{ijkl} is fixed via

$$2[ij]\langle jk\rangle[kl]\langle li\rangle = s_{ij}s_{kl} - s_{ik}s_{jl} + s_{il}s_{jk} + \epsilon_{ijkl}. \quad (5.6)$$

Here, the spinor products are defined as,

$$\begin{aligned} \langle ij \rangle &\equiv \lambda_i^\alpha \lambda_{j,\alpha}, \\ [ij] &\equiv \tilde{\lambda}_{i,\dot{\alpha}} \tilde{\lambda}_j^{\dot{\alpha}}, \end{aligned} \quad (5.7)$$

and the bi-spinor is given by

$$p_{i\mu} \sigma_{\alpha\dot{\beta}}^\mu = \lambda_{i\alpha} \tilde{\lambda}_{j\dot{\beta}}, \quad (5.8)$$

with the Pauli matrices $\sigma^\mu = (I_{2\times 2}, \sigma^1, \sigma^2, \sigma^3)$.

We also introduce the object

$$\begin{aligned} \Delta_6 &= \text{tr}(\gamma_5 \not{p}_1 \not{p}_2 \not{p}_3 \not{p}_4 \not{p}_5 \not{p}_6) \\ &= \langle 12 \rangle [23] \langle 34 \rangle [45] \langle 56 \rangle [61] - [12] \langle 23 \rangle [34] \langle 45 \rangle [56] \langle 61 \rangle, \end{aligned} \quad (5.9)$$

which naturally arises as the four-dimensional limit of the leading singularity of the one-loop hexagon integral (4.68). In the definition of Δ_6 we employ slashed momenta and the chiral γ_5 , both of which are 4×4 matrices given by

$$\not{p}_i = \begin{pmatrix} 0 & |i\rangle\langle i| \\ |i\rangle[i| & 0 \end{pmatrix}, \quad \gamma_5 = \begin{pmatrix} \mathbf{1}_{2\times 2} & 0 \\ 0 & -\mathbf{1}_{2\times 2} \end{pmatrix}. \quad (5.10)$$

Momentum Twistor Parametrization

Throughout this chapter, we will work with the momenta defined in $D_{\text{ext}} = 4$. Therefore, we need to solve the Gram determinant constraint (5.3).

We adopt momentum twistor variables [225], which have been proven to be valuable in studying scattering amplitudes. Momentum twistors automatically satisfy momentum conservation and massless on-shell conditions. Additionally, they hardwire the Gram determinant constraint, allowing us to describe the six-point kinematics in terms of eight unconstrained variables. For a more comprehensive understanding of momentum twistors and detailed definitions, interested readers can refer to [225].

For our purposes, it is sufficient to know that for an n -particle process, we encode the external kinematics via n momentum twistors

$$Z_i = (\lambda_i, \mu_i), \quad (5.11)$$

which are related to invariants built from consecutive sums of momenta via

$$(p_i + p_{i+1} + \cdots + p_{j-1})^2 = \frac{\langle i-1j-1j \rangle}{\langle i-1i \rangle \langle j-1j \rangle}, \quad (5.12)$$

with the momentum twistor four-bracket $\langle ijkl \rangle = \epsilon^{ijkl} Z_i Z_j Z_k Z_l$ and the ordinary spinor brackets $\langle ij \rangle = \langle ij I_\infty \rangle$ which are expressed in terms of momentum twistors using the infinity bitwistor

$$I_\infty = \begin{pmatrix} 0 & 0 \\ 0 & 0 \\ 0 & 1 \\ -1 & 0 \end{pmatrix}. \quad (5.13)$$

In the case of six external momenta, we can use $\text{SL}(4)$ -transformations of the momentum twistors, to pick a particular parametrization in terms of eight independent variables x_j , cf. [227]. To be explicit, in the remainder of this paper we will use

$$Z = \begin{pmatrix} 1 & 0 & x_1 & x_1 x_2 & x_1 x_3 & x_1 x_6 \\ 0 & 1 & 1 & x_8 & 1 & 1 \\ 0 & 0 & 0 & 1 & x_4 & 1 \\ 0 & 0 & 1 & 0 & x_5 & x_7 \end{pmatrix}, \quad (5.14)$$

where $\vec{x} = \{x_1, \dots, x_8\}$ are free variables. The parametrization in (5.14) can be written explicitly as,

$$\begin{aligned} s_{12} &= \frac{1}{x_1}, & s_{23} &= \frac{1}{x_1(x_2 - x_8)}, & s_{34} &= \frac{x_3 - x_2 x_4 - x_5}{x_1(x_3 x_8 - x_2)}, \\ s_{45} &= \frac{x_2(x_4(1 - x_7) + x_5 - 1) - x_5(x_6 + x_8 - 1) - (x_6 - x_7)(x_4 x_8 - 1) + x_3(x_7 + x_8 - 1)}{x_1(x_3 - x_6)(x_2 - x_8)}, \\ s_{56} &= -\frac{x_8 x_5 - x_5 + x_7 - x_4 x_7 x_8}{x_1(x_2 - x_3 x_8)}, & s_{61} &= -\frac{x_5 - x_4 x_7}{x_1(x_3 - x_6)}, \end{aligned}$$

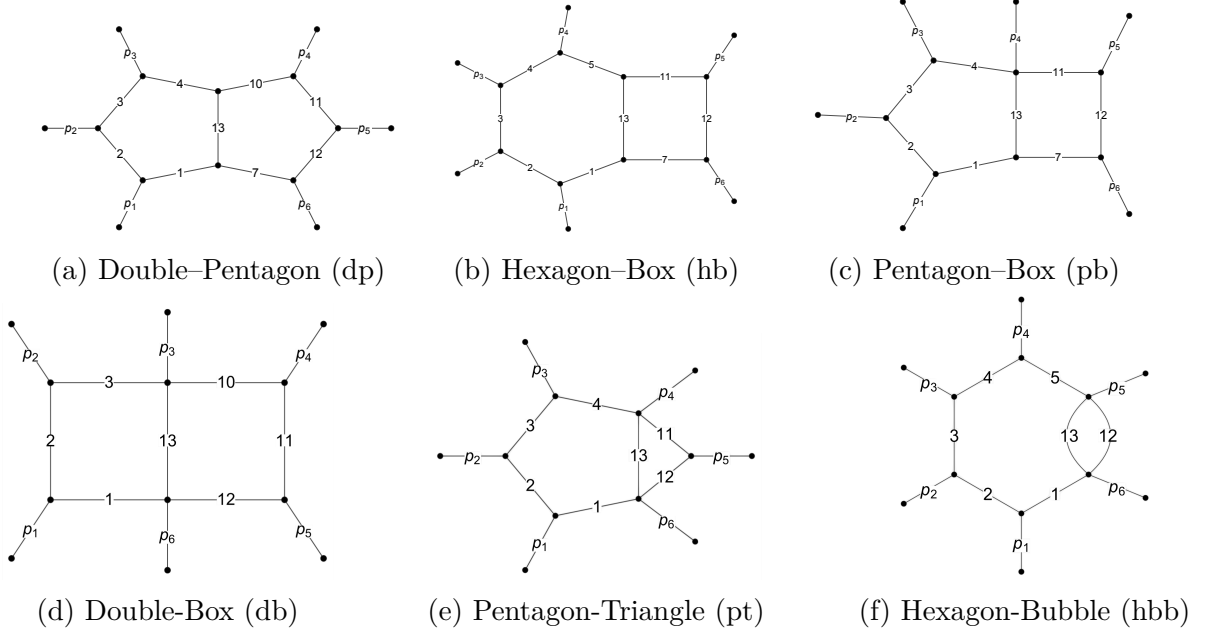


Figure 5.1: Two-loop six-point massless planar Feynman diagrams.

$$s_{123} = \frac{x_7 + x_8 - 1}{x_1(x_8 - x_2)}, \quad s_{234} = \frac{x_5}{x_1(x_2 - x_3x_8)}, \quad s_{345} = \frac{x_3 - x_5 - x_4x_6 + x_4x_7}{x_1(x_3 - x_6)}. \quad (5.15)$$

All ϵ_{ijkl} and Δ_6 , appearing in the alphabet and in the normalization of UT integrals, are rationalized by this parametrization, e.g.

$$\epsilon_{1234} = -\frac{x_7(x_3 + x_4x_8 - 1) + x_2(x_5 + x_4(x_8 - x_7) - 1)}{x_1^2(x_2 - x_8)(x_2 - x_3x_8)}. \quad (5.16)$$

Note that the parity degree of freedom is reflected in the momentum twistor space by the fact that (5.15) has two different solutions for any choice of Mandelstam invariants.

5.2 Integral Families

All planar two-loop hexagon integrals take the general form

$$I_{\bar{a}} = e^{2\epsilon\gamma_E} \int \frac{d^{4-2\epsilon}l_1}{i\pi^{2-\epsilon}} \frac{d^{4-2\epsilon}l_2}{i\pi^{2-\epsilon}} \frac{N}{\prod_{j=1}^{13} D_j^{\nu_j}}, \quad (5.17)$$

where $\nu_j \in \mathbb{Z}$, N is a numerator that possibly depends on the external and loop momenta, whereas the denominators D_j are chosen as

$$D_1 = -l_1^2, \quad D_2 = -(l_1 - p_1)^2, \quad D_3 = -(l_1 - p_1 - p_2)^2, \quad D_4 = -(l_1 - p_1 - p_2 - p_3)^2, \\ D_5 = -(l_1 - p_1 - p_2 - p_3 - p_4)^2, \quad D_6 = -(l_1 - p_1 - p_2 - p_3 - p_4 - p_5)^2,$$

$$\begin{aligned}
D_7 &= -l_2^2, & D_8 &= -(l_2 + p_1)^2, & D_9 &= -(l_2 + p_1 + p_2)^2, \\
D_{10} &= -(l_2 + p_1 + p_2 + p_3)^2, & D_{11} &= -(l_2 + p_1 + p_2 + p_3 + p_4)^2, \\
D_{12} &= -(l_2 + p_1 + p_2 + p_3 + p_4 + p_5)^2, & D_{13} &= -(l_1 + l_2)^2.
\end{aligned} \tag{5.18}$$

In Section 2.1, the propagators are defined with an overall minus sign compared to the propagators listed here. The difference between the two conventions is just an overall factor of $(-1)^\nu$ where $\nu = \sum_j \nu_j$.

In this chapter, we study the five out of six families in which at most nine of the ν_j take positive values. Up to permutations of the external legs, these families can be described by the Feynman diagrams in Figure 5.1, which we call top-topologies, and the diagrams which are obtained by pinching some of the internal legs, which we refer to as subtopologies. The calculation of the top-topology integrals is the main goal of this chapter. We are considering the following families distinguished by which ν_j 's are allowed to be non-negative:

$$\begin{aligned}
&\text{hexagon-box (hb): } \nu_1, \nu_2, \nu_3, \nu_4, \nu_5, \nu_7, \nu_{11}, \nu_{12}, \nu_{13} \geq 0, \\
&\text{pentagon-box (pb): } \nu_1, \nu_2, \nu_3, \nu_4, \nu_7, \nu_{11}, \nu_{12}, \nu_{13} \geq 0, \\
&\text{double-box (db): } \nu_1, \nu_2, \nu_3, \nu_{10}, \nu_{11}, \nu_{12}, \nu_{13} \geq 0, \\
&\text{pentagon-triangle (pt): } \nu_1, \nu_2, \nu_3, \nu_4, \nu_{11}, \nu_{12}, \nu_{13} \geq 0, \\
&\text{hexagon-bubble (hbb): } \nu_1, \nu_2, \nu_3, \nu_4, \nu_5, \nu_{12}, \nu_{13} \geq 0,
\end{aligned} \tag{5.19}$$

For the remaining values of j , we have $\nu_j \leq 0$.

Note that the set of propagators (5.18) is only linearly independent for external momenta defined in $D_{\text{ext}} > 4$ space-time dimensions. If the external momenta are four-dimensional, there are two identities connecting the propagators. This is because e.g. $p_5 \cdot l_1$ and $p_5 \cdot l_2$ may be expressed in terms of scalar products between the loop momenta and the first four external momenta. We could explicitly use these identities to eliminate two of the above propagators (irreducible scalar products). However, this involves making an arbitrary choice which propagators to remove. This obscures the simple structures of the UT integrals we describe in the following Section 5.3. Instead, we add the corresponding integral identities to the seeds of the IBP system. To be more explicit, we choose to rewrite the scalar products between loop momenta and p_5 or p_6 in terms of the other four momenta according to the following

$$\begin{aligned}
l_j \cdot p_k &= \frac{1}{G(1, 2, 3, 4)} \left[G \begin{pmatrix} p_k & p_2 & p_3 & p_4 \\ p_1 & p_2 & p_3 & p_4 \end{pmatrix} l_j \cdot p_1 + G \begin{pmatrix} p_1 & p_k & p_3 & p_4 \\ p_1 & p_2 & p_3 & p_4 \end{pmatrix} l_j \cdot p_2 + \right. \\
&\quad \left. G \begin{pmatrix} p_1 & p_2 & p_k & p_4 \\ p_1 & p_2 & p_3 & p_4 \end{pmatrix} l_j \cdot p_3 + G \begin{pmatrix} p_1 & p_2 & p_3 & p_k \\ p_1 & p_2 & p_3 & p_4 \end{pmatrix} l_j \cdot p_4 \right],
\end{aligned} \tag{5.20}$$

for $j = 1, 2$ and $k = 5, 6$. We then insert these identities as numerators into the seed integrals and treat them in the same manner as the ordinary IBP identities that are generated using LITERED [132].

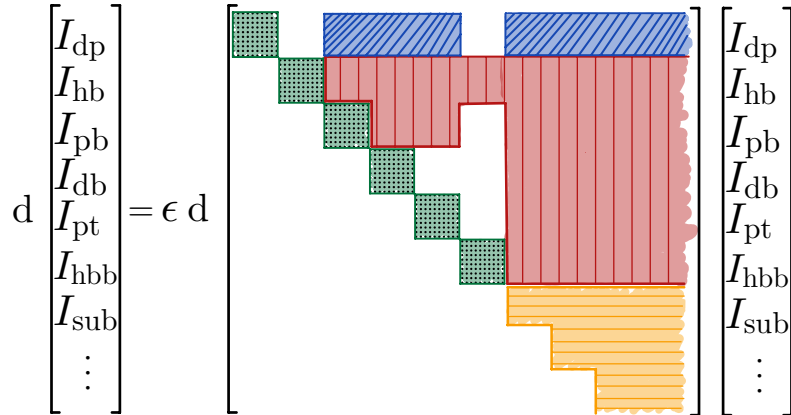


Figure 5.2: Schematic representation of the structure of the canonical differential equation (4.38) for the two-loop six-point planar integral families. The green blocks with a dotted pattern represent the maximal cut blocks computed in [226], the yellow blocks with horizontal lines represent the subsector integrals [116] and the red blocks with vertical lines are the ones discussed here. Moreover, the blue blocks with diagonal lines correspond to the off-diagonal blocks of the double-pentagon family. Their computation is left for future work.

As expected, for all six-point integral families, the number of master integrals with four-dimensional kinematics is lower than the number of master integrals for D -dimensional kinematics. The kinematic identities from relations like (5.20) reduce the number of master integrals.

5.3 Canonical Bases of Master Integrals

In Ref. [226] the UT basis for the two-loop hexagon families on their respective maximal cuts was discovered, and the corresponding canonical differential equation on the cut was calculated. This corresponds to the blocks on the diagonal of the matrix of the differential equation $d\tilde{A}$, see Figure 5.2. However, the full expression of the UT integrals or the canonical differential equation was unknown beyond the maximal cut. The definitions of the UT integrals beyond their maximal cuts for three of the top-sector families: the double-box, the pentagon-triangle, and the hexagon-bubble family (see Figure 5.1) were calculated in [263]. In the remainder of this section, we extend the definitions of the UT integrals beyond their maximal cuts for two additional families: the hexagon-box and pentagon-box families. In addition to the newly constructed top sector integrals, we use the known subsector integrals from Ref. [116] to complete the UT basis. Complete canonical differential equations, including the off-diagonal blocks, are obtained using the methods described in Chapter 4. Note that, at the time of writing this thesis, only the

off-diagonal blocks of the double-pentagon family are not known.

Finding a canonical basis at higher loops is much harder compared to one loop. One of the main difficulties arises from the fact that at higher loop orders we can have more than one master integral in each sector. Therefore, finding enough UT integrals in each sector can be a problem. The general strategy which we use to find “good” candidates for UT integrals, in this section, is to write them as “ D -dimensional” as possible. This means that we want to replace possible chiral numerators from Ref. [226], with numerators of definite parity and where scalar products are written in terms of Gram determinants. Moreover, we utilize known one-loop results (see Section 4.3) and dimension-shift identities (see Section 4.2) to write possible numerators of UT integrals.

5.3.1 Hexagon-Box Family

There is only one master integral in the top sector of this family. Here, we can find the UT integral by performing leading singularity analysis in the loop-by-loop Baikov representation introduced in Section 2.4.

We start with the right loop. There we have a one-loop box diagram with loop momenta l_2 and independent external momenta p_5 , p_6 , and l_1 . The Baikov polynomial and the Gram determinant that involve just the external momenta that appear in the Baikov representation (2.44) are

$$P_R = G(l_2, p_5, p_6, l_1), \quad G(p_5, p_6, l_1). \quad (5.21)$$

We are left with the left loop which is a pentagon integral with independent external momenta p_1, p_2, p_3, p_4 , and loop momentum l_1 . Hence, the Gram determinants we have to consider are

$$P_L = G(l_1, p_1, p_2, p_3, p_4), \quad G(p_1, p_2, p_3, p_4). \quad (5.22)$$

Since we are considering a box with four Baikov variables and a pentagon with five Baikov variables, we end up with a loop-by-loop representation which depends on nine variables

$$I_{hb}^{(LbL)} \sim \int d^9 z P_R^{\frac{D-5}{2}} [G(p_5, p_6, l_1)]^{-\frac{D+4}{2}} P_L^{\frac{D-6}{2}} [G(p_1, p_2, p_3, p_4)]^{-\frac{D+5}{2}} \prod_{k=1}^9 \frac{1}{z_k^{\nu_k}}. \quad (5.23)$$

The leading singularity is obtained by cutting all propagators $z_i = 0$, setting $D = 4$ and computing the residue

$$\text{LS} \left(I_{hb}^{(LbL)} \right) = \frac{[G(p_1, p_2, p_3, p_4)]^{\frac{1}{2}}}{s_{56}(l_1 \cdot p_6) P_L} \quad (5.24)$$

Therefore, the UT integral with constant leading singularity is

$$I_{hb} = \epsilon^4 e^{2\epsilon\gamma_E} \int \frac{d^{4-2\epsilon} l_1}{i\pi^{2-\epsilon}} \frac{d^{4-2\epsilon} l_2}{i\pi^{2-\epsilon}} \frac{N_{hb}}{D_1 D_2 D_3 D_4 D_5 D_7 D_{11} D_{12} D_{13}}, \quad (5.25)$$

where the numerator is

$$N_{hb} = s_{56} \frac{G(l_1, p_1, p_2, p_3, p_4)}{\epsilon_{1234}} (l_1 + p_6)^2. \quad (5.26)$$

In addition, there are 201 integrals in the basis coming from the subtopologies. Sixteen of those correspond to six–point integrals discussed in the remainder of this section and 185 are from five–point sectors. This is shown schematically in the figure 5.3.

5.3.2 Pentagon–Box Family

There are three master integrals in the top sector of the pentagon–box integral family. Similarly to the other integral families, we aim to have the UT integrals of definite parity and write the scalar products appearing in the numerators in terms of Gram determinants. This leads us to use a different basis compared to Ref. [226]. The three UT integrals can be written as

$$I_{\text{pb},i} = \epsilon^4 e^{2\epsilon\gamma_E} \int \frac{d^{4-2\epsilon}l_1 d^{4-2\epsilon}l_2}{i\pi^{2-\epsilon} i\pi^{2-\epsilon}} \frac{N_{\text{pb},i}}{D_1 D_2 D_3 D_4 D_7 D_{11} D_{12} D_{13}}, \quad i = 1, \dots, 3, \quad (5.27)$$

where the numerators are

$$N_{\text{pb},1} = s_{56} \frac{G(l_1, p_1, p_2, p_3, p_6)}{\epsilon_{6123}}, \quad (5.28)$$

$$N_{\text{pb},2} = s_{12} s_{23} s_{56} (l_1 + p_6)^2, \quad (5.29)$$

$$N_{\text{pb},3} = 4 \frac{-s_{12}\epsilon_{4561} + s_{123}\epsilon_{5612}}{G(p_1, p_2, p_3, p_6)} G \begin{pmatrix} l_1 & p_1 & p_2 & p_3 & p_6 \\ l_2 & p_1 & p_2 & p_3 & p_6 \end{pmatrix}. \quad (5.30)$$

These numerators can be obtained in the following way. We know that a one–loop pentagon is UT if normalized by its leading singularity in $D = 6$ dimensions and similarly a one–loop box is UT in $D = 4$ dimensions. Therefore, we can use a dimension–lowering relation (4.10) to lower the dimension of the pentagon loop to $D = 4$ and “glue” it to the one–loop box. This results in the numerator $N_{\text{pb},1}$. The second numerator can be obtained from leading singularity analysis in the loop–by–loop Baikov representation. Here, the additional $D_6 = (l_1 + p_6)^2$ in the numerator effectively turns the pentagon–box into a double–box whose leading singularity is $(s_{12} s_{23} s_{56})^{-1}$. Finally, the last numerator is obtained by computing a leading singularity of the pentagon–box integral with the following numerator

$$G \begin{pmatrix} l_1 & p_1 & p_2 & p_3 & p_6 \\ l_2 & p_1 & p_2 & p_3 & p_6 \end{pmatrix} \quad (5.31)$$

in the loop–by–loop Baikov representation.

Additionally, 114 integrals come from subtopologies. Seven of them are coming from the double–box family, one from the pentagon–triangle family, and the remaining ones from the five–point one–mass integrals.

5.3.3 Double–Box Family

The double–box top sector contains seven master integrals. In addition, the subsectors of the double–box family include 59 master integrals [116]. Although the integrals introduced

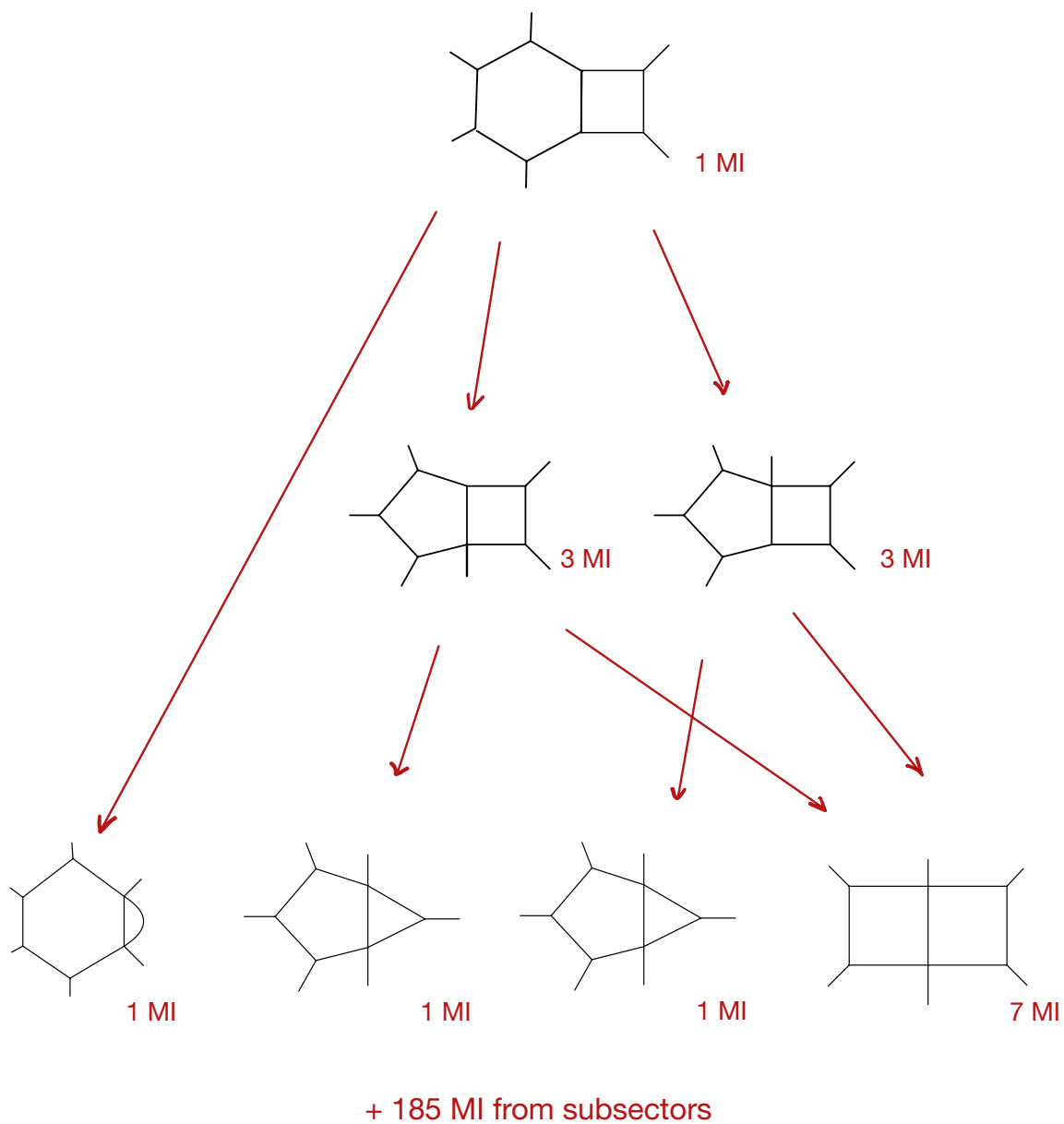


Figure 5.3: Schematic representation of the hexagon–box basis of integrals. The red arrows represent different pinches of propagators that lead to different six–point topologies. The number of master integrals (MI) for each of the topologies is written in the bottom right corner of the corresponding diagram.

in Ref. [226] produce an ϵ -factorised differential equation on the maximal cut (i.e., when all subsector integrals are set to zero), this property does not persist beyond the maximal cut. Therefore, it is necessary to modify the UT basis beyond the maximal cut. Essentially, the findings in Ref. [226] are not sensitive to redefinitions of the top-sector master integrals, which vanish on the maximal cut but might compromise the UT property of the integrals.

In the double-box sector given in Figure (5.1a), the seven double-box UT integrals can be chosen as,

$$I_{\text{db},i} = \epsilon^4 e^{2\epsilon\gamma_E} \int \frac{d^{4-2\epsilon}l_1 d^{4-2\epsilon}l_2}{i\pi^{2-\epsilon} i\pi^{2-\epsilon}} \frac{N_{\text{db},i}}{D_1 D_2 D_3 D_{10} D_{11} D_{12} D_{13}}, \quad i = 1, \dots, 6, \quad (5.32)$$

$$I_{\text{db},7} = \epsilon^4 e^{2\epsilon\gamma_E} \int \frac{d^{4-2\epsilon}l_1 d^{4-2\epsilon}l_2}{i\pi^{2-\epsilon} i\pi^{2-\epsilon}} \frac{N_{\text{db},7}}{D_1 D_2 D_3 D_{10} D_{11} D_{12} D_{13}^2}, \quad (5.33)$$

where

$$N_{\text{db},1} = -s_{12}s_{45}s_{156}, \quad (5.34)$$

$$N_{\text{db},2} = -s_{12}s_{45}(l_1 + p_5 + p_6)^2, \quad (5.35)$$

$$N_{\text{db},3} = \frac{s_{45}}{\epsilon_{5126}} G \begin{pmatrix} l_1 & p_1 & p_2 & p_5 + p_6 \\ p_1 & p_2 & p_5 & p_6 \end{pmatrix}, \quad (5.36)$$

$$N_{\text{db},4} = \frac{s_{12}}{\epsilon_{1543}} G \begin{pmatrix} l_2 - p_6 & p_5 & p_4 & p_1 + p_6 \\ p_1 & p_5 & p_4 & p_3 \end{pmatrix}, \quad (5.37)$$

$$N_{\text{db},5} = -\frac{1}{4} \frac{\epsilon_{1245}}{G(1, 2, 5, 6)} G \begin{pmatrix} l_1 & p_1 & p_2 & p_5 & p_6 \\ l_2 & p_1 & p_2 & p_5 & p_6 \end{pmatrix}, \quad (5.38)$$

$$N_{\text{db},6} = \frac{1}{8} G \begin{pmatrix} l_1 & p_1 & p_2 \\ l_2 - p_6 & p_4 & p_5 \end{pmatrix} + \frac{D_2 D_{11} (s_{123} + s_{345})}{8}, \quad (5.39)$$

$$N_{\text{db},7} = -\frac{1}{2\epsilon} \frac{\Delta_6}{G(1, 2, 4, 5)} G \begin{pmatrix} l_1 & p_1 & p_2 & p_4 & p_5 \\ l_2 & p_1 & p_2 & p_4 & p_5 \end{pmatrix}. \quad (5.40)$$

To get the above concise expression of UT integrals, we used two guiding principles: we aim at constructing integrals of definite parity and at writing scalar products in terms of Gram determinants. Even though there is no guarantee that the resulting integrals will be UT, we find empirically that these principles help us to find a canonical basis. The UT integrals on the maximal cut that were presented in Ref. [226] are constructed by employing chiral numerators in terms of spinor brackets, hence they transform non-trivially under parity and are only sensible in four-dimensional kinematics. For example, for the double-box top sector, consider a pair of conjugate chiral numerators in terms of spinor helicity formalism,

$$\mathcal{N}_A = s_{45} (\langle 15 \rangle [52] + \langle 16 \rangle [62]) l_1 \cdot (\lambda_2 \tilde{\lambda}_1), \quad (5.41)$$

$$\mathcal{N}_B = s_{45} ([15] \langle 52 \rangle + [16] \langle 62 \rangle) l_1 \cdot (\lambda_1 \tilde{\lambda}_2). \quad (5.42)$$

From the six-point four-dimensional kinematics, choose $\{p_1, p_2, p_5, p_6\}$ as a basis and a linear expansion shows,

$$\begin{aligned} & (\langle 15 \rangle [52] + \langle 16 \rangle [62]) \lambda_2 \tilde{\lambda}_1 + ([15] \langle 52 \rangle + [16] \langle 62 \rangle) \lambda_1 \tilde{\lambda}_2 \\ & = (s_{25} + s_{26}) p_1 + (s_{15} + s_{16}) p_2 - s_{12} p_5 - s_{12} p_6. \end{aligned} \quad (5.43)$$

Therefore the parity-even combination of two chiral numerators equals,

$$\begin{aligned} \mathcal{N}_A + \mathcal{N}_B &= -\frac{1}{2} s_{12} s_{45} (l_1 + p_5 + p_6)^2 + \frac{1}{2} s_{12} s_{45} s_{156} \\ &+ \left(\text{terms proportional to } D_1, \dots, D_7 \right). \end{aligned} \quad (5.44)$$

So we use $N_2 = s_{12} s_{45} (l_1 + p_5 + p_6)^2$ in (5.35) as a numerator to obtain a UT integral. The parity-odd combination has the following kinematic relation,

$$\mathcal{N}_A - \mathcal{N}_B = \frac{-8 s_{45} G \begin{pmatrix} l_1 & p_1 & p_2 & p_5 + p_6 \\ p_5 & p_1 & p_2 & p_6 \end{pmatrix}}{\epsilon_{5126}}, \quad (5.45)$$

so we formulate the expression of N_3 in (5.36) as another numerator to construct a UT integral. The numerator N_4 is also a parity-odd combination of chiral numerators.

The numerator N_6 originates from the product of two chiral numerators. The second term in (5.39) is obtained by transforming the whole differential equation, including the subsectors, to the canonical form. Furthermore, N_7 is discovered from the on-cut IBP reduction to the maximally cut UT basis of the double box in [226].

5.3.4 Penta-Triangle Family

There is one master integral in the top sector. An appropriate choice of uniform transcendentality integral is

$$I_{\text{pt}} = \epsilon^4 e^{2\epsilon\gamma_E} \int \frac{d^{4-2\epsilon} l_1}{i\pi^{2-\epsilon}} \frac{d^{4-2\epsilon} l_2}{i\pi^{2-\epsilon}} \frac{N_{\text{pt}}}{D_1 D_2 D_3 D_4 D_{11} D_{12} D_{13}}, \quad (5.46)$$

with numerator

$$N_{\text{pt}} = \frac{1}{32} \frac{G(l_1, p_1, p_2, p_3, p_5)}{\epsilon_{1235}}. \quad (5.47)$$

This is obtained by using a lowering dimension-shift relation (4.10) on the pentagon loop.

In addition, there are 43 integrals from subtopologies.

5.3.5 Hexagon-Bubble Family

There is one master integral in the top sector. An appropriate choice of uniform transcendentality integral is

$$I_{\text{hbb}} = \epsilon^3 e^{2\epsilon\gamma_E} \int \frac{d^{4-2\epsilon} l_1}{i\pi^{2-\epsilon}} \frac{d^{4-2\epsilon} l_2}{i\pi^{2-\epsilon}} \frac{N_{\text{hb}}}{D_1 D_2 D_3 D_4 D_5 D_{12} D_{13}^2}, \quad (5.48)$$

with numerator

$$N_{\text{hbb}} = \frac{1}{32} \frac{G(l_1, p_1, p_2, p_3, p_4)}{\epsilon_{1234}} (l_1 + p_6)^2. \quad (5.49)$$

Notice that the propagator D_{13} is doubled. This comes from a raising dimension–shift relation (4.13) acting on the bubble loop. Similarly, the numerator can be thought of as a dimension lowering operator acting on the hexagon loop. The additional irreducible scalar product in the numerator, $D_6 = (l_1 + p_6)^2$, transforms the hexagon into a pentagon and the fraction involving Gram determinants lowers the dimension of the pentagon from $D = 6$ to $D = 4$.

In addition, there are 31 integrals from subtopologies.

5.4 Efficiently Calculating Feynman Integrals

As described in Chapter 4, the method of differential equations has proved to be a very powerful tool for analytic computations of Feynman integrals. Since the derivatives of (5.17) with respect to the external variables can be expanded in terms of the same family of integrals, there is a completely algorithmic way to express them in terms of the master integrals of the respective family using IBP identities; see Section 4.1. However, the swell of intermediate expressions renders this approach unfeasible for state-of-the-art applications. Since this algorithm relies solely on linear algebra involving rational functions of kinematic variables, it can be drastically accelerated by using finite field reconstructions [137–139]. In a nutshell, the required calculations are performed for integer–valued kinematics modulo some large prime. Then, once enough information about the resulting rational functions is known, they can be reconstructed in an analytical form. However, in our particular application of eight–scale six–point integrals, the functional reconstruction itself poses a significant bottleneck of this computation. Hence, it is invaluable to provide as much analytic information about the function space as possible, to simplify this final reconstruction step.

Reconstruction and solving of differential equations is simplified by choosing a basis of master integrals \vec{I}_{fam} that consists of pure transcendental functions of uniform transcendental weight; see Section 4.3. Then, the derivatives for the integral family take the canonical form

$$d\vec{I}_{\text{fam}}(\epsilon, \vec{x}) = \epsilon d\tilde{A}_{\text{fam}}(\vec{x}) \cdot \vec{I}_{\text{fam}}(\epsilon, \vec{x}), \quad (5.50)$$

where the total differential is given in terms of the eight momentum twistor variables and the basis integrals are described in Section 5.3. Here and in the following we use the subscript $\text{fam} \in \{\text{hb}, \text{pb}, \text{db}, \text{pt}, \text{hbb}\}$ to distinguish the five families under study, see Figure 5.1. A special feature of eq. (5.50) is that the dependence on the dimensional regulator ϵ is via a factor on the R.H.S., so that the matrix $d\tilde{A}_{\text{fam}}$ depends on the kinematics only. This matrix is expanded in a basis of dlog forms according to

$$d\tilde{A}_{\text{fam}}(\vec{x}) = \sum_j c_j^{(\text{fam})} d\log(w_j(\vec{x})), \quad (5.51)$$

where the w_j are algebraic functions of the kinematic variables, whereas the $c_j^{(\text{fam})}$ are block upper triangular matrices whose entries are rational constants. The size of these matrices is determined by the number of master integrals for each of the families. There are 202, 117, 66, 44, and 32 master integrals for the hexagon-box, the pentagon-box, the double-box, the pentagon-triangle and the hexagon-bubble family, respectively. The required alphabet for the five families of integrals we are studying is described in Section 5.5. Moreover, machine-readable expressions for the UT basis, \tilde{A} matrices and the alphabet can be found at

github.com/antonela-matijasic/hexagon-functions.git.

We also note that the question of whether an integral basis can possibly form a canonical basis can be tested efficiently. It is sufficient to perform the finite field evaluation of the differential equation for a small set of kinematic configurations and for different values of ϵ to verify the ϵ -factorized form. Hence, this step does not require functional reconstruction.

Naively, to find the \tilde{A}_{fam} matrices, one would reconstruct the rational functions in the derivative matrices

$$\tilde{A}_{\text{fam}}^j = \frac{\partial \tilde{A}_{\text{fam}}}{\partial x_j}, \quad (5.52)$$

and integrate those into dlog forms sequentially. In the present case, where some of the leading singularities evaluate to square roots, the square roots have to be extracted from the derivative matrices first. This is straightforward to do, cf. Sec. 6.3 of [139]. However, reconstruction can be avoided entirely if the alphabet \mathbb{A} is known a priori [228]. Then, provided that a UT basis has been found, the only remaining objects to determine are the \mathbb{Q} -valued matrices $c_j^{(\text{fam})}$ in equation (5.51). This amounts to a linear fit problem. Since here the final step only consists in a rational reconstruction, instead of a functional reconstruction, this approach requires only a small number of finite field evaluations.

Ultimately, combined knowledge of the UT basis and the alphabet allows efficient determination of differential equations. Calculating the full differential equation in this setup takes around 1.25 hours, 41 minutes and 31 minutes for the double-box, pentagon-triangle and hexagon-bubble, respectively.¹ While for the families with more master integrals, the pentagon-box and the hexagon-box family, it took around 1 and 4 days, respectively, to solve the IBP system and to fit the alphabet.² In contrast, performing a partial functional reconstruction of the dependence on 7 out of the 8 variables on one single entry of the double-box partial differential equation takes roughly 41 hours on a more powerful machine³, rendering the whole reconstruction of all 8 partial derivatives for all non-vanishing elements highly inefficient.

¹The timings were obtained on AMD Ryzen 7 5700G, with 8 CPU cores and only involve solving the IBPs and the linear fit step.

²The timings were obtained on Intel(R) Xenon(R) Platinum 8160 CPU @ 2.10 GHz using 4 threads with 100 GB and 1 thread with 4 TB of memory for the pentagon-box and the hexagon-box, respectively.

³We used 4 threads on Intel(R) Xenon(R) Platinum 8160 CPU @ 2.10 GHz with 800 GB of memory.

5.5 The Hexagon Alphabet at Two Loops

The analytical structure of the function space of two-loop hexagon integrals is encoded in the hexagon alphabet \mathbb{A} .

The hexagon alphabet consists of letters known from two-loop five-point integrals with one off-shell leg [116] rewritten in terms of six-particle kinematics, letters from the maximal cut [226], letters from the one-loop hexagon integrals [79], and new letters appearing in the off-diagonal blocks of the differential equations.

The alphabet presented in the following sections is closed under the action of dihedral transformations. Hence, it will be sufficient to describe not only the integrals studied in this paper but also all of their dihedral images. The dihedral group is generated by cyclic permutations T defined via

$$T(p_i) = p_{i+1}, \quad i = 1, \dots, 6, \quad (p_7 \equiv p_1), \quad (5.53)$$

and reflections ρ

$$\rho(p_i) = p_{8-i}, \quad i = 1, \dots, 6, \quad (5.54)$$

where the indices on the right-hand side are defined modulo 6.

With permutations included, the two-loop hexagon alphabet has 283 letters, which we classify according to parity transformations and list in the following sections. The subset of letters appearing in the differential equations for different families considered is given in Table 5.2.

Note that the differential equations (4.38) are valid for four-dimensional kinematics, but we provide the letters in terms of nine scalar products s_{ij} . This allows for shorter expressions which are easily converted to four-dimensional kinematics using the map (5.15). Although the alphabet we provide in this section is multiplicatively independent as functions of the nine Mandelstam variables, there is a set of identities (App. A) that hold on the support of the Gram determinant constraint (4.144).

Of course, the well-known nine-letter alphabet for the six-point remainder function in $\mathcal{N} = 4$ sYM theory [192, 219] is contained within our alphabet.

5.5.1 Predicting Alphabet Letters

As described in Section 5.4, for an efficient calculation of the multi-scale differential equation, it is invaluable to know the alphabet letters a priori.

The letters describe the locations of possible singularities of the Feynman integrals, thus they are dictated by the Landau equations and more general by PLD; see Chapter 3. The letters produced by Landau analysis are rational functions of the kinematic variables. However, it has been observed that in situations where some of the leading singularities of the Feynman integrals under study evaluate to square roots, the alphabet that is required to describe the differential equation in the canonical form also contains algebraic letters of the form

$$w_k = \frac{P_k - \sqrt{Q_k}}{P_k + \sqrt{Q_k}}, \quad (5.55)$$

where both P_k and Q_k are homogeneous polynomials of the kinematic variables.

In order to predict the alphabet, we follow the approach described in Chapter 3. In this approach, we would solve the Landau equations (3.13) and detect/recognize possible square roots. This would give us the even part of the alphabet which can be used as input for the Algorithm 1 that produces algebraic letters.

Since the publicly available code for solving Landau equations [34, 35] became available after we have already conjectured the two–loop alphabet, we followed a slightly different approach. We assumed that all even letters, including the occurring square roots $\sqrt{Q_k}$, needed to fit the differential equation matrices, are already known in the literature [79, 116, 226]. This resulted in an overcomplete alphabet consisting of 400 letters where the first 90 letters are of degree one, 291 letters are of degree two, 18 letters are of degree three, and one letter is of degree five. A priori, we do not have a criterion which would reduce the size of the alphabet and therefore also the size of the ansatz.

In the construction of odd letters, we assume that the nine kinematic variables \vec{v} are independent. In particular, in these D –dimensional kinematics, all square roots in the problem are independent and square–free, i.e. no polynomial can be factored from under the square roots. The 39 square roots we consider are:

$$\left\{ \begin{aligned} &\sqrt{\lambda(s_{12}, s_{34}, s_{56})}, \sqrt{\lambda(s_{12}, s_{36}, s_{45})}, \sqrt{G(p_1, p_2, p_3, p_4)}, \sqrt{G(p_1, p_2, p_3, p_5)}, \sqrt{G(p_1, p_2, p_4, p_5)}, \\ &\sqrt{\Delta_6}, \sqrt{(s_{12}\epsilon_{1456} + s_{123}\epsilon_{1256})^2}, \sqrt{(s_{234}\epsilon_{6123} - s_{61}\epsilon_{1234})^2}, \\ &\sqrt{(s_{56}\epsilon_{1234} - s_{34}\epsilon_{1245} - (s_{34} - s_{234})\epsilon_{1345} - (s_{56} - s_{234})\epsilon_{2345})^2} \end{aligned} \right\} + \text{cyclic permutations}, \quad (5.56)$$

where Δ_6 is defined in equation (3.32). Furthermore, we also consider all products of two different square roots listed here. This allows us to construct the relevant odd letters using the approach described in Section 3.4.

Note that the square roots of Gram determinants listed in (5.56) can only be treated independently in D –dimensional kinematics. For D –dimensional on-shell six–point kinematics, the Gram determinants of four momenta satisfy the identities

$$\begin{aligned} G(p_i, p_j, p_k, p_l)G(p_i, p_j, p_m, p_n) &= G \begin{pmatrix} p_i & p_j & p_k & p_l \\ p_i & p_j & p_m & p_n \end{pmatrix}^2 - G(p_i, p_j, p_m + p_n)G(1, 2, 3, 4, 5) \\ G(p_i, p_j, p_k, p_l)G(p_i, p_j, p_k, p_n) &= G \begin{pmatrix} p_i & p_j & p_k & p_l \\ p_i & p_j & p_k & p_n \end{pmatrix}^2 - G(p_i, p_j, p_k)G(1, 2, 3, 4, 5), \end{aligned} \quad (5.57)$$

for all $i, j, k, l, m, n \in \{1, 2, 3, 4, 5, 6\}$. These relations imply that, in the four–dimensional limit where $G(1, 2, 3, 4, 5) \rightarrow 0$, the product of any two Gram determinants of four momenta turns into a perfect square. Hence, in four–dimensional kinematics, the square roots of Gram determinants of four momenta are no longer independent roots. Consequently, there is a set of identities among odd letters generated from the construction described

in Section 3.4. We use the momentum twistor parametrization (5.15) to satisfy the Gram constraint manifestly and to find these relations between the letters for four-dimensional external kinematics. We list the identities in App. A. Thus, we obtain a list of candidate letters to express the differential equation in four-dimensional kinematics.

Ultimately, the proof that we have constructed the full alphabet lies in the success of the linear fit to the equation (5.51). If some letters are missing from the ansatz, the corresponding entries of the differential equation cannot be determined. However, we find for the five families studied that the letters constructed via Algorithm 1 are sufficient to describe the entire respective differential equations.

In the following sections, we list all the letters that appear in the differential equations for the five families considered in this chapter.

5.5.2 Parity–Even Letters

The first part of the alphabet is parity–even letters that are given as scalar products of external momenta.

There are 48 letters linear in the Mandelstam variables s_{ij} :

$$w_1 = s_{12}, \quad w_{i+1} = T^i w_1, \quad i = 1, \dots, 5, \quad (5.58)$$

$$w_7 = s_{123}, \quad w_{i+7} = T^i w_7, \quad i = 1, 2, \quad (5.59)$$

$$w_{10} = -s_{12} - s_{23}, \quad w_{i+10} = T^i w_{10}, \quad i = 1, \dots, 5, \quad (5.60)$$

$$w_{16} = s_{12} - s_{123}, \quad w_{i+16} = T^i w_{16}, \quad i = 1, \dots, 5, \quad (5.61)$$

$$w_{22} = s_{12} - s_{345}, \quad w_{i+22} = T^i w_{22}, \quad i = 1, \dots, 5, \quad (5.62)$$

$$w_{28} = -s_{12} - s_{23} + s_{123}, \quad w_{i+28} = T^i w_{28}, \quad i = 1, \dots, 5, \quad (5.63)$$

$$w_{34} = s_{12} - s_{34} - s_{123}, \quad w_{i+34} = T^i w_{34}, \quad i = 1, \dots, 5, \quad (5.64)$$

$$w_{40} = s_{12} - s_{56} + s_{345}, \quad w_{i+40} = T^i w_{40}, \quad i = 1, \dots, 5, \quad (5.65)$$

$$w_{46} = s_{12} + s_{45} - s_{123} - s_{345}, \quad w_{i+46} = T^i w_{46}, \quad i = 1, 2. \quad (5.66)$$

The following 51 letters are quadratic in the Mandelstam variables s_{ij} :

$$w_{49} = -s_{12}s_{45} + s_{123}s_{345}, \quad w_{i+49} = T^i w_{49}, \quad i = 1, 2, \quad (5.67)$$

$$w_{52} = s_{12}s_{56} - s_{12}s_{123} + s_{34}s_{123}, \quad w_{i+52} = T^i w_{52}, \quad i = 1, \dots, 5, \quad (5.68)$$

$$w_{58} = -s_{12}s_{45} - s_{23}s_{345} + s_{123}s_{345}, \quad w_{i+58} = T^i w_{58}, \quad i = 1, \dots, 5, \quad (5.69)$$

$$w_{64} = -s_{12}s_{45} - s_{34}s_{123} + s_{123}s_{345}, \quad w_{i+64} = T^i w_{64}, \quad i = 1, \dots, 5, \quad (5.70)$$

$$w_{70} = s_{12}s_{56} - s_{123}s_{56} + s_{34}s_{123}, \quad w_{i+70} = T^i w_{70}, \quad i = 1, \dots, 5, \quad (5.71)$$

$$w_{76} = -s_{12}(s_{34} + s_{45}) - (s_{34} - s_{56} + s_{123})s_{345}, \quad w_{i+76} = T^i w_{76}, \quad i = 1, \dots, 5, \quad (5.72)$$

$$w_{82} = (s_{12} + s_{23})s_{45} + s_{123}(s_{61} - s_{23} - s_{345}), \quad w_{i+82} = T^i w_{82}, \quad i = 1, \dots, 5, \quad (5.73)$$

$$w_{88} = s_{12}(-s_{34} + s_{345}) + (s_{34} - s_{56} - s_{345})s_{345}, \quad w_{i+88} = T^i w_{88}, \quad i = 1, \dots, 5, \quad (5.74)$$

$$w_{94} = (s_{34} - s_{12} + s_{123})(s_{12} - s_{34} + s_{234}) - s_{23}s_{56},$$

$$w_{i+94} = T^i w_{94}, \quad i = 1, \dots, 5, \quad (5.75)$$

while another 18 letters are cubic in the scalar products s_{ij} :

$$\begin{aligned} w_{100} &= s_{23}s_{56}(-s_{34} + s_{345}) - (s_{61} - s_{234})(s_{12}s_{45} + s_{34}s_{123} - s_{123}s_{345}), \\ w_{i+100} &= T^i w_{100}, \quad i = 1, \dots, 5 \end{aligned} \quad (5.76)$$

$$\begin{aligned} w_{106} &= -s_{123}(s_{34} - s_{56})(s_{56} - s_{234}) - s_{12}s_{56}(s_{23} + s_{56} - s_{234}), \\ w_{i+106} &= T^i w_{106}, \quad i = 1, \dots, 5 \end{aligned} \quad (5.77)$$

$$\begin{aligned} w_{112} &= (s_{234} - s_{61})s_{23}^2 - (s_{56}s_{61} - s_{123}s_{61} + (s_{45} + s_{123})s_{234})s_{23} + s_{45}s_{123}s_{234}, \\ w_{i+112} &= T^i w_{112}, \quad i = 1, \dots, 5. \end{aligned} \quad (5.78)$$

The next five letters are square roots that remain square roots even in the momentum twistor parametrization. They are defined as:

$$w_{118} = r_1 = \sqrt{\lambda(s_{12}, s_{34}, s_{56})}, \quad (5.79)$$

$$w_{119} = r_2 = \sqrt{\lambda(s_{23}, s_{45}, s_{61})}, \quad (5.80)$$

$$w_{120} = r_3 = \sqrt{\lambda(s_{12}, s_{36}, s_{45})},$$

$$w_{i+120} = r_{i+3} = T^i w_{120}, \quad i = 1, 2, \quad (5.81)$$

where λ denotes the Källén function

$$\lambda(a, b, c) = a^2 + b^2 + c^2 - 2ab - 2ac - 2bc. \quad (5.82)$$

These letters change sign under the $\sqrt{\lambda} \rightarrow -\sqrt{\lambda}$ transformations, but $d \log(\sqrt{\lambda})$ is invariant.

The remaining 34 even letters including pseudo scalars:

$$w_{123} = \epsilon_{1234}, \quad w_{i+123} = T^i w_{123}, \quad i = 1, \dots, 5, \quad (5.83)$$

$$w_{129} = \epsilon_{1235}, \quad w_{i+129} = T^i w_{129}, \quad i = 1, \dots, 5, \quad (5.84)$$

$$w_{135} = \epsilon_{1245}, \quad w_{i+135} = T^i w_{135}, \quad i = 1, 2, \quad (5.85)$$

$$w_{138} = \Delta_6 \quad (5.86)$$

$$w_{139} = s_{12}\epsilon_{1456} + s_{123}\epsilon_{1256}, \quad w_{i+139} = T^i w_{139}, \quad i = 1, \dots, 5, \quad (5.87)$$

$$\begin{aligned} w_{145} &= s_{56}\epsilon_{1234} - s_{34}\epsilon_{1245} - (s_{34} - s_{234})\epsilon_{1345} - (s_{56} - s_{234})\epsilon_{2345}, \\ w_{i+145} &= T^i w_{145}, \quad i = 1, \dots, 5, \end{aligned} \quad (5.88)$$

$$w_{151} = s_{234}\epsilon_{6123} - s_{61}\epsilon_{1234}, \quad w_{i+151} = T^i w_{151}, \quad i = 1, \dots, 5. \quad (5.89)$$

A pseudo-scalar transforms as $w_j \rightarrow -w_j$ under parity transformations, but again $d \log w_j$ is invariant. Furthermore, all of the above pseudo-scalars are square roots in terms of Mandelstam variables s_{ij} which become rationalized in momentum twistor variables x_i .

To summarize, the parity-even part of the alphabet contains 156 letters closed under the action of the dihedral symmetry group. All of these letters are already known either

Family	# even letters in DE	# even letters from PLD.j1	Additional letters
Hexagon–box (hbb)	48	48 (+1)	–
Pentagon–triangle (pt)	57	48 (+1)	$w_{13}, w_{36}, w_{45}, w_{56}, w_{64},$ $w_{77}, w_{85}, w_{100}, w_{129}$
Double–box (db)	56	48 (+1)	$w_{36}, w_{39}, w_{41}, w_{44},$ $w_{96}, w_{99}, w_{120}, w_{135}$
Pentagon–box (pb)	67	48 (+1)	$w_{13}, w_{34}, w_{36}, w_{37}, w_{42},$ $w_{45}, w_{62}, w_{64}, w_{70}, w_{77},$ $w_{85}, w_{94}, w_{97}, w_{100}, w_{106},$ $w_{121}, w_{129}, w_{136}, w_{139}$
Hexagon–box (hb)	79	48 (+1)	$w_{13}, w_{14}, w_{34} - w_{37}, w_{40},$ $w_{42}, w_{45}, w_{56}, w_{62} - w_{65},$ $w_{70}, w_{77}, w_{78}, w_{85}, w_{94},$ $w_{97}, w_{100}, w_{101}, w_{106}, w_{115},$ $w_{121}, w_{129}, w_{130}, w_{136},$ $w_{139}, w_{145}, w_{154}$

Table 5.1: Comparison between the even letters predicted by PLD.j1 and even letters that appear in the differential equations. The package predicts the same singularities for all five families (and the Gram determinant constraint, represented by (+1) in the table).

from the two–loop six–point maximal cut differential equations or from the two–loop five–point integrals with one off–shell leg.

Recently, great progress has been made in finding even letters directly from the study of the Landau variety; see Section 3.2. We compared the even letters listed in this section with the components of the Landau singular locus of the five families, computed using the principal Landau determinants implemented in PLD.j1 [34, 35]. As noted in the preceding references, the current implementation of principle Landau determinants can miss some of the components of the singular locus. For the hexagon–bubble family, all letters are correctly predicted, while for the remaining families some letters are missed by the package PLD.j1. We list the additional letters needed for the DE in Table 5.1.

5.5.3 Parity–Odd Letters

This section lists the parity–odd letters that transform as $d \log(w_i) \rightarrow -d \log(w_i)$ under parity transformations.

First, there are 25 letters that change their sign under the sign change of a square root r_i :

$$w_{157} = \frac{s_{12} + s_{34} - s_{56} - r_1}{s_{12} + s_{34} - s_{56} + r_1}, \quad w_{157} = T w_{157}, \quad (5.90)$$

$$w_{159} = \frac{-s_{12} + s_{34} + s_{56} - r_1}{-s_{12} + s_{34} + s_{56} + r_1}, \quad w_{159} = T w_{159}, \quad (5.91)$$

$$w_{161} = \frac{s_{12} - s_{34} + s_{56} - 2s_{123} - r_1}{s_{12} - s_{34} + s_{56} - 2s_{123} + r_1}, \quad w_{i+161} = T^i w_{161}, \quad i = 1, \dots, 5, \quad (5.92)$$

$$w_{167} = \frac{s_{123} + s_{345} - r_3}{s_{123} + s_{345} + r_3}, \quad w_{i+167} = T^i w_{167}, \quad i = 1, 2, \quad (5.93)$$

$$w_{170} = \frac{s_{123} - s_{345} - r_3}{s_{123} - s_{345} + r_3}, \quad w_{i+170} = T^i w_{170}, \quad i = 1, 2, \quad (5.94)$$

$$w_{173} = \frac{s_{123} + s_{345} - 2s_{12} - r_3}{s_{123} + s_{345} - 2s_{12} + r_3}, \quad w_{i+173} = T^i w_{173}, \quad i = 1, 2, \quad (5.95)$$

$$w_{176} = \frac{s_{123} - s_{345} + 2s_{34} - 2s_{56} - r_3}{s_{123} - s_{345} + 2s_{34} - 2s_{56} + r_3}, \quad w_{i+176} = T^i w_{176}, \quad i = 1, 2, \quad (5.96)$$

$$w_{179} = \frac{s_{123} - s_{345} - 2s_{23} + 2s_{61} - r_3}{s_{123} - s_{345} - 2s_{23} + 2s_{61} + r_3}, \quad w_{i+179} = T^i w_{179}, \quad i = 1, 2, \quad (5.97)$$

These letters are already known from the two-loop five-particle integrals with one off-shell leg.

In addition, there are 87 letters that are odd with respect to the sign change of the pseudo scalars ϵ_{ijkl} and Δ_6 :

$$w_{182} = \frac{s_{12}s_{23} - s_{23}s_{34} + s_{23}s_{56} + s_{34}s_{123} - s_{234}(s_{12} + s_{123}) - \epsilon_{1234}}{s_{12}s_{23} - s_{23}s_{34} + s_{23}s_{56} + s_{34}s_{123} - s_{234}(s_{12} + s_{123}) + \epsilon_{1234}},$$

$$w_{i+182} = T^i w_{182}, \quad i = 1, \dots, 5, \quad (5.98)$$

$$w_{188} = \frac{s_{12}(s_{23} - s_{234}) - s_{23}(s_{34} + s_{56}) + s_{123}(s_{34} + s_{234}) - \epsilon_{1234}}{s_{12}(s_{23} - s_{234}) - s_{23}(s_{34} + s_{56}) + s_{123}(s_{34} + s_{234}) + \epsilon_{1234}},$$

$$w_{i+188} = T^i w_{188}, \quad i = 1, \dots, 5, \quad (5.99)$$

$$w_{194} = \frac{s_{12}(-s_{23} + s_{234}) + s_{23}(s_{34} + s_{56}) + s_{123}(s_{34} - s_{234}) - \epsilon_{1234}}{s_{12}(-s_{23} + s_{234}) + s_{23}(s_{34} + s_{56}) + s_{123}(s_{34} - s_{234}) + \epsilon_{1234}},$$

$$w_{i+194} = T^i w_{194}, \quad i = 1, \dots, 5, \quad (5.100)$$

$$w_{200} = \frac{s_{12}(s_{23} + s_{234}) + s_{23}(-s_{34} + s_{56}) + s_{123}(s_{34} - s_{234}) - \epsilon_{1234}}{s_{12}(s_{23} + s_{234}) + s_{23}(-s_{34} + s_{56}) + s_{123}(s_{34} - s_{234}) + \epsilon_{1234}},$$

$$w_{i+200} = T^i w_{200}, \quad i = 1, \dots, 5, \quad (5.101)$$

$$w_{206} = \frac{s_{12}(s_{23} + s_{234}) - s_{23}(s_{34} + s_{56} - 2s_{234}) + s_{123}(s_{34} - s_{234}) - \epsilon_{1234}}{s_{12}(s_{23} + s_{234}) - s_{23}(s_{34} + s_{56} - 2s_{234}) + s_{123}(s_{34} - s_{234}) + \epsilon_{1234}},$$

$$w_{i+206} = T^i w_{206}, \quad i = 1, \dots, 5, \quad (5.102)$$

$$w_{212} = \frac{s_{12}(s_{23} - s_{234}) + s_{23}(-s_{34} + s_{56} - 2s_{123}) + s_{123}(-s_{34} + s_{234}) - \epsilon_{1234}}{s_{12}(s_{23} - s_{234}) + s_{23}(-s_{34} + s_{56} - 2s_{123}) + s_{123}(-s_{34} + s_{234}) + \epsilon_{1234}},$$

$$w_{i+212} = T^i w_{212}, \quad i = 1, \dots, 5, \quad (5.103)$$

$$w_{218} = \frac{s_{12}(s_{23} + 2s_{56} - 2s_{123} - s_{234}) + s_{23}(-s_{34} + s_{56}) + s_{123}(s_{34} - s_{234}) - \epsilon_{1234}}{s_{12}(s_{23} + 2s_{56} - 2s_{123} - s_{234}) + s_{23}(-s_{34} + s_{56}) + s_{123}(s_{34} - s_{234}) + \epsilon_{1234}},$$

$$w_{i+218} = T^i w_{218}, \quad i = 1, \dots, 5, \quad (5.104)$$

$$w_{224} = \frac{2s_{12}^2 + s_{12}(s_{23} - 2s_{34} - 2s_{123} + s_{234}) + s_{23}(-s_{34} + s_{56}) + s_{123}(s_{34} - s_{234}) - \epsilon_{1234}}{2s_{12}^2 + s_{12}(s_{23} - 2s_{34} - 2s_{123} + s_{234}) + s_{23}(-s_{34} + s_{56}) + s_{123}(s_{34} - s_{234}) + \epsilon_{1234}},$$

$$w_{i+224} = T^i w_{224}, \quad i = 1, \dots, 5, \quad (5.105)$$

$$w_{230} = -\frac{s_{23}(s_{56} - s_{34}) + s_{12}(s_{23} + 2s_{56} - s_{234}) + s_{123}(s_{34} - 2s_{56} + s_{234}) - \epsilon_{1234}}{s_{23}(s_{56} - s_{34}) + s_{12}(s_{23} + 2s_{56} - s_{234}) + s_{123}(s_{34} - 2s_{56} + s_{234}) + \epsilon_{1234}},$$

$$w_{i+230} = T^i w_{230}, \quad i = 1, \dots, 5, \quad (5.106)$$

These 54 letters are known from the one-loop hexagon integral and the two-loop five-point integrals with one massive leg.

The following six letters appear for the first time in the off-diagonal block of the differential equations for pentagon-triangle integral family,

$$w_{236} = \frac{-s_{12}(s_{45} + s_{61} - s_{234}) + s_{23}(s_{34} + s_{56} - s_{345}) + s_{123}(-s_{34} + s_{61} - s_{234} + s_{345}) - \epsilon_{1235}}{-s_{12}(s_{45} + s_{61} - s_{234}) + s_{23}(s_{34} + s_{56} - s_{345}) + s_{123}(-s_{34} + s_{61} - s_{234} + s_{345}) + \epsilon_{1235}},$$

$$w_{i+236} = T^i w_{236}, \quad i = 1, \dots, 5. \quad (5.107)$$

Furthermore, the letters $\{w_{242}, \dots, w_{253}\}$ appear for the first time in the off-diagonal block of the double-box differential equation. These are defined as

$$w_{242} = \frac{P_1 - \epsilon_{1245}}{P_1 + \epsilon_{1245}}, \quad w_{i+242} = T^i w_{242}, \quad i = 1, 2, \quad (5.108)$$

$$w_{245} = \frac{P_2 - \epsilon_{1245}}{P_2 + \epsilon_{1245}}, \quad w_{i+245} = T^i w_{245}, \quad i = 1, 2, \quad (5.109)$$

$$w_{248} = \frac{P_3 - \epsilon_{1245}}{P_3 + \epsilon_{1245}}, \quad w_{i+248} = T^i w_{248}, \quad i = 1, 2, \quad (5.110)$$

$$w_{251} = \frac{P_4 - \epsilon_{1245}}{P_4 + \epsilon_{1245}}, \quad w_{i+251} = T^i w_{251}, \quad i = 1, 2, \quad (5.111)$$

where P_1, P_2, P_3 and P_4 are polynomials defined as

$$P_1 = s_{12}s_{45} + s_{23}(-s_{34} + s_{56} + s_{345}) + s_{61}(s_{34} - s_{56}) + s_{123}(s_{34} + s_{61} - s_{234}) + s_{345}(s_{56} - s_{123} - s_{234}), \quad (5.112)$$

$$P_2 = s_{12}s_{45} - s_{34}s_{61} + s_{56}s_{61} - s_{34}s_{123} + s_{123}(-s_{61} + s_{234} + s_{345}) + s_{23}(s_{34} - s_{56} - s_{345}) - s_{56}s_{345} + s_{234}s_{345}, \quad (5.113)$$

$$P_3 = s_{12}s_{45} + s_{123}(-s_{34} + s_{123}) + 2s_{23}^2 + s_{23}(s_{34} + s_{56} - 2(s_{61} + s_{123} + s_{234}) + s_{345}) + s_{61}(-s_{34} - s_{56} + s_{123} + 2s_{234}) + s_{345}(s_{56} - s_{123} - s_{234}), \quad (5.114)$$

$$P_4 = s_{12}s_{45} + s_{23}(s_{34} - s_{56} - s_{345}) + 2s_{34}^2 + s_{34}(-2s_{56} + s_{61} + s_{123} - 2(s_{234} + s_{345})) - s_{56}s_{61} + s_{61}s_{123} + 2s_{56}s_{234} - s_{123}s_{234} + s_{345}(s_{56} - s_{123} + s_{234}). \quad (5.115)$$

The following three odd letters are known from the one-loop hexagon integral,

$$w_{254} = \frac{-s_{12}s_{45}s_{234} + s_{34}s_{61}s_{123} + s_{345}(-s_{23}s_{56} + s_{123}s_{234}) - \Delta_6}{-s_{12}s_{45}s_{234} + s_{34}s_{61}s_{123} + s_{345}(-s_{23}s_{56} + s_{123}s_{234}) + \Delta_6},$$

$$w_{i+254} = T^i w_{254}, \quad i = 1, 2. \quad (5.116)$$

The last 12 letters appear for the first time in the pentagon-box family and in the off-diagonal terms of the hexagon-box family:

$$w_{257} = -\frac{P_5 - (s_{12}\epsilon_{1456} + s_{123}\epsilon_{1256})}{P_5 + (s_{12}\epsilon_{1456} + s_{123}\epsilon_{1256})},$$

$$w_{i+257} = T^i w_{257}, \quad i = 1, \dots, 5, \quad (5.117)$$

$$w_{263} = -\frac{P_6 - (s_{234}\epsilon_{6123} - s_{61}\epsilon_{1234})}{P_6 + (s_{234}\epsilon_{6123} - s_{61}\epsilon_{1234})},$$

$$w_{i+263} = T^i w_{263}, \quad i = 1, \dots, 5, \quad (5.118)$$

where the polynomials P_5 and P_6 are defined as follows

$$P_5 = s_{12} (s_{23}s_{56} - s_{61}s_{56} + s_{45} (s_{234} - s_{56}))$$

$$+ s_{123} (-s_{34}s_{61} - s_{234}s_{345} + s_{56} (s_{61} + s_{345})), \quad (5.119)$$

$$P_6 = s_{12} (s_{23} (s_{61} - s_{234}) + s_{45}s_{234}) + s_{123} (s_{234}s_{345} - s_{34}s_{61})$$

$$+ s_{23} (s_{34}s_{61} - s_{56}s_{61} - s_{234}s_{345}). \quad (5.120)$$

5.5.4 Letters with Mixed Parity Transformations

The last 15 letters in the hexagon alphabet transform non-trivially under the parity transformations. They are even under simultaneous changes of the sign of a square root r_i and a pseudo-scalar ϵ_{ijkl} , but odd under the sign change of just one of them.

The letters are defined as:

$$w_{269} = \frac{P_7 - r_1\epsilon_{1234}}{P_7 + r_1\epsilon_{1234}},$$

$$w_{i+269} = T^i w_{269}, \quad i = 1, \dots, 5, \quad (5.121)$$

$$w_{275} = \frac{P_8 - r_4\epsilon_{1234}}{P_8 + r_4\epsilon_{1234}},$$

$$w_{i+275} = T^i w_{275}, \quad i = 1, \dots, 5, \quad (5.122)$$

$$w_{281} = \frac{P_9 - r_3\epsilon_{1245}}{P_9 + r_3\epsilon_{1245}},$$

$$w_{i+281} = T^i w_{281}, \quad i = 1, 2, \quad (5.123)$$

where P_5 , P_6 and P_7 are the following polynomials:

$$P_7 = s_{12}^2 (s_{23} - s_{234}) + s_{12} (-2s_{23}(s_{34} + s_{56}) + s_{34}(-2s_{56} + s_{123}) + s_{234}(s_{34} + s_{56} + s_{123}))$$

$$+ (s_{34} - s_{56}) (s_{23}(s_{34} - s_{56}) + s_{123}(-s_{34} + s_{234})), \quad (5.124)$$

$$P_8 = s_{12} (s_{23}(2s_{56} - s_{123} + s_{234}) - s_{234}(s_{123} + s_{234})) - s_{123}(s_{34} - s_{234})(s_{123} + s_{234})$$

$$+ 2s_{23}^2 s_{56} + 2s_{23} (s_{34}(2s_{56} + s_{123} - s_{234}) - s_{56}(s_{123} + s_{234}) - 2s_{123}s_{234}), \quad (5.125)$$

$$P_9 = s_{12}s_{45} (2s_{23} + 2s_{34} + 2s_{56} + 2s_{61} - s_{123} - 4s_{234} - s_{345}) + (s_{123} + s_{345}).$$

$$(s_{23}(s_{34} - s_{56} - s_{345}) - s_{61}(s_{34} - s_{56}) - s_{123}(s_{34} + s_{61} - s_{234}) - s_{345}(s_{56} - s_{123} - s_{234})). \quad (5.126)$$

The first 12 letters are already known from the literature, while the letters $\{w_{281}, \dots, w_{283}\}$ are new. These new letters appear in the off-diagonal blocks of the double-box differential equations and consequently in all other families where a double-box appears as a subsector.

5.5.5 Summary of Two-Loop Hexagon Alphabet

Throughout previous sections we provided the two-loop hexagon alphabet closed under cyclic permutations and under reflections. In total, the alphabet has 283 letters, 156 of which are even, 112 odd, and 15 with mixed parity behavior. To express the DEs of the particular orientations of the integral families shown in Figure 5.1, only a subset of letters is needed.

The specific letters appearing in the differential equations for each of the families are listed in Table 5.2. The letters are classified according to the weight at which they first appear in the symbol. Moreover, only letters appearing up to weight four are listed, since they also contribute to the relevant function space.

For all of the families except for the hexagon-bubble family, there are letters which appear at weight five or six for the first time. For the hexagon-box, these letters are

$$\begin{aligned} \mathbb{A}_{hb}^{(5)} &= \{w_{94}, w_{97}, w_{106}, w_{115}, w_{121}, w_{129}, w_{130}, w_{177}, w_{180}, w_{224}, w_{227}, w_{230}, w_{260}, w_{269}, w_{272}\}, \\ \mathbb{A}_{hb}^{(6)} &= \{w_{136}, w_{139}, w_{145}, w_{154}\}, \end{aligned} \quad (5.127)$$

while in the pentagon-box family, they are

$$\begin{aligned} \mathbb{A}_{pb}^{(5)} &= \{w_{94}, w_{97}, w_{106}, w_{121}, w_{129}, w_{177}, w_{180}, w_{224}, w_{227}, w_{230}, w_{269}, w_{272}\}, \\ \mathbb{A}_{pb}^{(6)} &= \{w_{136}, w_{139}\}. \end{aligned} \quad (5.128)$$

Starting from weight seven, all letters will appear in the symbol. On the other hand, for the double-box family and the pentagon-triangle family, all letters will appear already at weight six, while the new letters at weight five are

$$\begin{aligned} \mathbb{A}_{db}^{(5)} &= \{w_{96}, w_{99}, w_{120}, w_{176}, w_{179}, w_{226}, w_{229}, w_{271}, w_{274}\}, \\ \mathbb{A}_{pt}^{(5)} &= \{w_{129}\}. \end{aligned} \quad (5.129)$$

5.6 Solving the Differential Equations

In this section, we describe how to solve the canonical differential equations (4.38) for the double-box, pentagon-triangle and hexagon-bubble families. The general solution to the canonical differential equations is given as a Chen's iterated integral (4.80); see Section 4.4. To fully determine the solution, we provide boundary constants for all integrals in the

three families up to transcendental weight four. Following similar steps as in the one-loop hexagon, described in Section 4.6, we fix the full functional dependence in the Euclidean region in terms of classical polylogarithms up to weight two. Moreover, we describe how to define one-fold integral representations for all functions up to weight four, which can be used to provide fast numerical evaluations of the integrals.

Note that the determination of boundary values for the hexagon-box and pentagon-box families is still ongoing and, as such, is not included in this thesis. As a result, solutions for these integrals are also not provided.

5.6.1 Boundary Constants

To uniquely fix a solution of the first-order canonical DE, we have to provide boundary information for all of the integrals at a single point. Similarly to the one-loop example presented in Chapter 4, we fix the boundary constants analytically by imposing regularity of our basis of integrals throughout the Euclidean region. We record the values of our integral bases at the symmetric reference point

$$\vec{v}_0 = \{-1, \dots, -1\}. \quad (5.130)$$

While the basis should be regular all through the Euclidean region, defined by

$$s_{ij} < 0, \quad s_{ijk} < 0, \quad (5.131)$$

this is not true for the differential equation matrices. Instead, the Euclidean region is crossed by hypersurfaces defined by the vanishing of any alphabet letter

$$w_j = 0. \quad (5.132)$$

Schematically, the situation is depicted in Figure 4.2, where solid black lines denote the boundaries of the Euclidean region, while the dashed lines depict the spurious hypersurfaces defined by vanishing of one of some alphabet letters. Imposing the absence of singularities on these spurious surfaces puts constraints on the boundary constants. The constraints arising from the hypersurfaces that contain the boundary point \vec{v}_0 are labeled Type-I in Figure 4.2. The constraints from all other spurious hypersurfaces, which we call Type-II constraints, must first be transported to the boundary point using the differential equation along some path γ .

We find that solving the DEs on the one-parameter curve defined by

$$\begin{aligned} s_{12} &= s_{34} = s_{56} = -1, \\ s_{23} &= s_{45} = s_{61} = -(x-1)^2, \\ s_{123} &= s_{234} = s_{345} = x-1, \end{aligned} \quad (5.133)$$

and requiring regularity at the points $x = 0, \rho, \bar{\rho}$ with $\rho = \frac{1}{2}(1 - i\sqrt{3})$ is sufficient to fix all boundary constants up to weight four up to an overall rescaling. The latter is fixed once

we substitute the known expansion for our UT choice for the sunrise integrals

$$\begin{aligned} I_{\text{sunrise}}(\vec{v}_0) &= -e^{2\gamma_E\epsilon} \frac{\Gamma(1-\epsilon)^3\Gamma(1+2\epsilon)}{2\Gamma(1-3\epsilon)} \\ &= -\frac{1}{2} + \frac{\pi^2}{12}\epsilon^2 + \frac{16}{3}\zeta_3\epsilon^3 + \frac{19\pi^4}{240}\epsilon^4 + \mathcal{O}(\epsilon^5). \end{aligned} \quad (5.134)$$

On the curve defined by equation (5.133), the alphabet of the three families under study simplifies massively, so that all remaining nonconstant logarithms have arguments from the set

$$\mathbb{A}_{\text{line}} = \{x, x-1, 1-x+x^2\}. \quad (5.135)$$

Since the last letter can be factorized over the complex numbers as

$$1-x+x^2 = \left[x - \frac{1}{2}(1-i\sqrt{3})\right] \left[x - \frac{1}{2}(1+i\sqrt{3})\right] \quad (5.136)$$

we can express the general solution to the DEs on this curve in terms of Goncharov G -functions (4.82) with entries in the set $\{0, 1, \rho, \bar{\rho}\}$. Hence, the boundary constants can be expressed in terms of linear combinations of polylogarithms at the sixth roots of unity [212], as we already saw in the one-loop hexagon in Section 4.5.

Using the function `DecomposeToLyndonWords` from `POLYLOGTOOLS` [23], it is straightforward to isolate the log-divergent contributions in the limits $x \rightarrow 0, \rho, \bar{\rho}$. Imposing their vanishing order-by-order in ϵ fixes the boundary constants relative to each other. Here we provide the boundary values for the top-sector integrals,

$$\begin{aligned} I_{\text{db},1}(\vec{v}_0) &= 1 + \frac{\pi^2}{6}\epsilon^2 + \frac{38}{3}\zeta_3\epsilon^3 + \left(\frac{49\pi^4}{216} + \frac{32}{3} \text{Im}[\text{Li}_2(\rho)]^2\right)\epsilon^4, \\ I_{\text{db},2}(\vec{v}_0) &= 1 + \frac{\pi^2}{6}\epsilon^2 + \frac{34}{3}\zeta_3\epsilon^3 + \left(\frac{71\pi^4}{360} + 20 \text{Im}[\text{Li}_2(\rho)]^2\right)\epsilon^4, \\ I_{\text{db},3}(\vec{v}_0) &= I_{\text{db},4}(\vec{v}_0) = I_{\text{db},5}(\vec{v}_0) = 0, \\ I_{\text{db},6}(\vec{v}_0) &= -\left(\frac{\pi^4}{540} + \frac{4}{3} \text{Im}[\text{Li}_2(\rho)]^2\right)\epsilon^4, \\ I_{\text{db},7}(\vec{v}_0) &= I_{\text{pt}}(\vec{v}_0) = I_{\text{hbb}}(\vec{v}_0) = 0. \end{aligned} \quad (5.137)$$

All boundary values for the subsector integrals are written in a similar manner, but we do not list them here, since the list would be quite long. Machine-readable analytic expressions for the boundary values of the double-box, pentagon-triangle, and hexagon-bubble families can be found in the ancillary files of Ref. [263].

5.6.2 Analytic Properties of the Hexagon Function Space

A formal solution to canonical differential equations is discussed in Section 4.4, where we also introduce the notion of the symbol. In this section, we provide a brief reminder of what

a formal solution entails. Moreover, we use the symbol to examine the analytic properties of the two–loop hexagon function space.

The solutions to the canonical differential equations can be found as a series expansion in the dimensional regulator ϵ . By construction, the expansion starts at $\mathcal{O}(\epsilon^0)$,

$$\vec{I}_{\text{fam}}(\vec{v}, \epsilon) = \sum_{k=0}^{\infty} \epsilon^k \vec{I}_{\text{fam}}^{(k)}(\vec{v}), \quad (5.138)$$

where \vec{I}_{fam} denotes the basis integrals for one of the five families. The weight k solution is then given as k –fold iterated integral

$$\vec{I}_{\text{fam}}^{(k)}(\vec{v}) = \vec{I}_{\text{fam}}^{(k)}(\vec{v}_0) + \int_{\gamma} (d\tilde{A}(\vec{v}')) \vec{I}_{\text{fam}}^{(k-1)}(\vec{v}'), \quad (5.139)$$

where $\vec{I}_{\text{fam}}^{(k)}(\vec{v}_0)$ are weight k boundary values described in the previous section and γ is a path connecting the boundary point \vec{v}_0 and some other point \vec{v} .

The integral in equation (5.139) can be written as

$$\vec{I}_{\text{fam}}^{(k)}(\vec{v}) = \sum_{k'=0}^k \sum_{i_1, \dots, i_{k'}=1}^{283} a^{(a_1)} \dots a^{(i_{k'})} \vec{I}_{\text{fam}}^{(k-k')}(\vec{v}_0) [w_{i_1}, \dots, w_{i_{k'}}]_{\vec{v}_0}(\vec{v}), \quad (5.140)$$

where we use the recursive definition of Chen iterated integrals (4.81) of weight k

$$[w_{i_1}, \dots, w_{i_k}]_{\vec{v}_0}(\vec{v}) = \int_{\gamma} d \log w_{i_k}(\vec{v}') [w_{i_1}, \dots, w_{i_{k-1}}]_{\vec{v}_0}(\vec{v}') \quad (5.141)$$

with $[\]_{\vec{v}_0} = 1$. The differential equations ensure that only homotopy invariant linear combinations of iterated integrals appear in the solution (5.140), while a single term is not homotopy invariant.

One useful tool for studying the properties of polylogarithmic functions is the symbol. The symbol map \mathcal{S} can be defined by its action on the Chen iterated integrals (4.93). It maps the k –fold iterated integral into the k –fold tensor product. Using the symbol map, we classify the alphabet letters according to the weight at which they appear in the symbol for the first time for each family. We record this information in Table 5.2 and in Section 5.5.5. Moreover, we use it to predict the function space for the basis integrals at weight one and weight two described in the following section.

Furthermore, we confirm the validity of the extended Steinmann relations [264] for all integrals in the basis of all five families considered. These relations state that double discontinuities in partially overlapping channels vanish [265, 266] and require that the three–point kinematic variables s_{123} , s_{234} and s_{345} never appear next to each other in the symbol. Physically, they reflect the incompatibility of the different three–particle cuts on all possible Riemann sheets. The differential equation matrices $A_{(\text{fam})}$ ensure that the Steinmann relations hold at any order in ϵ at any depth into the symbol [199]

$$c_j^{(\text{fam})} \cdot c_k^{(\text{fam})} = 0, \quad j \neq k, \quad j, k = 7, 8, 9. \quad (5.142)$$

In practice, these adjacency conditions imply that any two letters w_j and w_k for which this identity holds will never appear as consecutive letters in the symbol.

Constraints like these are very important for bootstrap approaches to amplitudes or other observables. For example, one such observable is the Wilson loop with Lagrangian insertion in $\mathcal{N} = 4$ sYM [267]. It was observed that it is related to all-plus amplitudes in pure Yang–Mills theory [268, 269], and hence depends on the same function space.

If the alphabet for an object is known, one can make an ansatz in terms of all possible functions built from this alphabet and determine the respective coefficients from physical properties of the result, see e.g. [192, 193, 195]. However, for large alphabets and with growing weight, the size of the required function basis grows rapidly. Then, a priori knowledge about the structure of the function space, like the above adjacency conditions, cuts down the size of the required ansatz. Motivated by this application, we also consider the adjacency constraints for all other pairs of letters in our alphabet. Considering the overlap of all five families, we find 1052 forbidden pairs of letters. Of course, this number of forbidden pairs is not preserved under basis changes for the function alphabet. Additionally, it is possible that some of these forbidden pairs are accidental at the two-loop level and will not continue to hold at higher loops.

5.6.3 One-Fold Integral Representation for Numerical Evaluations

In Section 4.6, we motivated a hybrid approach to write a solution to the canonical differential equations where one part of the solution is given in terms of the function basis and the rest as a one-fold integral representation. In this section, we are following the same approach. We are interested in the solution to the canonical differential equations (5.50) up to weight four in the dimensional regulator ϵ .

At weights one and two, iterated integrals (5.139) are explicitly integrated into special functions, ensuring that they are well-defined across the entire Euclidean region. Furthermore, only the integrals of the subsectors contribute at these weights, so their functional space is already established [213–215]. At weight one, the only function that can appear is the logarithm

$$\begin{aligned} f_i^{(1)} &= \log(-s_{ii+1}), \quad i = 1, \dots, 6, \\ f_{i+6}^{(1)} &= \log(-s_{ii+1i+2}), \quad i = 1, \dots, 3. \end{aligned} \tag{5.143}$$

The function basis at weight two is given by genuine weight two functions and products of weight one functions. Genuine weight two functions that appear are:

$$\begin{aligned} f_1^{(2)} &= \text{Li}_2\left(1 - \frac{s_{12}}{s_{123}}\right), \quad f_{i+1}^{(2)} = T^i f_1^{(2)}, \quad i = 1, \dots, 5, \\ f_7^{(2)} &= \text{Li}_2\left(1 - \frac{s_{23}}{s_{123}}\right), \quad f_{i+7}^{(2)} = T^i f_7^{(2)}, \quad i = 1, \dots, 5, \\ f_{13}^{(2)} &= \text{Li}_2\left(1 - \frac{s_{12}s_{45}}{s_{123}s_{345}}\right), \quad f_{i+13}^{(2)} = T^i f_{13}^{(2)}, \quad i = 1, \dots, 2, \end{aligned}$$

$$f_{16}^{(2)} = \text{Tri}(s_{12}, s_{34}, s_{56}), \quad f_{17}^{(2)} = \text{Tri}(s_{23}, s_{45}, s_{61}), \quad (5.144)$$

where the $\text{Tri}(a, b, c)$ function is the Bloch–Wigner dilogarithm

$$\text{Tri}(a, b, c) = \text{BW}(z, \bar{z})|_{z\bar{z}=a/b, (1-z)(1-\bar{z})=c/b} \quad (5.145)$$

defined via

$$\text{BW}(z, \bar{z}) = 2\text{Li}_2(z) - 2\text{Li}_2(\bar{z}) + \log(z\bar{z}) [\log(1-z) - \log(1-\bar{z})]. \quad (5.146)$$

This basis of special functions is sufficient to express the solution up to weight two for any master integral in our basis for the three families considered in [263]. For the two remaining families, we expect that the same basis of functions is sufficient to express the solutions since there are no new letters appearing in the symbol at these weights. Moreover, this basis perfectly agrees with the basis found at one-loop in Section 4.6.

We still need to get weight three and four parts of the solution. Since we know the boundary value at the point \vec{v}_0 up to weight four, we can use that information to set up a one-fold integration over the weight-two functions along a straight line to some other point within the Euclidean region. This representation is well-suited for fast numerical evaluations with high precision.

We start by setting up a straight line between our starting point \vec{v}_0 and an end point. When considering such a path, we need to ensure that the path satisfies the Gram constraint (4.144), otherwise our differential equations are no longer valid. To do this, we use the momentum twistor parametrization (5.15) and set straight paths between two points in terms of momentum twistor variables. The starting point \vec{v}_0 in this parametrization is

$$\vec{x}_0 = \{-1, 1, 0, 0, 1, 1, 0, 0\}, \quad (5.147)$$

and a straight line between our starting point and an endpoint is

$$\vec{x}_1(t) = (1-t)\vec{x}_0 + t\vec{x}_1. \quad (5.148)$$

The solution at weight three is given as a one-fold integration over the weight two functions

$$\vec{I}_{\text{fam}}^{(3)} = \vec{I}_{\text{fam}}^{(3)}(\vec{x}_0) + \int_0^1 dt \frac{d\tilde{A}_{\text{fam}}}{dt} \vec{f}^{(2)}(t), \quad (5.149)$$

where $\vec{I}_{\text{fam}}^{(3)}(\vec{x}_0)$ is the boundary value at weight three and $\vec{f}^{(2)}$ are the weight two functions expressed in terms of the momentum twistor variables. At weight four, we use integration by parts to rewrite two-fold integration over the weight-two functions as a one-fold integration

$$\begin{aligned} \vec{I}_{\text{fam}}^{(4)} &= \vec{I}_{\text{fam}}^{(4)}(\vec{x}_0) + \int_0^1 dt \frac{d\tilde{A}_{\text{fam}}}{dt} \vec{I}_{\text{fam}}^{(3)}(\vec{x}_0) + \int_0^1 dt_1 \int_0^{t_1} dt_2 \frac{d\tilde{A}_{\text{fam}}}{dt_1} \frac{d\tilde{A}_{\text{fam}}}{dt_2} \vec{f}^{(2)}(t_2) \\ &= \vec{I}_{\text{fam}}^{(4)}(\vec{x}_0) + \int_0^1 dt \left(\frac{d\tilde{A}_{\text{fam}}}{dt} \vec{I}_{\text{fam}}^{(3)}(\vec{x}_0) + (\tilde{A}_{\text{fam}}(1) - \tilde{A}_{\text{fam}}(t)) \frac{d\tilde{A}_{\text{fam}}}{dt} \vec{f}^{(2)}(t) \right). \end{aligned} \quad (5.150)$$

We use the one-fold integral representation to numerically evaluate all basis integrals of the double-box, pentagon-triangle and hexagon-bubble families at four different points in the bulk of the Euclidean region:

$$\begin{aligned}
\vec{x}_1 &= \left\{ -\frac{299}{300}, \frac{221}{200}, \frac{1}{300}, \frac{1}{200}, \frac{53}{50}, \frac{21}{20}, \frac{1}{100}, \frac{1}{700} \right\}, \\
\vec{x}_2 &= \left\{ -\frac{31}{30}, \frac{161}{150}, \frac{43}{875}, -\frac{17}{630}, \frac{10153}{9450}, \frac{243}{250}, -\frac{22}{75}, \frac{1}{30} \right\}, \\
\vec{x}_3 &= \left\{ -\frac{17}{10}, \frac{51}{50}, \frac{109}{3670}, -\frac{197}{5505}, \frac{3799}{3670}, \frac{774}{815}, -\frac{3}{20}, \frac{1}{25} \right\}, \\
\vec{x}_4 &= \left\{ -1, \frac{9021}{8950}, \frac{7}{1250}, -\frac{17}{250}, \frac{2003}{1790}, \frac{466}{475}, -\frac{637}{3580}, \frac{5}{179} \right\}.
\end{aligned} \tag{5.151}$$

The numerical values obtained through one-fold integration are in complete agreement with the numerical values obtained with AMFLOW up to the desired precision of 20 digits.

A proof-of-concept implementation of the one-fold integration in `Mathematica` is provided in the auxiliary files of Ref. [263]. Although the representations given in equations (5.149) and (5.150) hold globally, both the weight-two functions and the differential equation matrix \tilde{A}_{fam} are multi-valued functions that must be analytically continued appropriately across their branch cuts. This is beyond the scope of our work and hence our implementation is suitable for fast evaluations in the Euclidean region on the paths that do not cross any branch cuts. We leave the analytic continuation to the entire Euclidean region and the physical scattering regions for future work.

In this section, we have identified the function space for three families of six-point Feynman integrals up to weight four in the dimensional regulator. Following the hybrid approach, the function space up to weight two is given in terms of a basis of special functions, while at weight three and four we employ a one-fold integral representation. Extending this result to the remaining two families is still a work in progress, since we do not have complete boundary values for these families.

	Hexagon-box	Pentagon-box	Double-box	Pentagon-triangle	Hexagon-bubble
Weight 1	$w_1 - w_9$	$w_1 - w_9$	$w_1 - w_9$	$w_1 - w_9$	$w_1 - w_9$
Weight 2	$w_{16} - w_{27},$ $w_{49} - w_{51},$ $w_{157} - w_{160}$	$w_{16} - w_{27},$ $w_{49} - w_{51},$ $w_{157} - w_{160}$	$w_{16} - w_{27},$ $w_{49} - w_{51},$ $w_{157} - w_{160}$	$w_{16} - w_{27},$ $w_{49} - w_{51},$ $w_{157} - w_{160}$	$w_{16} - w_{27},$ $w_{49} - w_{51},$ $w_{157} - w_{160}$
Weight 3	$w_{28} - w_{33},$ $w_{46} - w_{48},$ $w_{62} - w_{65}$ $w_{88} - w_{93}, w_{118},$ $w_{119}, w_{161} - w_{166},$ $w_{182} - w_{190}, w_{194}, w_{195},$ $w_{196}, w_{206} - w_{211},$ $w_{218} - w_{220},$ $w_{263} - w_{266}$	$w_{28} - w_{33},$ $w_{46} - w_{48},$ $w_{62}, w_{64}, w_{88} - w_{93},$ $w_{118}, w_{119}, w_{161} - w_{166},$ $w_{182} - w_{190},$ $w_{194} - w_{196},$ $w_{206} - w_{211}$ $w_{218} - w_{220}$ $w_{263} - w_{266}$	$w_{28} - w_{33},$ $w_{46} - w_{48},$ $w_{88} - w_{93}, w_{118}, w_{119},$ $w_{161} - w_{166},$ $w_{182} - w_{190},$ $w_{194} - w_{196},$ $w_{206}, -w_{211},$ $w_{218} - w_{220},$ $w_{263} - w_{266}$	$w_{28} - w_{33}$ $w_{46} - w_{48},$ $w_{62}, w_{64}, w_{88} - w_{93},$ $w_{118}, w_{119}, w_{161} - w_{166},$ $w_{182} - w_{190},$ $w_{194} - w_{196},$ $w_{206} - w_{211},$ $w_{218} - w_{220},$ $w_{263} - w_{266}$	$w_{28} - w_{33},$ $w_{46} - w_{48},$ $w_{88} - w_{93},$ $w_{118}, w_{119},$ $w_{161} - w_{166},$ $w_{182} - w_{190},$ $w_{194} - w_{196},$ $w_{206} - w_{223},$ $w_{263} - w_{268}$
Weight 4	$w_{13}, w_{14}, w_{34}, w_{36}, w_{37},$ $w_{40}, w_{42}, w_{45}, w_{56}, w_{70},$ $w_{77}, w_{78}, w_{85}, w_{86}, w_{100},$ $w_{101}, w_{123} - w_{128}, w_{138},$ $w_{171}, w_{174}, w_{197}, w_{198},$ $w_{202}, w_{203}, w_{236}, w_{237}$	$w_{13}, w_{14}, w_{36}, w_{37}, w_{42},$ $w_{45}, w_{70}, w_{77}, w_{85}, w_{100},$ $w_{123} - w_{128}, w_{138}, w_{168},$ $w_{171}, w_{174}, w_{197}, w_{202}, w_{236},$	$w_{36}, w_{39}, w_{41}, w_{44},$ $w_{123} - w_{128}, w_{138},$ $w_{167}, w_{170}, w_{173}, w_{268}$	$w_{13}, w_{36}, w_{45}, w_{77},$ $w_{85}, w_{100}, w_{123} - w_{128},$ $w_{138}, w_{197}, w_{202}, w_{236}$	$w_{123} - w_{128},$ w_{138}
> Weight 4	19	14	9	1	—
Total	131	115	101	95	100

Table 5.2: List of the alphabet letters appearing in the differential equations for each of the families considered. Note that all of the letters from the weight $k - 1$ of the symbol also appear at the symbol of weight k .

Chapter 6

Conclusions and Outlook

Scattering amplitudes play an important role in the study of the fundamental laws of the universe. They allow us to make precise comparisons with data from collider experiments and provide insight into the intricate mathematical structure of a theory. Scattering amplitudes are computed in the perturbative expansion. Beyond the leading order, the calculation of the contributing Feynman integrals becomes one of the most important and increasingly challenging tasks. A well-known approach for the analytic computation of Feynman integrals, which we followed in this thesis, is to derive a system of ordinary differential equations in the canonical form so that solutions in terms of known functions can be readily obtained. An alternative approach is to bypass the evaluation of Feynman integrals and directly bootstrap the amplitudes from an understanding of their physical properties. In both approaches, understanding the symbol alphabets associated with the singularity structure of Feynman integrals is essential.

The question of when a Feynman integral can develop kinematic singularities is closely connected to the Landau equations. In this thesis, we reviewed these equations and a modern method for finding their solutions. The solutions to the Landau equations correspond to the zeros and singularities of the symbol letters. Indeed, the irreducible components of the principal Landau determinant correspond to the polynomial part of the alphabet. Nevertheless, the algebraic part of the alphabet cannot be accessed directly through the Landau equations. A conjectured factorization property of these letters allows for an algorithmic identification of missing algebraic letters. However, for cutting-edge applications, a naive approach rapidly becomes infeasible. In light of the above, we propose an efficient algorithm for identifying the algebraic letters in question, based on the observed factorization property. Assuming that the factorization property holds, we define a criterion to filter the polynomial letters that enter the ansatz. This drastically reduces the size of the problem and allows us to complete the alphabet with algebraic letters in minutes.

The proposed algorithm can be used in a wide range of examples with non-rational symbol alphabets. In this thesis, we demonstrated its usage on a highly non-trivial example of the two-loop hexagon alphabet. Moreover, the proposed two-loop alphabet was used to fit the differential equation matrices for the hexagon-box, pentagon-box, double-box, pentagon-triangle, and hexagon-bubble integral families where several previously unknown

letters appear.

Furthermore, the results for the letters of the five integral families provided in this thesis constitute valuable data that may be used as a benchmark for independent approaches that aim at predicting the singular locus of Feynman integrals, for example, based on an analysis of the Landau equations [34–36, 99], or via other methods [38, 42].

Based on the findings discussed in this thesis, there are several interesting directions for future study:

1. *How to systematically find all components of the Landau variety for massless scattering?* Landau equations have been known for more than sixty years, and recently received a lot of renewed attention, yet there are still several unresolved questions. The question of systematically finding components of the singular locus in the presence of massless particles and UV/IR divergences was addressed in Ref. [34, 35]. However, as we saw in Section 5.5, it does not yield the complete set of letters beyond the simplest family. Hence, an open question is how to systematically find the missing components.
2. *Assumed form of algebraic letters and nested square roots.* When constructing algebraic letters, we assumed that all square roots are independent and square-free, i.e. no polynomial can be factored from under the square root. However, there are cases in the literature, for example [117], where an additional polynomial appears in front of the square root (3.47). This is not an obstacle for the proposed algorithm. Nevertheless, it would be interesting to understand when such algebraic letters are necessary, which polynomials can actually appear in front of the square root and what their connection is to the leading singularities.

In addition, there are several examples in the literature [117, 270] where nested square roots appear as a normalization in the canonical basis. The corresponding letters do not satisfy the factorization (3.39) and therefore are outside the scope of the algorithm.

3. *Obtaining the full six-point alphabet for two-loop massless amplitudes.* The 283 alphabet letters identified here are likely to constitute the main part of the full hexagon alphabet, but we also expect more letters to be needed for the remaining integral family. There is evidence from both a leading singularity calculation and Schubert analysis [42] that the double-pentagon integral for D -dimensional external states involves elliptic integrals. For four-dimensional external states (i.e. in the dimensional reduction scheme), all leading singularities for this family are algebraic [226]. Hence, while more new letters might appear in the remaining family, we still expect the differential equations to be epsilon-factorizable and expressible in terms of logarithmic one-forms.

However, the leading singularity of the double-pentagon integral in $D = 6 - 2\epsilon$ is rather involved, and the corresponding odd letters [226] do not satisfy the factorization condition (3.39) in the momentum twistor parametrization. It remains an

open question as to how the presented algorithm for predicting symbol letters can be applied to the aforementioned special case.

Moreover, understanding the entire planar six-particle alphabet could enable possible bootstrap applications. For instance, the Wilson loop with Lagrangian insertion in $\mathcal{N} = 4$ sYM [267] has been found to be connected to all-plus amplitudes in pure Yang–Mills theory [268, 269], and therefore depends on the same function space.

4. *Computing the remaining planar two-loop six-point Feynman integrals.* In this thesis, we have presented the results for the hexagon–box, pentagon–box, double–box, pentagon–triangle, and hexagon–bubble integral families. Therefore, the only missing planar family is the double–pentagon family whose UT basis on the maximal cut was obtained in [226]. We expect that by following similar steps as in Section 5.3, it should be possible to extend its definition beyond the maximal cut and derive and solve the complete canonical differential equation.
5. *Two-loop six-point function space.* The availability of canonical differential equations together with boundary values allows for systematic classification of the relevant function space. We can straightforwardly write the needed functions in terms of iterated integrals for any permutation of the considered integral families, see Figure 5.1. However, these functions are generally not independent and some of them are reducible, i.e. they can be written as a products of lower weight functions. Therefore, once we have all differential equations, it will be interesting to see how many irreducible functions appear at each weight up to weight four.
6. *Providing solutions valid in the physical region for four-jet production.* This is crucial for applying these Feynman integrals to phenomenology. One method of accomplishing this is to transport the known analytic boundary value to various kinematic regions. Alternatively, as explored in [214], we can compute the boundary value for a specific point in the desired physical region using the physical constraints discussed here, or through numerical computation, and subsequently solve the canonical differential equation within this region.

Appendix A

Identities among Letters in Four–Dimensional Kinematics

In Section 5.5, we provide an alphabet that is closed under cyclic permutations of the external legs and multiplicatively independent as functions of nine Mandelstam variables. However, in four–dimensional kinematics, the relations between Gram determinants (5.57) together with the Gram determinant constraint (4.144) lead to a set of identities among the letters, which we provide in this section.

Identities among rationalized letters. Since the ϵ_{ijkl} become rationalized in the four–dimensional limit, many previously algebraic letters turn into purely rational letters in terms of the momentum twistor parametrization. Here, we list a basis of 33 identities between letters in our alphabet that hold, provided that the external momenta lie in a four–dimensional space.

$$\begin{aligned} 0 &= T^j(-W_{182} - W_{231} + W_{258}), \quad j = 0, \dots, 5, \\ 0 &= T^j(-W_{183} - W_{190} + W_{256}), \quad j = 0, \dots, 5, \\ 0 &= T^j(-W_{184} - W_{187} + W_{244}), \quad j = 0, 1, 2, \\ 0 &= T^j(-W_{182} + W_{188} - W_{207} + W_{217}), \quad j = 0, \dots, 5, \\ 0 &= T^j(-W_{183} + W_{189} + W_{195} + W_{219} + W_{226} + W_{251}), \quad j = 0, 1, 2, \\ 0 &= T^j(W_{195} + W_{196} + W_{219} + W_{220} + W_{246}), \quad j = 0, \dots, 4, \\ 0 &= T^j(W_{182} - W_{188} - W_{224} - W_{226} + W_{249} - W_{251}), \quad j = 0, 1, \\ 0 &= W_{186} + W_{189} + W_{197} + W_{221} - W_{229} + W_{248}, \\ 0 &= -W_{226} + W_{192} + W_{194} + W_{218} + W_{228} + W_{253} + W_{256}. \end{aligned} \tag{A.1}$$

Again, T is the generator of a cyclic permutation of the external legs, while $W_j = \log w_j$. We note that the remaining permutations of the last four identities also hold; however, they are not independent of the previous identities.

Identities among odd letters. Our alphabet contains five square roots which are not rationalized by the momentum twistor parametrization. For the odd letters related to each of these square roots, there is one identity. The identities are given by

$$\begin{aligned} 0 &= T^j(W_{269} + W_{271} - W_{273}), & j = 0, 1, \\ 0 &= T^j(W_{275} - W_{278} - W_{282}), & j = 0, 1, 2. \end{aligned} \tag{A.2}$$

List of Figures

2.1	One-loop hexagon integral. In our examples, both the external momenta p_i and the propagators are considered to be massless.	10
2.2	The set of spanning trees \mathcal{T}_1 for the one-loop hexagon graph contributing to the \mathcal{U} polynomial.	13
2.3	The set of spanning 2-forests \mathcal{T}_2 for the one-loop hexagon graph contributing to the \mathcal{F} polynomial.	14
2.4	Double-pentagon graph and corresponding dual graph. Black lines represent the double-pentagon graph, red lines represent its dual graph and the blue dashed lines represent the irreducible scalar products.	19
4.1	Graphical representations of the integrals in the IBP basis of the one-loop hexagon integral family. The figure is adapted from Ref. [79].	51
4.2	Schematic representation of the Euclidean region R which is bounded by the inequalities $s_{ij} < 0$ and $s_{ijk} < 0$ (solid black lines). The dashed lines represent different hypersurfaces where some alphabet letters W_j vanish.	61
5.1	Two-loop six-point massless planar Feynman diagrams.	77
5.2	Schematic representation of the structure of the canonical differential equation (4.38) for the two-loop six-point planar integral families. The green blocks with a dotted pattern represent the maximal cut blocks computed in [226], the yellow blocks with horizontal lines represent the subsector integrals [116] and the red blocks with vertical lines are the ones discussed here. Moreover, the blue blocks with diagonal lines correspond to the off-diagonal blocks of the double-pentagon family. Their computation is left for future work.	79
5.3	Schematic representation of the hexagon-box basis of integrals. The red arrows represent different pinches of propagators that lead to different six-point topologies. The number of master integrals (MI) for each of the topologies is written in the bottom right corner of the corresponding diagram.	82

List of Tables

4.1	Numerical evaluation of the hexagon integral at several kinematic points. The values correspond to the UT hexagon integral and are obtained using the one-fold integral representation.	67
5.1	Comparison between the even letters predicted by PLD.j1 and even letters that appear in the differential equations. The package predicts the same singularities for all five families (and the Gram determinant constraint, represented by (+1) in the table).	91
5.2	List of the alphabet letters appearing in the differential equations for each of the families considered. Note that all of the letters from the weight $k - 1$ of the symbol also appear at the symbol of weight k	102

Bibliography

- [1] S. Weinberg, *The Quantum Theory of Fields*. Cambridge University Press, 1995.
- [2] M. E. Peskin and D. V. Schroeder, *An Introduction to quantum field theory*. Addison-Wesley, Reading, USA, 1995.
- [3] M. D. Schwartz, *Quantum Field Theory and the Standard Model*. Cambridge University Press, 3, 2014.
- [4] G. Gabrielse, D. Hanneke, T. Kinoshita, M. Nio and B. Odom, *New determination of the fine structure constant from the electron g value and $q\epsilon d$* , *Phys. Rev. Lett.* **97** (2006) 030802.
- [5] D. Hanneke, S. F. Hoogerheide and G. Gabrielse, *Cavity Control of a Single-Electron Quantum Cyclotron: Measuring the Electron Magnetic Moment*, *Phys. Rev. A* **83** (2011) 052122 [1009.4831].
- [6] P. W. Higgs, *Broken symmetries, massless particles and gauge fields*, *Phys. Lett.* **12** (1964) 132.
- [7] F. Englert and R. Brout, *Broken Symmetry and the Mass of Gauge Vector Mesons*, *Phys. Rev. Lett.* **13** (1964) 321.
- [8] P. W. Higgs, *Broken Symmetries and the Masses of Gauge Bosons*, *Phys. Rev. Lett.* **13** (1964) 508.
- [9] ATLAS collaboration, *Observation of a new particle in the search for the Standard Model Higgs boson with the ATLAS detector at the LHC*, *Phys. Lett. B* **716** (2012) 1 [1207.7214].
- [10] CMS collaboration, *Observation of a New Boson at a Mass of 125 GeV with the CMS Experiment at the LHC*, *Phys. Lett. B* **716** (2012) 30 [1207.7235].
- [11] S. J. Parke and T. R. Taylor, *An Amplitude for n Gluon Scattering*, *Phys. Rev. Lett.* **56** (1986) 2459.
- [12] G. Travaglini et al., *The SAGEX review on scattering amplitudes*, *J. Phys. A* **55** (2022) 443001 [2203.13011].

- [13] LIGO SCIENTIFIC, VIRGO collaboration, *Tests of general relativity with GW150914*, *Phys. Rev. Lett.* **116** (2016) 221101 [1602.03841].
- [14] P. Benincasa, *Amplitudes meet Cosmology: A (Scalar) Primer*, 2203.15330.
- [15] G. Heinrich, *Sector Decomposition*, *Int. J. Mod. Phys. A* **23** (2008) 1457 [0803.4177].
- [16] G. Heinrich, S. P. Jones, M. Kerner, V. Magerya, A. Olsson and J. Schlenk, *Numerical scattering amplitudes with pySecDec*, *Comput. Phys. Commun.* **295** (2024) 108956 [2305.19768].
- [17] X. Liu, Y.-Q. Ma and C.-Y. Wang, *A Systematic and Efficient Method to Compute Multi-loop Master Integrals*, *Phys. Lett. B* **779** (2018) 353 [1711.09572].
- [18] X. Liu and Y.-Q. Ma, *AMFlow: A Mathematica package for Feynman integrals computation via auxiliary mass flow*, *Comput. Phys. Commun.* **283** (2023) 108565 [2201.11669].
- [19] M. Borinsky, *Tropical Monte Carlo quadrature for Feynman integrals*, 2008.12310.
- [20] A. V. Smirnov, N. D. Shapurov and L. I. Vysotsky, *FIESTA5: numerical high-performance Feynman integral evaluation*, 2110.11660.
- [21] M. Borinsky, H. J. Munch and F. Tellander, *Tropical Feynman integration in the Minkowski regime*, *Comput. Phys. Commun.* **292** (2023) 108874 [2302.08955].
- [22] E. Panzer, *Algorithms for the symbolic integration of hyperlogarithms with applications to Feynman integrals*, *Comput. Phys. Commun.* **188** (2015) 148 [1403.3385].
- [23] C. Duhr and F. Dulat, *PolyLogTools — polylogs for the masses*, *JHEP* **08** (2019) 135 [1904.07279].
- [24] J. Blümlein and C. Schneider, *Analytic computing methods for precision calculations in quantum field theory*, *Int. J. Mod. Phys. A* **33** (2018) 1830015 [1809.02889].
- [25] V. A. Smirnov, *Analytic tools for Feynman integrals*, vol. 250. 2012, 10.1007/978-3-642-34886-0.
- [26] J. M. Henn, *Lectures on differential equations for Feynman integrals*, *J. Phys. A* **48** (2015) 153001 [1412.2296].
- [27] J. D. Bjorken, *Experimental tests of Quantum electrodynamics and spectral representations of Green's functions in perturbation theory*, Ph.D. thesis, Stanford U., 1959.

- [28] L. D. Landau, *On analytic properties of vertex parts in quantum field theory*, *Nucl. Phys.* **13** (1959) 181.
- [29] N. Nakanishi, *Ordinary and Anomalous Thresholds in Perturbation Theory*, *Progress of Theoretical Physics* **22** (1959) 128
[<https://academic.oup.com/ptp/article-pdf/22/1/128/5427385/22-1-128.pdf>].
- [30] R. J. Eden, P. V. Landshoff, D. I. Olive and J. C. Polkinghorne, *The analytic S-matrix*. Cambridge Univ. Press, Cambridge, 1966.
- [31] F. Pham, *Singularités des processus de diffusion multiple*, *Annales de l'institut Henri Poincaré. Section A, Physique Théorique* **6** (1967) 89.
- [32] F. Pham, *Singularities of Multiple Scattering Processes*. Springer US, Boston, MA, 1968, 10.1007/978-1-4684-7727-6_2.
- [33] F. C. S. Brown, *On the periods of some Feynman integrals*, 0910.0114.
- [34] C. Fevola, S. Mizera and S. Telen, *Principal Landau determinants*, *Comput. Phys. Commun.* **303** (2024) 109278 [2311.16219].
- [35] C. Fevola, S. Mizera and S. Telen, *Landau Singularities Revisited: Computational Algebraic Geometry for Feynman Integrals*, *Phys. Rev. Lett.* **132** (2024) 101601 [2311.14669].
- [36] M. Helmer, G. Papathanasiou and F. Tellander, *Landau Singularities from Whitney Stratifications*, 2402.14787.
- [37] J. Chen, C. Ma and L. L. Yang, *Alphabet of one-loop Feynman integrals **, *Chin. Phys. C* **46** (2022) 093104 [2201.12998].
- [38] X. Jiang, J. Liu, X. Xu and L. L. Yang, *Symbol letters of Feynman integrals from Gram determinants*, 2401.07632.
- [39] Q. Yang, *Schubert problems, positivity and symbol letters*, *JHEP* **08** (2022) 168 [2203.16112].
- [40] S. He, J. Liu, Y. Tang and Q. Yang, *Symbology of Feynman integrals from twistor geometries*, *Sci. China Phys. Mech. Astron.* **67** (2024) 231011 [2207.13482].
- [41] S. He, Z. Li, R. Ma, Z. Wu, Q. Yang and Y. Zhang, *A study of Feynman integrals with uniform transcendental weights and their symbology*, *JHEP* **10** (2022) 165 [2206.04609].
- [42] S. He, X. Jiang, J. Liu and Q. Yang, *On symbology and differential equations of Feynman integrals from Schubert analysis*, *JHEP* **12** (2023) 140 [2309.16441].

- [43] M. Heller, A. von Manteuffel and R. M. Schabinger, *Multiple polylogarithms with algebraic arguments and the two-loop EW-QCD Drell-Yan master integrals*, *Phys. Rev. D* **102** (2020) 016025 [1907.00491].
- [44] L. J. Dixon, *Scattering amplitudes: the most perfect microscopic structures in the universe*, *J. Phys. A* **44** (2011) 454001 [1105.0771].
- [45] J. Andersen et al., *Les Houches 2023: Physics at TeV Colliders: Standard Model Working Group Report*, in *Physics of the TeV Scale and Beyond the Standard Model: Intensifying the Quest for New Physics*, 6, 2024, 2406.00708.
- [46] G. Passarino and M. J. G. Veltman, *One Loop Corrections for $e^+ e^-$ Annihilation Into $\mu^+ \mu^-$ in the Weinberg Model*, *Nucl. Phys. B* **160** (1979) 151.
- [47] O. V. Tarasov, *Connection between Feynman integrals having different values of the space-time dimension*, *Phys. Rev. D* **54** (1996) 6479 [hep-th/9606018].
- [48] O. V. Tarasov, *Generalized recurrence relations for two loop propagator integrals with arbitrary masses*, *Nucl. Phys. B* **502** (1997) 455 [hep-ph/9703319].
- [49] G. 't Hooft and M. Veltman, *Regularization and renormalization of gauge fields*, *Nuclear Physics B* **44** (1972) 189.
- [50] C. G. Bollini and J. J. Giambiagi, *Dimensional Renormalization: The Number of Dimensions as a Regularizing Parameter*, *Nuovo Cim. B* **12** (1972) 20.
- [51] G. M. Cicuta and E. Montaldi, *Analytic renormalization via continuous space dimension*, *Lett. Nuovo Cim.* **4** (1972) 329.
- [52] C. A. Nelson, *Origin of Cancellation of Infrared Divergences in Coherent State Approach: Forward Process $qq \rightarrow qq + \text{Gluon}$* , *Nucl. Phys. B* **181** (1981) 141.
- [53] H. F. Contopanagos and M. B. Einhorn, *Theory of the asymptotic S matrix for massless particles*, *Phys. Rev. D* **45** (1992) 1291.
- [54] F. Bloch and A. Nordsieck, *Note on the Radiation Field of the electron*, *Phys. Rev.* **52** (1937) 54.
- [55] T. Kinoshita, *Mass singularities of Feynman amplitudes*, *J. Math. Phys.* **3** (1962) 650.
- [56] T. D. Lee and M. Nauenberg, *Degenerate Systems and Mass Singularities*, *Phys. Rev.* **133** (1964) B1549.
- [57] C. Frye, H. Hannesdottir, N. Paul, M. D. Schwartz and K. Yan, *Infrared Finiteness and Forward Scattering*, *Phys. Rev. D* **99** (2019) 056015 [1810.10022].

- [58] H. Hannesdottir and M. D. Schwartz, *S -Matrix for massless particles*, *Phys. Rev. D* **101** (2020) 105001 [1911.06821].
- [59] N. Agarwal, L. Magnea, C. Signorile-Signorile and A. Tripathi, *The infrared structure of perturbative gauge theories*, *Phys. Rept.* **994** (2023) 1 [2112.07099].
- [60] E. Byckling and K. Kajantie, *Particle Kinematics: (Chapters I-VI, X)*. University of Jyväskylä, Jyväskylä, Finland, 1971.
- [61] S. Mizera, *Bounds on Crossing Symmetry*, *Phys. Rev. D* **103** (2021) 081701 [2101.08266].
- [62] J. Henn and P. Raman, *Positivity properties of scattering amplitudes*, 2407.05755.
- [63] J. M. Henn, K. Melnikov and V. A. Smirnov, *Two-loop planar master integrals for the production of off-shell vector bosons in hadron collisions*, *JHEP* **05** (2014) 090 [1402.7078].
- [64] C. Bogner and S. Weinzierl, *Feynman graph polynomials*, *Int. J. Mod. Phys. A* **25** (2010) 2585 [1002.3458].
- [65] R. N. Lee and A. A. Pomeransky, *Critical points and number of master integrals*, *JHEP* **11** (2013) 165 [1308.6676].
- [66] I. Gelfand, M. Kapranov and A. Zelevinsky, *Generalized euler integrals and a-hypergeometric functions*, *Advances in Mathematics* **84** (1990) 255.
- [67] S.-J. Matsubara-Heo, S. Mizera and S. Telen, *Four lectures on Euler integrals*, *SciPost Phys. Lect. Notes* **75** (2023) 1 [2306.13578].
- [68] P. A. Baikov, *Explicit solutions of n loop vacuum integral recurrence relations*, hep-ph/9604254.
- [69] P. A. Baikov, *Explicit solutions of the multiloop integral recurrence relations and its application*, *Nucl. Instrum. Meth. A* **389** (1997) 347 [hep-ph/9611449].
- [70] J. Chen, X. Jiang, C. Ma, X. Xu and L. L. Yang, *Baikov representations, intersection theory, and canonical Feynman integrals*, *JHEP* **07** (2022) 066 [2202.08127].
- [71] S. Weinzierl, *Feynman Integrals*. Springer Cham, 1, 2022, 10.1007/978-3-030-99558-4, [2201.03593].
- [72] J. M. Drummond, J. Henn, V. A. Smirnov and E. Sokatchev, *Magic identities for conformal four-point integrals*, *JHEP* **01** (2007) 064 [hep-th/0607160].
- [73] H. Frellesvig and C. G. Papadopoulos, *Cuts of Feynman Integrals in Baikov representation*, *JHEP* **04** (2017) 083 [1701.07356].

- [74] A. B. Goncharov, M. Spradlin, C. Vergu and A. Volovich, *Classical Polylogarithms for Amplitudes and Wilson Loops*, *Phys. Rev. Lett.* **105** (2010) 151605 [1006.5703].
- [75] J. Maldacena, D. Simmons-Duffin and A. Zhiboedov, *Looking for a bulk point*, *JHEP* **01** (2017) 013 [1509.03612].
- [76] J. Golden, A. B. Goncharov, M. Spradlin, C. Vergu and A. Volovich, *Motivic Amplitudes and Cluster Coordinates*, *JHEP* **01** (2014) 091 [1305.1617].
- [77] S. Caron-Huot, L. J. Dixon, A. McLeod and M. von Hippel, *Bootstrapping a Five-Loop Amplitude Using Steinmann Relations*, *Phys. Rev. Lett.* **117** (2016) 241601 [1609.00669].
- [78] L. J. Dixon and Y.-T. Liu, *An eight loop amplitude via antipodal duality*, *JHEP* **09** (2023) 098 [2308.08199].
- [79] J. M. Henn, A. Matijašić and J. Miczajka, *One-loop hexagon integral to higher orders in the dimensional regulator*, *JHEP* **01** (2023) 096 [2210.13505].
- [80] J. Hadamard, *Théorème sur les séries entières*, *Acta Mathematica* **22** (1899) 55.
- [81] J. C. Polkinghorne and G. R. Screaton, *The analytic properties of perturbation theory — I*, *Nuovo Cim.* **15** (1960) 289.
- [82] J. C. Polkinghorne and G. R. Screaton, *The analytic properties of perturbation theory — II*, *Nuovo Cim.* **15** (1960) 925.
- [83] H. S. Hannesdottir, A. J. McLeod, M. D. Schwartz and C. Vergu, *Constraints on sequential discontinuities from the geometry of on-shell spaces*, *JHEP* **07** (2023) 236 [2211.07633].
- [84] H. S. Hannesdottir, A. J. McLeod, M. D. Schwartz and C. Vergu, *Implications of the Landau equations for iterated integrals*, *Phys. Rev. D* **105** (2022) L061701 [2109.09744].
- [85] M. Berghoff and E. Panzer, *Hierarchies in relative Picard-Lefschetz theory*, 2212.06661.
- [86] J. B. Boyling, *A homological approach to parametric feynman integrals*, *Il Nuovo Cimento A (1965-1970)* **53** (1968) 351.
- [87] S. Bloch, H. Esnault and D. Kreimer, *On Motives associated to graph polynomials*, *Commun. Math. Phys.* **267** (2006) 181 [math/0510011].
- [88] S. Mizera, *Physics of the analytic S-matrix*, *Phys. Rept.* **1047** (2024) 1 [2306.05395].

- [89] I. Gelfand, M. Kapranov and A. Zelevinsky, *Discriminants, Resultants, and Multidimensional Determinants*, Modern Birkhäuser Classics. Birkhäuser Boston, 2009.
- [90] R. P. Klausen, *Hypergeometric feynman integrals*, Ph.D. thesis, Mainz U., 2023. 2302.13184. 10.25358/openscience-8527.
- [91] R. P. Klausen, *Kinematic singularities of Feynman integrals and principal A-determinants*, *JHEP* **02** (2022) 004 [2109.07584].
- [92] C. Dlapa, M. Helmer, G. Papathanasiou and F. Tellander, *Symbol alphabets from the Landau singular locus*, *JHEP* **10** (2023) 161 [2304.02629].
- [93] S. Mizera and S. Telen, *Landau discriminants*, *JHEP* **08** (2022) 200 [2109.08036].
- [94] T. Dennen, M. Spradlin and A. Volovich, *Landau Singularities and Symbology: One- and Two-loop MHV Amplitudes in SYM Theory*, *JHEP* **03** (2016) 069 [1512.07909].
- [95] T. Dennen, I. Prlina, M. Spradlin, S. Stanojevic and A. Volovich, *Landau Singularities from the Amplituhedron*, *JHEP* **06** (2017) 152 [1612.02708].
- [96] I. Prlina, M. Spradlin and S. Stanojevic, *All-loop singularities of scattering amplitudes in massless planar theories*, *Phys. Rev. Lett.* **121** (2018) 081601 [1805.11617].
- [97] T. Bitoun, C. Bogner, R. P. Klausen and E. Panzer, *Feynman integral relations from parametric annihilators*, *Lett. Math. Phys.* **109** (2019) 497 [1712.09215].
- [98] D. Agostini, C. Fevola, A.-L. Sattelberger and S. Telen, *Vector spaces of generalized Euler integrals*, *Commun. Num. Theor. Phys.* **18** (2024) 327 [2208.08967].
- [99] S. Caron-Huot, M. Correia and M. Giroux, *Recursive Landau Analysis*, 2406.05241.
- [100] A. B. Goncharov, *Multiple polylogarithms, cyclotomy and modular complexes*, *Math. Res. Lett.* **5** (1998) 497 [1105.2076].
- [101] C. Duhr, H. Gangl and J. R. Rhodes, *From polygons and symbols to polylogarithmic functions*, *JHEP* **10** (2012) 075 [1110.0458].
- [102] I. Prlina, M. Spradlin, J. Stankowicz, S. Stanojevic and A. Volovich, *All-Helicity Symbol Alphabets from Unwound Amplituhedra*, *JHEP* **05** (2018) 159 [1711.11507].
- [103] I. Prlina, M. Spradlin, J. Stankowicz and S. Stanojevic, *Boundaries of Amplituhedra and NMHV Symbol Alphabets at Two Loops*, *JHEP* **04** (2018) 049 [1712.08049].
- [104] N. Arkani-Hamed and J. Trnka, *The Amplituhedron*, *JHEP* **10** (2014) 030 [1312.2007].

- [105] N. Arkani-Hamed and J. Trnka, *Into the Amplituhedron*, *JHEP* **12** (2014) 182 [1312.7878].
- [106] J. Mago, A. Schreiber, M. Spradlin and A. Volovich, *Symbol alphabets from plabic graphs*, *JHEP* **10** (2020) 128 [2007.00646].
- [107] L. Ren, M. Spradlin and A. Volovich, *Symbol alphabets from tensor diagrams*, *JHEP* **12** (2021) 079 [2106.01405].
- [108] S. Abreu, R. Britto, C. Duhr and E. Gardi, *From multiple unitarity cuts to the coproduct of Feynman integrals*, *JHEP* **10** (2014) 125 [1401.3546].
- [109] S. Abreu, R. Britto and H. Grönqvist, *Cuts and coproducts of massive triangle diagrams*, *JHEP* **07** (2015) 111 [1504.00206].
- [110] S. Abreu, R. Britto, C. Duhr and E. Gardi, *Cuts from residues: the one-loop case*, *JHEP* **06** (2017) 114 [1702.03163].
- [111] S. Abreu, R. Britto, C. Duhr and E. Gardi, *Algebraic Structure of Cut Feynman Integrals and the Diagrammatic Coaction*, *Phys. Rev. Lett.* **119** (2017) 051601 [1703.05064].
- [112] S. Abreu, R. Britto, C. Duhr and E. Gardi, *Diagrammatic Hopf algebra of cut Feynman integrals: the one-loop case*, *JHEP* **12** (2017) 090 [1704.07931].
- [113] N. Arkani-Hamed and E. Y. Yuan, *One-Loop Integrals from Spherical Projections of Planes and Quadrics*, 1712.09991.
- [114] X. Jiang and L. L. Yang, *Recursive structure of Baikov representations: Generics and application to symbology*, *Phys. Rev. D* **108** (2023) 076004 [2303.11657].
- [115] J. Chen, B. Feng and L. L. Yang, *Intersection theory rules symbology*, *Sci. China Phys. Mech. Astron.* **67** (2024) 221011 [2305.01283].
- [116] S. Abreu, H. Ita, F. Moriello, B. Page, W. Tschernow and M. Zeng, *Two-Loop Integrals for Planar Five-Point One-Mass Processes*, *JHEP* **11** (2020) 117 [2005.04195].
- [117] F. Febres Cordero, G. Figueiredo, M. Kraus, B. Page and L. Reina, *Two-Loop Master Integrals for Leading-Color $pp \rightarrow t\bar{t}H$ Amplitudes with a Light-Quark Loop*, *JHEP* **07** (2024) 084 [2312.08131].
- [118] PARTICLE DATA GROUP collaboration, *Review of Particle Physics*, *PTEP* **2022** (2022) 083C01.
- [119] S. Abreu, H. Ita, B. Page and W. Tschernow, *Two-loop hexa-box integrals for non-planar five-point one-mass processes*, *JHEP* **03** (2022) 182 [2107.14180].

- [120] N. Arkani-Hamed, H. Frost, G. Salvatori, P.-G. Plamondon and H. Thomas, *All Loop Scattering as a Counting Problem*, 2309.15913.
- [121] N. Arkani-Hamed, Q. Cao, J. Dong, C. Figueiredo and S. He, *Scalar-Scaffolded Gluons and the Combinatorial Origins of Yang-Mills Theory*, 2401.00041.
- [122] A. Kotikov, *Differential equations method: New technique for massive Feynman diagrams calculation*, *Phys. Lett. B* **254** (1991) 158.
- [123] E. Remiddi, *Differential equations for Feynman graph amplitudes*, *Nuovo Cim. A* **110** (1997) 1435 [hep-th/9711188].
- [124] F. V. Tkachov, *A Theorem on Analytical Calculability of Four Loop Renormalization Group Functions*, *Phys. Lett.* **100B** (1981) 65.
- [125] K. G. Chetyrkin and F. V. Tkachov, *Integration by Parts: The Algorithm to Calculate beta Functions in 4 Loops*, *Nucl. Phys.* **B192** (1981) 159.
- [126] A. Smirnov and A. Petukhov, *The Number of Master Integrals is Finite*, *Lett. Math. Phys.* **97** (2011) 37 [1004.4199].
- [127] S. Laporta, *High precision calculation of multiloop Feynman integrals by difference equations*, *Int. J. Mod. Phys. A* **15** (2000) 5087 [hep-ph/0102033].
- [128] A. V. Smirnov, *Algorithm FIRE – Feynman Integral REDuction*, *JHEP* **10** (2008) 107 [0807.3243].
- [129] A. V. Smirnov and F. S. Chuharev, *FIRE6: Feynman Integral REDuction with Modular Arithmetic*, *Comput. Phys. Commun.* **247** (2020) 106877 [1901.07808].
- [130] C. Studerus, *Reduze-Feynman Integral Reduction in C++*, *Comput. Phys. Commun.* **181** (2010) 1293 [0912.2546].
- [131] A. von Manteuffel and C. Studerus, *Reduze 2 - Distributed Feynman Integral Reduction*, 1201.4330.
- [132] R. N. Lee, *Presenting LiteRed: a tool for the Loop InTEgrals REDuction*, 1212.2685.
- [133] R. N. Lee, *LiteRed 1.4: a powerful tool for reduction of multiloop integrals*, *J. Phys. Conf. Ser.* **523** (2014) 012059 [1310.1145].
- [134] P. Maierhöfer, J. Usovitsch and P. Uwer, *Kira—A Feynman integral reduction program*, *Comput. Phys. Commun.* **230** (2018) 99 [1705.05610].
- [135] J. Klappert, F. Lange, P. Maierhöfer and J. Usovitsch, *Integral reduction with Kira 2.0 and finite field methods*, *Comput. Phys. Commun.* **266** (2021) 108024 [2008.06494].

- [136] X. Guan, X. Liu, Y.-Q. Ma and W.-H. Wu, *Blade: A package for block-triangular form improved Feynman integrals decomposition*, 2405.14621.
- [137] A. von Manteuffel and R. M. Schabinger, *A novel approach to integration by parts reduction*, *Phys. Lett. B* **744** (2015) 101 [1406.4513].
- [138] T. Peraro, *Scattering amplitudes over finite fields and multivariate functional reconstruction*, *JHEP* **12** (2016) 030 [1608.01902].
- [139] T. Peraro, *FiniteFlow: multivariate functional reconstruction using finite fields and dataflow graphs*, *JHEP* **07** (2019) 031 [1905.08019].
- [140] K. J. Larsen and Y. Zhang, *Integration-by-parts reductions from unitarity cuts and algebraic geometry*, *Phys. Rev. D* **93** (2016) 041701 [1511.01071].
- [141] J. Böhm, A. Georgoudis, K. J. Larsen, H. Schönemann and Y. Zhang, *Complete integration-by-parts reductions of the non-planar hexagon-box via module intersections*, *JHEP* **09** (2018) 024 [1805.01873].
- [142] D. Bendle, J. Böhm, W. Decker, A. Georgoudis, F.-J. Pfreundt, M. Rahn et al., *Integration-by-parts reductions of Feynman integrals using Singular and GPI-Space*, *JHEP* **02** (2020) 079 [1908.04301].
- [143] P. Mastrolia and S. Mizera, *Feynman Integrals and Intersection Theory*, *JHEP* **02** (2019) 139 [1810.03818].
- [144] H. Frellesvig, F. Gasparotto, M. K. Mandal, P. Mastrolia, L. Mattiazzi and S. Mizera, *Vector Space of Feynman Integrals and Multivariate Intersection Numbers*, *Phys. Rev. Lett.* **123** (2019) 201602 [1907.02000].
- [145] H. Frellesvig, F. Gasparotto, S. Laporta, M. K. Mandal, P. Mastrolia, L. Mattiazzi et al., *Decomposition of Feynman Integrals on the Maximal Cut by Intersection Numbers*, *JHEP* **05** (2019) 153 [1901.11510].
- [146] H. Frellesvig, F. Gasparotto, S. Laporta, M. K. Mandal, P. Mastrolia, L. Mattiazzi et al., *Decomposition of Feynman Integrals by Multivariate Intersection Numbers*, *JHEP* **03** (2021) 027 [2008.04823].
- [147] J. Gluza, K. Kajda and D. A. Kosower, *Towards a Basis for Planar Two-Loop Integrals*, *Phys. Rev. D* **83** (2011) 045012 [1009.0472].
- [148] J. Böhm, A. Georgoudis, K. J. Larsen, M. Schulze and Y. Zhang, *Complete sets of logarithmic vector fields for integration-by-parts identities of Feynman integrals*, *Phys. Rev. D* **98** (2018) 025023 [1712.09737].
- [149] M. Barakat, R. Brüser, C. Fieker, T. Huber and J. Piclum, *Feynman integral reduction using Gröbner bases*, *JHEP* **05** (2023) 168 [2210.05347].

- [150] R. N. Lee, *Space-time dimensionality D as complex variable: Calculating loop integrals using dimensional recurrence relation and analytical properties with respect to D* , *Nucl. Phys. B* **830** (2010) 474 [0911.0252].
- [151] A. V. Kotikov, *Differential equation method: The Calculation of N point Feynman diagrams*, *Phys. Lett. B* **267** (1991) 123.
- [152] J. M. Henn, *Multiloop integrals in dimensional regularization made simple*, *Phys. Rev. Lett.* **110** (2013) 251601 [1304.1806].
- [153] R. N. Lee, *Reducing differential equations for multiloop master integrals*, *JHEP* **04** (2015) 108 [1411.0911].
- [154] M. Prausa, *epsilon: A tool to find a canonical basis of master integrals*, *Comput. Phys. Commun.* **219** (2017) 361 [1701.00725].
- [155] C. Meyer, *Transforming differential equations of multi-loop Feynman integrals into canonical form*, *JHEP* **04** (2017) 006 [1611.01087].
- [156] O. Gituliar and V. Magerya, *Fuchsia: a tool for reducing differential equations for Feynman master integrals to epsilon form*, *Comput. Phys. Commun.* **219** (2017) 329 [1701.04269].
- [157] M. Höschele, J. Hoff and T. Ueda, *Adequate bases of phase space master integrals for $gg \rightarrow h$ at NNLO and beyond*, *JHEP* **09** (2014) 116 [1407.4049].
- [158] C. Dlapa, J. Henn and K. Yan, *Deriving canonical differential equations for Feynman integrals from a single uniform weight integral*, *JHEP* **05** (2020) 025 [2002.02340].
- [159] C. Dlapa, J. M. Henn and F. J. Wagner, *An algorithmic approach to finding canonical differential equations for elliptic Feynman integrals*, *JHEP* **08** (2023) 120 [2211.16357].
- [160] F. Cachazo, *Sharpening The Leading Singularity*, 0803.1988.
- [161] N. Arkani-Hamed, J. L. Bourjaily, F. Cachazo and J. Trnka, *Local Integrals for Planar Scattering Amplitudes*, *JHEP* **06** (2012) 125 [1012.6032].
- [162] R. Britto, F. Cachazo and B. Feng, *Generalized unitarity and one-loop amplitudes in $N=4$ super-Yang-Mills*, *Nucl. Phys. B* **725** (2005) 275 [hep-th/0412103].
- [163] M. Spradlin and A. Volovich, *Symbols of One-Loop Integrals From Mixed Tate Motives*, *JHEP* **11** (2011) 084 [1105.2024].
- [164] N. Arkani-Hamed, J. L. Bourjaily, F. Cachazo, A. B. Goncharov, A. Postnikov and J. Trnka, *Grassmannian Geometry of Scattering Amplitudes*. Cambridge University Press, 4, 2016, 10.1017/CBO9781316091548, [1212.5605].

- [165] N. Arkani-Hamed, J. L. Bourjaily, F. Cachazo and J. Trnka, *Singularity Structure of Maximally Supersymmetric Scattering Amplitudes*, *Phys. Rev. Lett.* **113** (2014) 261603 [1410.0354].
- [166] E. Herrmann and J. Parra-Martinez, *Logarithmic forms and differential equations for Feynman integrals*, *JHEP* **02** (2020) 099 [1909.04777].
- [167] P. Wasser, *Analytic properties of Feynman integrals for scattering amplitudes*, Ph.D. thesis, Mainz U., 2018.
- [168] J. Henn, B. Mistlberger, V. A. Smirnov and P. Wasser, *Constructing d -log integrands and computing master integrals for three-loop four-particle scattering*, *JHEP* **04** (2020) 167 [2002.09492].
- [169] K.-T. Chen, *Iterated path integrals*, *Bull. Am. Math. Soc.* **83** (1977) 831.
- [170] E. Kummer, *Ueber die transcendenten, welche aus wiederholten integrationen rationaler formeln entstehen.*, *Journal für die reine und angewandte Mathematik* **1840** (1840) 74.
- [171] E. Kummer, *Ueber die transcendenten, welche aus wiederholten integrationen rationaler formeln entstehen. (fortsetzung).*, *Journal für die reine und angewandte Mathematik* **1840** (1840) 193.
- [172] E. Kummer, *Ueber die transcendenten, welche aus wiederholten integrationen rationaler formeln entstehen. (fortsetzung).*, *Journal für die reine und angewandte Mathematik* **21** (1840) 328.
- [173] H. Poincaré, *Sur les groupes des équations linéaires*, *Acta Mathematica* **4** (1884) 201.
- [174] J. A. Lappo-Danilevsky, *Mémoires sur la théorie des systèmes des équations différentielles linéaires.*, *The Mathematical Gazette* **38** (1954) 229.
- [175] A. B. Goncharov, *Multiple polylogarithms and mixed Tate motives*, math/0103059.
- [176] A. B. Goncharov, *Multiple ζ -numbers, hyperlogarithms and mixed Tate motives*, Preprint MSRI 058–93.
- [177] A. B. Goncharov, *The double logarithm and Manin’s complex for modular curves*, *Math. Res. Letters* **4** (1997) 617.
- [178] A. Sabry, *Fourth order spectral functions for the electron propagator*, *Nuclear Physics* **33** (1962) 401.
- [179] A. Levin and G. Racinet, *Towards multiple elliptic polylogarithms*, *arXiv Mathematics e-prints* (2007) math/0703237 [math/0703237].

- [180] F. C. S. Brown and A. Levin, *Multiple Elliptic Polylogarithms*, *arXiv e-prints* (2011) arXiv:1110.6917 [1110.6917].
- [181] F. Brown, *Multiple Modular Values and the relative completion of the fundamental group of $M_{1,1}$* , *arXiv e-prints* (2014) arXiv:1407.5167 [1407.5167].
- [182] Y. I. Manin, *Iterated integrals of modular forms and noncommutative modular symbols*, *arXiv Mathematics e-prints* (2005) math/0502576 [math/0502576].
- [183] S. Bloch, M. Kerr and P. Vanhove, *A Feynman integral via higher normal functions*, *Compos. Math.* **151** (2015) 2329 [1406.2664].
- [184] J. L. Bourjaily, Y.-H. He, A. J. McLeod, M. Von Hippel and M. Wilhelm, *Traintracks through Calabi-Yau Manifolds: Scattering Amplitudes beyond Elliptic Polylogarithms*, *Phys. Rev. Lett.* **121** (2018) 071603 [1805.09326].
- [185] J. L. Bourjaily, A. J. McLeod, C. Vergu, M. Volk, M. Von Hippel and M. Wilhelm, *Embedding Feynman Integral (Calabi-Yau) Geometries in Weighted Projective Space*, *JHEP* **01** (2020) 078 [1910.01534].
- [186] A. Klemm, C. Nega and R. Safari, *The l -loop Banana Amplitude from GKZ Systems and relative Calabi-Yau Periods*, *JHEP* **04** (2020) 088 [1912.06201].
- [187] K. Bönisch, F. Fischbach, A. Klemm, C. Nega and R. Safari, *Analytic structure of all loop banana integrals*, *JHEP* **05** (2021) 066 [2008.10574].
- [188] K. Bönisch, C. Duhr, F. Fischbach, A. Klemm and C. Nega, *Feynman integrals in dimensional regularization and extensions of Calabi-Yau motives*, *JHEP* **09** (2022) 156 [2108.05310].
- [189] S. Abreu, R. Britto and C. Duhr, *The SAGEX review on scattering amplitudes Chapter 3: Mathematical structures in Feynman integrals*, *J. Phys. A* **55** (2022) 443004 [2203.13014].
- [190] A. Goncharov, *A simple construction of grassmannian polylogarithms*, *Advances in Mathematics* **241** (2013) 79.
- [191] A. B. Goncharov, *Galois symmetries of fundamental groupoids and noncommutative geometry*, *Duke Math. J.* **128** (2005) 209 [math/0208144].
- [192] L. J. Dixon, J. M. Drummond and J. M. Henn, *Bootstrapping the three-loop hexagon*, *JHEP* **11** (2011) 023 [1108.4461].
- [193] L. J. Dixon, J. M. Drummond and J. M. Henn, *Analytic result for the two-loop six-point NMHV amplitude in $N=4$ super Yang-Mills theory*, *JHEP* **01** (2012) 024 [1111.1704].

- [194] L. J. Dixon, J. Drummond, T. Harrington, A. J. McLeod, G. Papathanasiou and M. Spradlin, *Heptagons from the Steinmann Cluster Bootstrap*, *JHEP* **02** (2017) 137 [1612.08976].
- [195] S. Caron-Huot, L. J. Dixon, J. M. Drummond, F. Dulat, J. Foster, O. Gürdoğan et al., *The Steinmann Cluster Bootstrap for $N = 4$ Super Yang-Mills Amplitudes*, *PoS CORFU2019* (2020) 003 [2005.06735].
- [196] L. J. Dixon and Y.-T. Liu, *Lifting Heptagon Symbols to Functions*, *JHEP* **10** (2020) 031 [2007.12966].
- [197] J. Drummond, J. Foster and O. Gürdoğan, *Cluster Adjacency Properties of Scattering Amplitudes in $N = 4$ Supersymmetric Yang-Mills Theory*, *Phys. Rev. Lett.* **120** (2018) 161601 [1710.10953].
- [198] J. Drummond, J. Foster and O. Gürdoğan, *Cluster adjacency beyond MHV*, *JHEP* **03** (2019) 086 [1810.08149].
- [199] D. Chicherin, J. M. Henn and G. Papathanasiou, *Cluster algebras for Feynman integrals*, *Phys. Rev. Lett.* **126** (2021) 091603 [2012.12285].
- [200] S. Fomin, L. Williams and A. Zelevinsky, *Introduction to cluster algebras. chapters 1-3*, 2021.
- [201] S. Fomin, L. Williams and A. Zelevinsky, *Introduction to cluster algebras. chapters 4-5*, 2021.
- [202] S. Fomin, L. Williams and A. Zelevinsky, *Introduction to cluster algebras. chapter 6*, 2021.
- [203] S. Fomin, L. Williams and A. Zelevinsky, *Introduction to cluster algebras. chapter 7*, 2021.
- [204] G. Papathanasiou, *The sageX review on scattering amplitudes, chapter 5: Analytic bootstraps for scattering amplitudes and beyond*, *Journal of Physics A: Mathematical and Theoretical* **55** (2022) 443006.
- [205] K.-T. Chen, *Iterated path integrals*, *Bulletin of the American Mathematical Society* **83** (1977) 831 .
- [206] G. Heinrich, *QCD calculations for the LHC: status and prospects*, in *5th Large Hadron Collider Physics Conference*, 10, 2017, 1710.04998.
- [207] S. Borowka, G. Heinrich, S. Jahn, S. P. Jones, M. Kerner and J. Schlenk, *A GPU compatible quasi-Monte Carlo integrator interfaced to pySecDec*, *Comput. Phys. Commun.* **240** (2019) 120 [1811.11720].

- [208] G. Heinrich, S. Jahn, S. P. Jones, M. Kerner, F. Langer, V. Magerya et al., *Expansion by regions with pySecDec*, *Comput. Phys. Commun.* **273** (2022) 108267 [2108.10807].
- [209] J. M. Henn, A. V. Smirnov and V. A. Smirnov, *Evaluating single-scale and/or non-planar diagrams by differential equations*, *JHEP* **03** (2014) 088 [1312.2588].
- [210] D. Chicherin, T. Gehrmann, J. M. Henn, N. A. Lo Presti, V. Mitev and P. Wasser, *Analytic result for the nonplanar hexa-box integrals*, *JHEP* **03** (2019) 042 [1809.06240].
- [211] D. E. Radford, *A natural ring basis for the shuffle algebra and an application to group schemes*, *Journal of Algebra* **58** (1979) 432.
- [212] J. M. Henn, A. V. Smirnov and V. A. Smirnov, *Evaluating Multiple Polylogarithm Values at Sixth Roots of Unity up to Weight Six*, *Nucl. Phys. B* **919** (2017) 315 [1512.08389].
- [213] T. Gehrmann, J. M. Henn and N. A. Lo Presti, *Pentagon functions for massless planar scattering amplitudes*, *JHEP* **10** (2018) 103 [1807.09812].
- [214] D. Chicherin and V. Sotnikov, *Pentagon Functions for Scattering of Five Massless Particles*, *JHEP* **12** (2020) 167 [2009.07803].
- [215] D. Chicherin, V. Sotnikov and S. Zoia, *Pentagon functions for one-mass planar scattering amplitudes*, *JHEP* **01** (2022) 096 [2110.10111].
- [216] D. Zagier, *The Dilogarithm Function*, in *Les Houches School of Physics: Frontiers in Number Theory, Physics and Geometry*, pp. 3–65, 2007, DOI.
- [217] S. Caron-Huot and J. M. Henn, *Iterative structure of finite loop integrals*, *JHEP* **06** (2014) 114 [1404.2922].
- [218] Z. Bern, L. J. Dixon, D. A. Kosower, R. Roiban, M. Spradlin, C. Vergu et al., *The Two-Loop Six-Gluon MHV Amplitude in Maximally Supersymmetric Yang-Mills Theory*, *Phys. Rev. D* **78** (2008) 045007 [0803.1465].
- [219] L. J. Dixon, J. M. Drummond and J. M. Henn, *The one-loop six-dimensional hexagon integral and its relation to MHV amplitudes in $N=4$ SYM*, *JHEP* **06** (2011) 100 [1104.2787].
- [220] D. B. Melrose, *Reduction of Feynman diagrams*, *Nuovo Cim.* **40** (1965) 181.
- [221] Z. Bern, L. J. Dixon and D. A. Kosower, *Dimensionally regulated one loop integrals*, *Phys. Lett. B* **302** (1993) 299 [hep-ph/9212308].
- [222] Z. Bern, L. J. Dixon and D. A. Kosower, *Dimensionally regulated pentagon integrals*, *Nucl. Phys. B* **412** (1994) 751 [hep-ph/9306240].

- [223] T. Binoth, J. P. Guillet and G. Heinrich, *Reduction formalism for dimensionally regulated one loop N point integrals*, *Nucl. Phys. B* **572** (2000) 361 [hep-ph/9911342].
- [224] T. Binoth, J. P. Guillet, G. Heinrich, E. Pilon and C. Schubert, *An Algebraic/numerical formalism for one-loop multi-leg amplitudes*, *JHEP* **10** (2005) 015 [hep-ph/0504267].
- [225] A. Hodges, *Eliminating spurious poles from gauge-theoretic amplitudes*, *JHEP* **05** (2013) 135 [0905.1473].
- [226] J. Henn, T. Peraro, Y. Xu and Y. Zhang, *A first look at the function space for planar two-loop six-particle Feynman integrals*, *JHEP* **03** (2022) 056 [2112.10605].
- [227] S. Badger, H. Frellesvig and Y. Zhang, *A Two-Loop Five-Gluon Helicity Amplitude in QCD*, *JHEP* **12** (2013) 045 [1310.1051].
- [228] S. Abreu, B. Page and M. Zeng, *Differential equations from unitarity cuts: nonplanar hexa-box integrals*, *JHEP* **01** (2019) 006 [1807.11522].
- [229] S. Abreu, L. J. Dixon, E. Herrmann, B. Page and M. Zeng, *The two-loop five-point amplitude in $\mathcal{N} = 4$ super-Yang-Mills theory*, *Phys. Rev. Lett.* **122** (2019) 121603 [1812.08941].
- [230] D. Chicherin, T. Gehrmann, J. M. Henn, P. Wasser, Y. Zhang and S. Zoia, *All Master Integrals for Three-Jet Production at Next-to-Next-to-Leading Order*, *Phys. Rev. Lett.* **123** (2019) 041603 [1812.11160].
- [231] T. Gehrmann, J. M. Henn and N. A. Lo Presti, *Analytic form of the two-loop planar five-gluon all-plus-helicity amplitude in QCD*, *Phys. Rev. Lett.* **116** (2016) 062001 [1511.05409].
- [232] S. Badger, C. Brønnum-Hansen, H. B. Hartanto and T. Peraro, *First look at two-loop five-gluon scattering in QCD*, *Phys. Rev. Lett.* **120** (2018) 092001 [1712.02229].
- [233] S. Badger, C. Brønnum-Hansen, H. B. Hartanto and T. Peraro, *Analytic helicity amplitudes for two-loop five-gluon scattering: the single-minus case*, *JHEP* **01** (2019) 186 [1811.11699].
- [234] S. Abreu, F. Febres Cordero, H. Ita, B. Page and M. Zeng, *Planar Two-Loop Five-Gluon Amplitudes from Numerical Unitarity*, *Phys. Rev. D* **97** (2018) 116014 [1712.03946].
- [235] H. A. Chawdhry, M. Czakon, A. Mitov and R. Poncelet, *Two-loop leading-color helicity amplitudes for three-photon production at the LHC*, *JHEP* **06** (2021) 150 [2012.13553].

- [236] S. Abreu, B. Page, E. Pascual and V. Sotnikov, *Leading-Color Two-Loop QCD Corrections for Three-Photon Production at Hadron Colliders*, *JHEP* **01** (2021) 078 [2010.15834].
- [237] S. Abreu, J. Dormans, F. Febres Cordero, H. Ita and B. Page, *Analytic Form of Planar Two-Loop Five-Gluon Scattering Amplitudes in QCD*, *Phys. Rev. Lett.* **122** (2019) 082002 [1812.04586].
- [238] S. Badger, D. Chicherin, T. Gehrmann, G. Heinrich, J. Henn, T. Peraro et al., *Analytic form of the full two-loop five-gluon all-plus helicity amplitude*, *Phys. Rev. Lett.* **123** (2019) 071601 [1905.03733].
- [239] S. Abreu, F. F. Cordero, H. Ita, B. Page and V. Sotnikov, *Leading-color two-loop QCD corrections for three-jet production at hadron colliders*, *JHEP* **07** (2021) 095 [2102.13609].
- [240] B. Agarwal, F. Buccioni, F. Devoto, G. Gambuti, A. von Manteuffel and L. Tancredi, *Five-parton scattering in QCD at two loops*, *Phys. Rev. D* **109** (2024) 094025 [2311.09870].
- [241] H. A. Chawdhry, M. Czakon, A. Mitov and R. Poncelet, *Two-loop leading-colour QCD helicity amplitudes for two-photon plus jet production at the LHC*, *JHEP* **07** (2021) 164 [2103.04319].
- [242] B. Agarwal, F. Buccioni, A. von Manteuffel and L. Tancredi, *Two-Loop Helicity Amplitudes for Diphoton Plus Jet Production in Full Color*, *Phys. Rev. Lett.* **127** (2021) 262001 [2105.04585].
- [243] G. De Laurentis, H. Ita and V. Sotnikov, *Double-virtual NNLO QCD corrections for five-parton scattering. II. The quark channels*, *Phys. Rev. D* **109** (2024) 094024 [2311.18752].
- [244] G. De Laurentis, H. Ita, M. Klinkert and V. Sotnikov, *Double-virtual NNLO QCD corrections for five-parton scattering. I. The gluon channel*, *Phys. Rev. D* **109** (2024) 094023 [2311.10086].
- [245] S. Badger, C. Brønnum-Hansen, D. Chicherin, T. Gehrmann, H. B. Hartanto, J. Henn et al., *Virtual QCD corrections to gluon-initiated diphoton plus jet production at hadron colliders*, *JHEP* **11** (2021) 083 [2106.08664].
- [246] S. Kallweit, V. Sotnikov and M. Wiesemann, *Triphoton production at hadron colliders in NNLO QCD*, *Phys. Lett. B* **812** (2021) 136013 [2010.04681].
- [247] M. Czakon, A. Mitov and R. Poncelet, *Next-to-Next-to-Leading Order Study of Three-Jet Production at the LHC*, *Phys. Rev. Lett.* **127** (2021) 152001 [2106.05331].

- [248] H. A. Chawdhry, M. Czakon, A. Mitov and R. Poncelet, *NNLO QCD corrections to diphoton production with an additional jet at the LHC*, *JHEP* **09** (2021) 093 [2105.06940].
- [249] S. Badger, M. Czakon, H. B. Hartanto, R. Moodie, T. Peraro, R. Poncelet et al., *Isolated photon production in association with a jet pair through next-to-next-to-leading order in QCD*, *JHEP* **10** (2023) 071 [2304.06682].
- [250] S. Badger, T. Gehrmann, M. Marcoli and R. Moodie, *Next-to-leading order QCD corrections to diphoton-plus-jet production through gluon fusion at the LHC*, *Phys. Lett. B* **824** (2022) 136802 [2109.12003].
- [251] D. D. Canko, C. G. Papadopoulos and N. Syrrakos, *Analytic representation of all planar two-loop five-point Master Integrals with one off-shell leg*, *JHEP* **01** (2021) 199 [2009.13917].
- [252] S. Abreu, D. Chicherin, H. Ita, B. Page, V. Sotnikov, W. Tschernow et al., *All Two-Loop Feynman Integrals for Five-Point One-Mass Scattering*, *Phys. Rev. Lett.* **132** (2024) 141601 [2306.15431].
- [253] Z. Bern, G. Diana, L. J. Dixon, F. Febres Cordero, S. Hoeche, D. A. Kosower et al., *Four-Jet Production at the Large Hadron Collider at Next-to-Leading Order in QCD*, *Phys. Rev. Lett.* **109** (2012) 042001 [1112.3940].
- [254] S. Badger, B. Biedermann, P. Uwer and V. Yundin, *Next-to-leading order QCD corrections to five jet production at the LHC*, *Phys. Rev. D* **89** (2014) 034019 [1309.6585].
- [255] R. K. Ellis, W. T. Giele and G. Zanderighi, *The One-loop amplitude for six-gluon scattering*, *JHEP* **05** (2006) 027 [hep-ph/0602185].
- [256] D. C. Dunbar, *The six gluon one-loop amplitude*, *Nucl. Phys. B Proc. Suppl.* **183** (2008) 122.
- [257] G. Mahlon, *One loop multiphoton helicity amplitudes*, *Phys. Rev. D* **49** (1994) 2197.
- [258] G. Ossola, C. G. Papadopoulos and R. Pittau, *Numerical evaluation of six-photon amplitudes*, *JHEP* **07** (2007) 085 [0704.1271].
- [259] T. Binoth, G. Heinrich, T. Gehrmann and P. Mastrolia, *Six-Photon Amplitudes*, *Phys. Lett. B* **649** (2007) 422 [hep-ph/0703311].
- [260] C. Bernicot and J. P. Guillet, *Six-Photon Amplitudes in Scalar QED*, *JHEP* **01** (2008) 059 [0711.4713].
- [261] D. C. Dunbar, G. R. Jehu and W. B. Perkins, *Two-loop six gluon all plus helicity amplitude*, *Phys. Rev. Lett.* **117** (2016) 061602 [1605.06351].

-
- [262] D. C. Dunbar, J. H. Godwin, G. R. Jehu and W. B. Perkins, *Analytic all-plus-helicity gluon amplitudes in QCD*, *Phys. Rev. D* **96** (2017) 116013 [1710.10071].
- [263] J. M. Henn, A. Matijašić, J. Miczajka, T. Peraro, Y. Xu and Y. Zhang, *A computation of two-loop six-point Feynman integrals in dimensional regularization*, 2403.19742.
- [264] S. Caron-Huot, L. J. Dixon, F. Dulat, M. Von Hippel, A. J. McLeod and G. Papathanasiou, *The Cosmic Galois Group and Extended Steinmann Relations for Planar $\mathcal{N} = 4$ SYM Amplitudes*, *JHEP* **09** (2019) 061 [1906.07116].
- [265] O. Steinmann, *Über den Zusammenhang zwischen den Wightmanfunktionen und den retardierten Kommutatoren*, *Helv. Physica Acta* **33** (1960) 257.
- [266] O. Steinmann, *Wightman-Funktionen und retardierte Kommutatoren. II*, *Helv. Physica Acta* **33** (1960) 347.
- [267] L. F. Alday, E. I. Buchbinder and A. A. Tseytlin, *Correlation function of null polygonal Wilson loops with local operators*, *JHEP* **09** (2011) 034 [1107.5702].
- [268] D. Chicherin and J. M. Henn, *Symmetry properties of Wilson loops with a Lagrangian insertion*, *JHEP* **07** (2022) 057 [2202.05596].
- [269] D. Chicherin and J. Henn, *Pentagon Wilson loop with Lagrangian insertion at two loops in $\mathcal{N} = 4$ super Yang-Mills theory*, *JHEP* **07** (2022) 038 [2204.00329].
- [270] S. Badger, M. Becchetti, N. Giraudo and S. Zoia, *Two-loop integrals for $t\bar{t}$ -jet production at hadron colliders in the leading colour approximation*, *JHEP* **07** (2024) 073 [2404.12325].

Acknowledgments

I would like to express my deepest gratitude to my supervisor, Johannes Henn, for his guidance, support and encouragement throughout my doctoral studies. I am especially grateful for the introduction to the field of Feynman integrals and scattering amplitudes, numerous discussions and all the constructive feedback. His ability to balance guidance with autonomy allowed me to grow as a researcher. I feel fortunate to have had the opportunity to work under his supervision.

I am thankful to Julian Miczajka for always finding time to discuss physics, research, and everyday life. I am especially grateful for countless tips and tricks for using `Mathematica` and for his help with the German summary of this thesis.

In addition, I would like to thank Markus Ebert, Manuel Ettengruber, Filip Rešćić, Darren Scott and William Torres Bobadilla for making life in Munich during the pandemic so much more enjoyable. I am thankful to fellow PhD students Andreas Bischof, Sèrgio Carrôlo, Davide De Biasio, Sara Ditsch, Ana Fernandes Alexandre, Felix Hagemann, Jungwon Lim, Elia Mazzucchelli, Francisco Vazão for sharing this journey. I would also like to thank Daniel Buchin, Giacomo Contri, Moritz Kellermann, Giorgio Pirola and Alessandro Ratti for sharing with me the responsibility of being the PhD representatives.

Moreover, I would like to thank my collaborators Julian Miczajka, Tiziano Peraro, Yingxuan Xu, and Yang Zhang, from whom I learned a lot during our joint work. Further thanks to Paolo Benincasa, Dmitrii Chicherin, Claudia Fevola, Wojciech Flieger, Martín Lagares, Anders Ohrberg Schreiber, Giulio Salvatori, Anna–Laura Sattelberger, Vasily Sotnikov, Bernd Sturmfels, Prashanth Raman, Simon Telen, Shun-Qing Zhang and Simone Zoia for enlightening discussions.

I would also like to thank Frank Steffen and Vera Weber for helping me with various administrative tasks. In addition, I am grateful to Stephan Stieberger for serving as an external supervisor in the IMPRS advisory panel system. Further thanks to Sorana Scholtes and Barbara Wankerl for encouraging me to participate in various outreach activities.

Special thanks are due to Sara Ditsch and Julian Miczajka, who were kind enough to read an earlier version of this thesis and to provide helpful comments.

Finally, I would like to thank Adriana, Paula, Iva, Ivana and Nemanja for being great friends at different stages of my education and for supporting me in this challenging adventure. And most importantly, I am truly grateful to my parents, sisters and grandparents for their unconditional love, support and for always believing in me.

This work received funding from the European Union's Horizon 2020 research and innovation programme *Novel structures in scattering amplitudes* (grant agreement No 725110).